Advances in
BIOTECHNOLOGY

Advances in Biotechnology

Chapter 1

Optimum Filtered Backprojection Images by Geometric Modeling: With Application to Medical Imaging

Atefeh Hasan-Zadeh[*]

Fouman Faculty of Engineering, College of Engineering, University of Tehran, Guilan, Iran, P. O. Box 43581-39115.

Email: hasanzadeh.a@ut.ac.ir

Abstract

This article pays to prove that the number of times that the projections from some angles in filtered backprojection image (which are equally spaced) can be calculated by the surface area of the convex body and (symplectic) Holmes-Thompson volume in notions of Fourier transform, Finsler metrics and Minkowski spaces. For this purpose, these parameters are calculated by the surface area of a convex body of the corresponding projective spaces and Holmes-Thompson volume in notions of integral geometry (Radon and Fourier transform), Finsler Geometry (and Minkowski spaces) and symplectic geometry. This lead to some correspondence between basic notions of medical imaging such as the projections from some angles which are equally spaced, the number of times that the projections from some angles which are equally spaced, the low image correctness, and the notions of Finsler geometry.

Keywords: Minkowski space; Finsler metric; Fourier transform; Backprojection images; Medical imaging.

1. Introduction

Medical imaging has led to a modern medical revolution in various ways. Many efforts have been made in this field since 1901 to date, [1-3]. The mathematical concepts of medical imaging are based on linear integrals and Fourier transforms, followed by the Radon transform, [4]. In fact, Radon transformation gives us a method for obtaining a Fourier transform of a function given by a density of its line integral.

On the other hand, many problems in geometry and physics can be easily solved by a change of viewpoint. For example, if one considers the line, or the plane, instead of the point as the basic object of geometry, the outlook changes completely. This change in viewpoint leads naturally to integral geometry. This paper is concerned with some analogy of various classical formulas from integral geometry and its relation with Finsler geometry and symplectic geometry.

This deep connection between these three geometries takes place by the type of volume named as Holmes-Thompson volume [5], which its ties to convex geometry, integral geometry, and Finsler geometry. The other advantage of working with Holmes-Thompson definition is that there is a remarkably simple formula for the Holmes-Thompson area density of a Minkowski space in terms of the Fourier transform of its norm [6-8], which is the main object in this paper.

Section 2 of this paper contains some preliminaries about Minkowski spaces, Finsler geometry and Integral geometry to cover all the key concepts in its entirety. Section 3, is about basic medical imaging concepts, too. In the sequel, the application of the triple chain of three geometries in financial markets has been proposed.

The proposed methodology, results in the calculation of the number of times that the projections from some angles in filtered backprojection image which are equally spaced in concepts of the surface area of the convex body and (symplectic) Holmes-Thompson volume in notions of Fourier transform, Finsler metrics and Minkowski spaces. This fact has been proved in Theorem 1.

2. Basic Geometric Concepts

Let V be vector space and $\mathsf{j}: V \to [0,\infty)$ be a norm that is smooth outside the origin. Set $L = \dfrac{\mathsf{j}^2}{2}$ and consider the exterior derivative of L, dL, as a map from $V \setminus \{0\}$ to $V^* \setminus \{0\}$. The norm j is said to be a Minkowski norm if dL is a diffeomorphism. For any nonzero vector $v \in V$, there is an invertible linear map $D(dL)(v): T_v V \to T_{dL(v)} V^*$. In fact, using the natural identification of $T_v V$ with V, and $T_{dL(v)} V^*$ with V^*, it may be think of $g_{\mathsf{j}}(v) := D(dL)(v)$ as a (symmetric) bilinear form on V: $g_{\mathsf{j}}(v)(\mathsf{w}_1, \mathsf{w}_2) := (D(dL)(v)(\mathsf{w}_1))(\mathsf{w}_2)$

. The norm g_j is a Minkowski norm if and only if g_j is positive definite.

When the vector v belongs to the unit sphere, structure $g_j(v)$ denoted as the osculating Euclidean structure at v and the ellipsoid $E_v := \{w \in V : g_j(w,w) = 1\}$, as the osculating ellipsoid at v. A smooth hypersurface in a finite-dimensional real vector space V is said to be quadratically convex if its osculating quadrics are all ellipsoids. A vector space V provided with a norm $\|.\|$ such that the unit sphere is quadratically convex is called a Minkowski space.

A Finsler metric on a manifold M is a continuous function defined on its tangent bundle such that is smooth (away from the zero section) and its restriction to each tangent space is a Minkowski norm, means that the hypersurface is quadratically convex and encloses the origin, is called a Finsler manifold.

Throughout this chapter, M is a compact manifold and for every $m \in M$ and any compact hypersurface $H \subset T^*M$, the intersection $H \cap T^*M$ is a convex hypersurface of enclosing the origin and in each cotangent space $T^*_m M$ the intersection $H \cap T^*M$ is a quadratically convex hypersurface enclosing the origin. In this way, it can be defined the Holmes-Thompson volume:

The Holmes-Thompson volume of a n-dimensional Finsler manifold (M,j), $vol_n(M,j)$, is the symplectic volume of its unit co-disc bundle divided by the volume of the Euclidean n-dimensional unit ball $vol_n(M,j) = \frac{1}{e_n n} \int_{S^*_H M} a \wedge (da)^{n-1}$, where e_n is the volume of the Euclidean unit ball of dimension n.

If K is a convex body, then it admits at least one supporting hyperplane H (affine here) for any point x of its boundary. If the convex body K be star-shaped with respect to origin in $\square^n$ and the boundary of K is continuous in the sense that the Minkowski functional of K defined by $\|x\|_K = \min\{a \geq 0 : x \in aK\}$ is a continuous function on $\square^n$, then the Minkowski functional is a homogeneous function of degree 1 on $\square^n$ is strictly positive outside of the origin, and $K = \{x \in \square^n : \|x\|_K \leq 1\}$. The radial function of a star body K is defined by $r_K(x) = \|x\|_K^{-1}$, $x \in \square^n$. If $x \in S^{n-1}$, then $r_K(x)$ is the radius of K in the direction of x, i.e., the distance from the origin to the boundary of K in the direction of x.

Lemma 1: [9] Let K be an origin-symmetric star body in $\square^n$. Then, for $0 < p < n$, the function $\|x\|_K^{-p}$ is locally integrable on $\square^n$. Also, if f is a bounded integrable function on $\square^n$, then the function $\|x\|_K^{-p} f(.)$ is integrable on $\square^n$.

In this way, for $x \in S^{n-1}$ can be defined the parallel section function of K in the direction of x as a function on $\square$ given by $A_{K,x}(t) = vol_{n-1}(K \cap \{x^\perp + tx\})$ where $\{x^\perp + tx\}$ is the hyperplane perpendicular to x at distance t from the origin and can be stated as the following: $A_{K,x}(t) = \int_{\langle x,x \rangle = t} c(\|x\|_K) dx$ which $c(\|x\|_K)$ is the indicator function of the body K. For $t = 0$, writing the integral in the right-hand side of the function $A_{K,x}(t)$ in the polar coordinates of

the hyperplane $\langle x, x \rangle = 0$, result in the polar formula for the volume of central hyperplane sections

$$
\begin{aligned}
A_{K,\mathbf{x}}(0) = vol_{n-1}(K \cap \mathbf{x}^{\perp}) &= \int\limits_{\langle x,x \rangle = t} \mathsf{c}\left(\|x\|_K\right) dx = \int\limits_{S^{n-1} \cap \mathbf{x}^{\perp}} \left(\int_0^{\infty} r^{n-2} \mathsf{c}\left(r\|\mathsf{q}\|_K\right) dr\right) d\mathsf{q} \\
&= \int\limits_{S^{n-1} \cap \mathbf{x}^{\perp}} \left(\int_0^{\frac{1}{\|\mathsf{q}\|_K}} r^{n-2} dr\right) d\mathsf{q} = \frac{1}{n-1} \int\limits_{S^{n-1} \cap \mathbf{x}^{\perp}} \|\mathsf{q}\|_K^{-n+1} d\mathsf{q} \\
&= \frac{1}{n-1} \int\limits_{S^{n-1} \cap \mathbf{x}^{\perp}} \mathsf{r}_K^{n-1}(\mathsf{q}) d\mathsf{q}
\end{aligned}
\tag{1}
$$

If f be an integrable function on $\square^n$, which is also integrable on every hyperplane, then the Radon transform of the function f is defined as a function of $(\mathsf{x};t)$, $\Re\mathsf{f}(\mathsf{x};t) = \int\limits_{\langle x,x \rangle = t} \mathsf{f}(x) dx$, $\mathsf{x} \in S^{n-1}$, $t \in \square$. Using (1), one can express the volume of central hyperplane sections in terms of the spherical Radon transform:

$$
A_{K,\mathbf{x}}(0) = vol_{n-1}(K \cap \mathbf{x}^{\perp}) = \frac{1}{n-1} \Re(\|\cdot\|_K^{-n+1})(\mathbf{x})
\tag{2}
$$

for every origin-symmetric star body K in $\square^n$ and every $\mathsf{x} \in S^{n-1}$. Furthermore, for $(n-1)$-dimensional linear subspaces of $\square^n$, instead of $\mathsf{x}^{\perp}$, the spherical Radon transform is self-dual, means that for any function $f, g \in C(S^{n-1})$;

$$
\int\limits_{S^{n-1}} \Re f(\mathsf{x}) g(\mathsf{x}) d\mathsf{x} = \int\limits_{S^{n-1}} f(\mathsf{x}) \Re g(\mathsf{x}) d\mathsf{x}
\tag{3}
$$

There is a well-known connection between the Radon and Fourier transform:

Lemma 2: [9] For a fixed x, the Fourier transform of the function $g(t) = \Re\mathsf{f}(\mathsf{x};t)$, $t \in \square$ is equal to the function $z \to \hat{\mathsf{f}}(z\mathsf{x})$, $z \in \square$.

The Fourier transform of distributions is the main tool used the proof of Theorem 1 in the sequel. More details about the concepts mentioned in this section can be found in the references [10-15].

3. Application to Medical Imaging

Unfortunately, the transformations applied to medical imaging does not work well on non-uniform networks. For this purpose, several mathematical approaches are used, most notably:

1) Sample a Fourier transform on a polar coordinate grid

2) Interpolation of the polar grid onto a standard rectangular grid

3) Using the Fourier transform in polar coordinates

4) Localization of Radon transform

5) Nonlocalization of Radon transform

And some other methods in [4] and the references therein.

In all ways, the image is the filtered backprojection image using the projections from some angles which are equally spaced. Checking the sequence of the resulting images shows that the progressively improving images have more and more angular projections, until it reaches the image uses projections from the most angles. Each projection has many individual line integrals.

In this way, to preserve the image of its projections in such a way that its properties can be preserved, the following theorem can be proved.

Theorem 1: As above notions, the number of times that the projections from some angles in filtered backprojection image (which are equally spaced and has been assessed by the point lies in quotation hyperplane in projective geometry) can be calculated by the surface area of the convex body and (symplectic) Holmes-Thompson volume in notions of Fourier transform, Finsler metrics and Minkowski spaces.

Proof. Using of Lemma 1, Lemma 2 and self-duality of spherical Radon-transform, relation (3), it can be achieved the connection between the volume of sections of symmetric star bodies and the Fourier transform:

If f be an even homogeneous function of degree $-n+1$ on $\square^{n}$ and continuous on the sphere S^{n-1}, then the Fourier transform of f is even homogeneous of degree -1 and continuous on $\square^{n} \setminus \{0\}$ function such that, for every $\mathsf{x} \in S^{n-1}$, $\Re f(\mathsf{x}) = \int_{S^{n-1} \cap \mathsf{x}^{\perp}} f(\mathsf{q}) d\mathsf{q} = \frac{1}{\mathsf{p}}(\hat{f}(\mathsf{x}))$.

In this way, and by relation (2), it can be concluded that if K is an origin-symmetric star body in $\square^{n}$, then the Fourier transform of the function $\|.\|_{K}^{-n+1}$ is homogeneous of degree -1 function on $\square^{n}$ and continuous on $\square^{n} \setminus \{0\}$ such that, for every $\mathsf{x} \in S^{n-1}$, $A_{K,\mathsf{x}}(0) = vol_{n-1}(K \cap \mathsf{x}^{\perp}) = \frac{1}{\mathsf{p}}(n-1)(\mathsf{F} \ (\|.\|_{K}^{-n+1})(\mathsf{x}))$.

If (V,f) is an n-dimensional Minkowski space and $N \subset V$ is an immersed submanifold of dimension k, $1 \leq k < n$, then the formula for the Holmes-Thompson k-area of N will be

$vol_{k}(N) = \frac{1}{\mathsf{e}_{k}}(\int_{N} \mathsf{f}_{k})$, where e_{k} denotes the volume of the Euclidean unit ball of dimension k,

$\mathsf{f}_{k}(v_{1} \wedge ... \wedge v_{k}) := \int_{(\mathsf{x}_{1} \wedge ... \wedge \mathsf{x}) \in S^{*k}} |\mathsf{x}_{1} \wedge ... \wedge \mathsf{x}_{k}.v_{1} \wedge ... \wedge v_{k}| \breve{\mathsf{f}}_{k}$, S^{*} is any closed hypersurface in $V^{*} \setminus \{0\}$

k that is star-shaped with respect to the origin and $\breve{\mathsf{f}}_{k} = -\frac{1}{4}(2\mathsf{p})^{n-1}(\mathsf{f} \ d\mathsf{x}_{1} \wedge ... \wedge d\mathsf{x}_{n})\big|_{X_{E}}$ is the

$V^{*} \setminus \{0\}$ contraction of standard (distributional) Fourier transform of f with the Euler vector field $X_{E}(\mathsf{x}) = \mathsf{x}$ in V^{*}.

In effect, there exists a smooth, translation-invariant, and possibly signed measure Φ_{n-k} on the manifold H_{n-k} of $(n-k)$-flats of V such that if $N \subset V$ is an immersed k-dimensional submanifold. Then

$$vol_k(N) = \frac{1}{e_k}(\int_{l \in H_{n-k}} \#(N \cap l)\Phi_{n-k}) \qquad [14\text{-}15] \qquad (4)$$

where e_k is the volume of the Euclidean unit ball of dimension k.

Eventually, for a projective Finsler metric j on an open convex domain $D \subseteq \Box P^n$ and a natural number k, $1 \le k \le n-1$, equation (4) is satisfied with D instead of $(V, \|.\|)$, that means

$$vol_k(N) = \frac{1}{e_k}(\int_{x \in H_{n-k}(D)} \#(N \cap l)\Phi_{n-k}).$$

In this way, geometric modeling of medical imaging result in the following correspondence:

the projections from some angles which are equally spaced $\Leftrightarrow$ point lies in quotation hyperplane

the number of times that the projections from some angles which are equally spaced $\Leftrightarrow$ surface area of convex body and (symplectic) Holmes-Thompson volume in notions of Fourier transform, Finsler metrics and Minkowski spaces

low image correctness $\Leftrightarrow$ minimality of the volume in corresponding notions of geometry

In connection with the third correspondence, this should be explained that as the proof of Theorem 1, formula (4) for the Holmes-Thompson volume implies that the tangent spaces of a projective Finsler metric are hypermetric if and only if the measures Φ_{n-k}, $k = 1,...,n$, are projective. Then, just like in the case of the standard Riemannian metric on $\Box P^n$, projective subspaces are area-minimizing.

4. Conclusion

In this paper, a new geometric approach was presented to calculate the number of times that the projections from some angles in filtered backprojection image which are equally spaced using of the surface area of the convex body and (symplectic) Holmes-Thompson volume. In fact, the calculations were made in terms of the volume of the Holmes-Thomson (as the bridge between Finsler geometry, integral geometry, and symplectic geometry). The projections from some angles which are equally spaced, the number of times that the projections from some angles which are equally spaced, and the low image correctness was corresponded to the notions of Finsler geometry. In this way, the proposed geometric approach can provide an appropriate answer to some medical imaging issues in optimum filtered backprojection images.

5. References

1. Olson, T., De Stefano, J. Wavelet localization of the radon transform, IEEE Signal Process, 1994.

2. Olson, T. Optimal time-frequency projections for localized tomography, Ann. Biomed, Eng., 1995.

3. Stanton, A., Wilhelm, CR. On a new kind of rays: translation of a paper read before the Würzburg Physical and Medical Society, Nature. 1895; 253: 274–276.

4. Olson, T., Applied Fourier Analysis: From Signal Processing to Medical Imaging, Springer, 2017.

5. Holmes, RD., Thompson, AC., N-dimensional area and content in Minkowski spaces, Pacific Journal of Mathematics, 1979; 85(1): 77-110.

6. Paiva, JCA, Fernandes, E., Fourier transforms and Holmes-Thompson volume of Finsler manifolds, International Mathematics Research Notices, 1999; 19: 1031-1042.

7. Paiva, JCA, Thompson, AC., Volumes on normed and Finsler spaces, Chapter book of a Sampler of Riemann-Finsler Geometry, Cambridge University Press, 2004, 1-48.

8. Gelfand, IM, Smirnov, M., Lagrangians satisfying Crofton formulas, Radon transforms, and nonlocal differentials, Advances in Mathematics, 1994; 109(2): 188-227.

9. Gromov, M., Filling Riemannian manifolds, Journal of Differential Geometry, 1998; 18(1): 1-147.

10. Rudin, W., Functional Analysis, Mc Graw-Hil., New York, 1973.

11. McDuff, D., Salamon, D., Introduction to symplectic topology, Oxford Mathematical Monographs, Clarendon Press, 1998.

12. Dym, H., McKean HP., Fourier series and Integrals, Academic Press, New York, 1972.

13. Schneider, R, on integral geometry in projective Finsler spaces, Izvestiya Natsional'noĭ Akademii Nauk Armenii. Matematika, 2002; 37: 34-51.

14. Schneider, R., Wieacker, JA, Integral geometry in Minkowski spaces, Advances in Mathematics, 1997; 129(2): 222-260.

15. Paiva, JCA., Fernandes, E., Crofton formulas in Projective Finsler spaces, Electronic Research Announcements of the American Mathematical Society, 1998; 4: 91-100.

Advances in Biotechnology

Chapter 2

Ubiquitous Role of Ribosomal DNA in the Viability of Living Cells and Organisms

Natalia S Kupriyanova[1]; Andrey A Vergun[1,2]; Alexey P Ryskov[1]*

[1]Laboratory of Genome Organization, Institute of Gene Biology of the Russian Academy of Sciences, Vavilova Str., 34/5, Moscow 119334, Russia.

[2]Department of Biochemistry, Molecular biology and Genetics, Moscow State Pedagogical University, M. Pirogovskaya Str., 1/1, Moscow 119991, Russia.

*[*]**Correspondense to: Alexey P Ryskov,** Laboratory of Genome Organization, Institute of Gene Biology of the Russian Academy of Sciences, Vavilova Str., 34/5, Moscow 119334, Russia.*

Tel: +7-495-135-87-41; Email: ryskov@mail.ru, vermand@mail.ru

Abstract

Ribosomes are among the most ancient and important substructures of the cell, retaining the organization of common features in all living organisms. The genes responsible for the synthesis of nucleic acids and proteins that form ribosomes, as well as those that serve the processes of these genes, the maturation of transcription products, and the transition of mature products to the active state, together form the largest polygenic complex, the coordinated work of which depends on the viability of individual cells and the whole body generally. In humans, tandem rDNA clusters are located on the short arms of five acrocentric chromosomes and form the so-called nucleolar organizers (NORs), specific sites of chromosomes where nucleoli form during mitotic telophase. Ribosomal DNA, by its very nature, is susceptible to recombination. Recombination events can result in a change of the repeat copy numbers or in DNA mutations. To prevent these, multiple DNA repair mechanisms are in place to retain rDNA repeat integrity. Here, we examine the literature and our own data on various aspects of

studying the structure and functions of rDNA, particularly the regulatory elements of rRNA transcription; intrachromosomal, interchromosomal, and evolutionary variability; and the characterization of extended genome regions adjacent to rDNA clusters in NOR. In addition, we present new findings on the association of nucleolar stress, cellular dysfunction, and human diseases, including cancer, cardiovascular, neurodegenerative, and autoimmune disorders; and infectious and metabolic disorders. Considerable attention is focused on rDNA in its native state, and on mechanisms providing its variability.

1. Introduction

The growth and division of the bulk of human body cells are tightly connected. Ribosome and protein synthesis are necessary for cell growth and, in return, the control of cell growth is inevitably connected with the control of ribosome formation. rDNA is formed by two zones, one of which encodes the ribosomal RNA (rRNA) precursor (pre-rRNA), and the other the ribosomal intergenic spacer (rIGS). Today, it is clear that the rIGS is a highly complicated structure consisting of functionally specific segments that can be easily transported to different genomic regions. Although the structure and function of rDNA repeating units are rather similar in all vertebrates, the extent of certain features is specific to humans and higher primates [1, 2]. Considerable attention has recently been devoted to rDNA as a whole, and on RNAs being coded in the rIGS. It has turns out that rDNA, while being a factory producing rRNAs, also carries out many important functions, and damage to rDNA can lead to the development of different pathologies.

2. Structural and Functional Organization of Human rDNA

In the human genome, rDNA clusters are placed on acrocentric chromosomes 13, 14, 15, 21, and 22, forming so-called nucleolar organizers (NORs). Structurally, the nucleolus consists of a fibrillary center (FC) surrounded by and associated with dense fibrillar components (DFCs). This construction is embedded in a granular component (GC) composed of granules surrounding the fibrillary components. Many segments similar to rDNA can also be detected on NOR⁻ chromosomes [3]. The peculiarities of ribosome biogenesis and nonribosomal nucleolar functions have become much clearer over the last few years. A number of studies have indicated that the nucleolus has functional activities in ribosomal as well as nonribosomal processes, such as development, aging, cell cycle, gene stability, lifespan regulation, and progeria, to name but a few. Damage to the nucleolar structure and function (nucleolar stress) is often connected with human diseases.

In all vertebrate genomes, rDNA exists in the form of abundant discrete clusters. Tandemly arranged rDNA repeats comprise NORs—specific chromosomal regions where nucleoli form during mitotic telophase. Each rDNA unit consists of a coding region for the rRNA precursor (pre-rRNA) and ribosomal intergenic spacer (rIGS) **(Figure 1).**
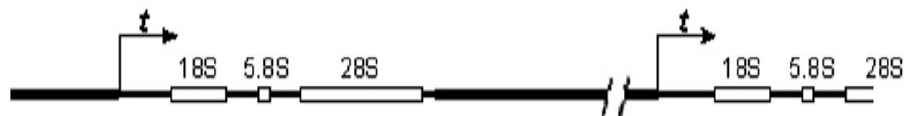

Figure 1: Ribosomal DNA repeat unit organization in mammalian genomes [3].

In **Figure 1**, the rDNA regions coding 18S, 5.8S, and 28S rRNA are represented as white rectangles. Transcribed spacers and rIGS are respectively shown as thin and thick black lines. The transcription start point is denoted as *t*.

The coding region being formed by external transcribed spacer (5'-ETS)–18S rDNA–internal transcribed spacer1 (ITS1)–5.8S rDNA-internal transcribed spacer 2 (ITS2)–28S rDNA–(3'-ETS) is transcribed by RNA polymerase I (Pol I) in the nucleolus as an inextricably linked extensive (40S–47S) pre-rRNA. The mature rRNA molecules (28S, 18S, and 5.8S) are formed after a series of specific endo- and exonucleolytic cleavage reactions. Ribosomal RNA accounts for no less than 80% of total steady-state cellular RNA. In the course of evolution, the length of 18S and 28S rDNA genes and transcribing spacers has increased, but common principles of the structural organization of the transcribing regions has remained invariant [4,5].

In a genome, apart from rDNA clusters, there exist so-called orphans, which are discrete elements similar to rDNA which have diverged from the major rDNA clusters. Evidence in flies and mammals shows that rIGS-like and 18S-like regions form long tandem blocks outside of rDNA clusters [6]. Several rDNA-like sequences were detected on human chromosome 22 at the distal position relative to the rDNA cluster area that included 28S rDNA-like and rIGS similar segments. At the same time, there was an absence of segments homologous to rDNA at the proximal area of the human chromosome 22 rDNA cluster [7, 8].

It is universally accepted that rDNA tandem repeats at five pairs of human chromosomes homogenize as a result of recombination and gene conversion. However, switching on both of these mechanisms can lead to opposite results: the correction of new sequence variants, as well as their propagation over all individual clusters among homologous and nonhomologous chromosomes, and also during the course of interbreeding of different populations. Many scientists have tried to elucidate the question of which mechanism dominates the homogenization process, gene conversion or nonequal crossover, and what exchanges occur most often: intrachromatid, between sister chromatids, or between homologous or nonhomologous chromosomes.

Various contradictory results were obtained. Data were obtained that verify the existence of interchromosomal exchange as a result of nonequal crossover, leading to the origination of variability in the rDNA spacers on nonhomologous chromosomes [9-12] which is enhanced over generations [13]. On the other hand, there are data concerning intrachromosomal exchanges of human rDNA leading to imbalance over generations [14], familiar inheritance of spacer variants according to Mendel [15], and the presence of synteny in the inheritance of human rDNA spacer variants [16]. Today synteny is defined as the conservation of blocks of order within two sets of chromosomes that are being compared with each other.

As mentioned earlier, the transcribing rDNA regions are divided by rIGS. It turned out that rIGS length can vary in the genomes of discrete individuals, just as inside the genome [17-20]. These differences are conditioned by the different numbers of repeats in clusters entering into the rIGS that are generated by different elementary monomers: from thousands of nucleotides to 2–6 nucleotides (microsatellite clusters). Highly polymorphic markers, such as microsatellites (mcs), appear to be the major instruments for making up genetic chromosomal maps and for mapping of disease loci [21-23] **(Table 1).**

Table 1: Frequency of occurrence of seven microsatellite motifs in the ribosomal DNA (rDNA)

Motif	M_p/M	L	M	Q
TCC	0.84	21	124	60
GACA	0.78	23	113	56
GA	0.69	26	110	50
CAC	0.50	36	72	36
GACT	0.42	43	60	30
TCG	0.14	260	10	10
GATG	0.01	2600	1	1

M, total number of cosmid clones; M_p, number of clones hybridized with microsatellite (mcs) probes; L, average spacing between loci (tpn); M, number of concrete loci in rDNA region; Q, number of rDNA copies containing the motif of interest.

Polymorphism of the rDNA nucleotide sequences is defined by the presence of variable zones in the rIGS, as well as by mutations in the transcribing region of rRNA genes. The obtained results suggest relative autonomy of the evolution of nucleotide sequences belonging to the nucleolar organizer. A number of data show that the extent of representation of some functionally important repeats in the pre-promoter region can affect the expression of rRNA genes and, accordingly, the power of the protein synthesizing cell system and, consequently, the common organism status [24, 25].

The other widely distributed type of polymorphism is represented by point mutations, often occurring in the rDNA pre-promoter region. This type of polymorphism has long been

known, and was detected for the first time as a polymorphism of the restriction fragment length manifesting as the result of different restrictions on endonuclease cleavage [26–28]. The high extent of nucleotide replacement in the regions connected with rDNA transcription management changes the specificity of the transcription factors, and provides the molecular mechanisms of species formation during evolution.

Our sequencing study of the 5'- and 3'-ends of recombinant rDNA inserts from the cosmid library of human chromosome 13 revealed that *Sau*3A sites on DNA depleted of protein were not digested stochastically, but that some of them appeared to be hypersensitive to endonuclease attack [29]. A similar phenomenon was observed early on SV40 DNA depleted of protein, but the reason remained unclear [30].

Analysis of the sequences adjacent to hypersensitive digestion sites indicated that, as a rule, they are either incorporated into *Alu* retroposon sequences or are adjacent to them. Many regulatory elements have been identified, including the promoter and terminator sites for RNA polymerase III (Pol III) and the points often used for in vivo rDNA recombination [31–33].

In performing blot hybridization analysis of cosmid clones containing different rIGS fragments of chromosome 13, we detected two clones with huge (10 and 26 tbp) deletions in the rIGS (Figure 2) [34, 35]. The deletion mapping of recombinant inserts in cosmid clones 36G10 and 47H2 after sequencing shows that in both cases, the cut points were located in microsatellite clusters $(TC)_n$, which probably represent unstable genomic loci.
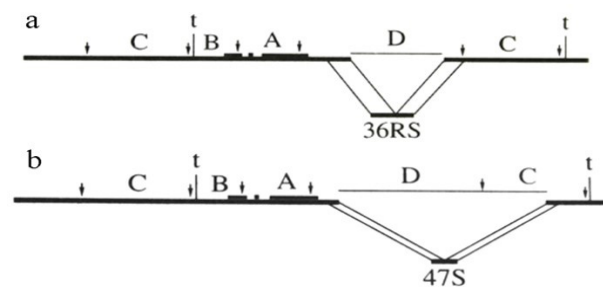

Figure 2: Graphical representation of two clones with huge deletions from the ribosomal intergenic spacer (rIGS) of human chromosome 13 [34, 35].

Comparative fluorescence in situ hybridization (FISH) of genomic DNA with native rIGS fragments and with DNA of the deleted clone 47H2 was also performed. It showed that in mild hybridization conditions, 47H2 binding was observed on all five pairs of acrocentric chromosomes, whereas when more stringent washing-off conditions were used, hybridization only occurred with chromosomes 13 and 21 [36]. This points to the presence of rDNA repeats carrying deletions in the rIGS in the human genome.

The results obtained are evidence of the frequent intrachromosomal homologous and nonhomologous exchanges between coding rRNA and regulatory and distal rDNA regions. There are a number of factors that favor such frequent exchanges between these regions

beyond the dependence of the exchange mechanism. First, the protein nucleolin, which takes an active part in transcription, pre-rRNA processing, and ribosomal maturation, can favor recombination [37, 38]. Second, hypomethylation of the coding and regulatory rDNA regions is also favorable to the activation of rDNA chain exchange [39–42]. Warmerdam et al. [2] have previously proposed that the observed HR-mediated loss of repeats after breaks in the rDNA occurs in trans, through recombination between sisters' chromatids or rDNA repeats on different chromosomes. Unlike in S/G2, homology-dependent repair in G1/G0 might be more prone to occur in cis, by using unrepaired repeats on the same tandem array **(Figure 3).**
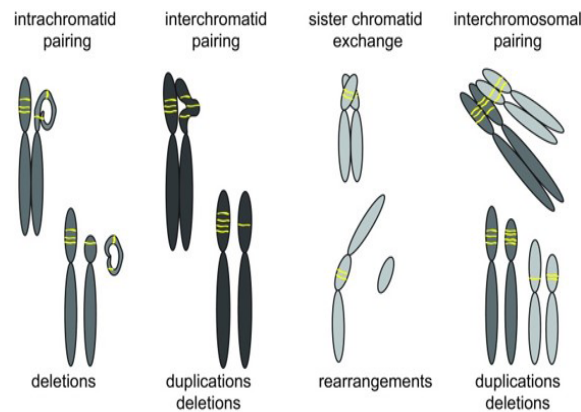

Figure 3: Interactions between chromosomes with repeats that can cause structural chromosomal rearrangements [2]. Repair of repeats can result in repeat expansions, contractions, and structural chromosomal aberrations.

It is also known that human rDNA contains a great many consensus sites for topoisomerase I (TOPO I), particularly in nucleoli on TC-enriching rIGS chains during active rRNA transcription in complexes with Pol I [43, 44]. Recombination under TOPO I participation can assist in homogenization of the regions between TOPO I sites. Also important is the factor of extensive rDNA saturation by $(CT)_n$, $(CTTT)_n$, $(TG)_n$, poly-G, and GC-enriched segments, which is typical for hotspots of recombination [45–47]. It seems reasonable to say that coding and regulatory rDNA regions are homogenized uniformly along the entire length by patching modified segments ("patch-like" manner), whereas rIGS homogenization reveals local characteristics favorable for the formation of homogenous subclusters. Subsequent homologous nonequal exchange between sister chromatids or between homologous and nonhomologous chromosomes can lead to the fixation, increase, or decrease in the number and a loss of blocks containing specific rIGS variants. Clusters in the vicinity of $(CT)_n/(AG)_n$ can assist in fragment homogenization, since it was shown that these sequences can initiate recombination and gene conversion [48].

Evolutionary conservation of the sequences surrounding rDNA clusters suggests that the NORs occupy a chromosome scope beyond proper rDNA, representing a significant capture of subtelomeric space. By cloning the X/21 translocation DNA fragment that is responsible for the development of Duchenne muscular dystrophy, the clones were obtained containing the frontier segment (DJ) between rDNA and adjacent nonribosomal DNA. Using these clones, it was found that transcription from the rDNA cluster on acrocentric chromosome occurs in the

direction of the centromere [49, 50]. The study of DJ-containing clones allowed to determine the primary structure of 8.3 kbp of nonribosomal DNA adjacent to the 5'-end of the head repeat in the rDNA cluster on chromosome 21 [51]. On human chromosome 22, a proximal connecting link between the 3'-end of the rDNA cluster and nonribosomal DNA was also estimated [52]. It enters into the ITS1 and represents a unique 68 bp sequence followed by a tandemly organized cluster formed by 147 bp monomers. This cluster is detected in all acrocentric chromosomes and participates in the formation of genomic repeates of higher order (6.4–6.8 kbp).

3. rDNA Polymorphism and Chromosomal Abnormalities

Variability in the lengths of human rDNA monomers was originally demonstrated by electron microscopy [53]. A link was detected between rRNA gene copy numbers, their transcription activity, and the survival of individuals with a variety of rDNA chromosomal abnormalities and different diseases [54–57]. A number of active ribosomal genes (AcRGs) were estimated to be the cause of chromosomal abnormalities (CAs) in conditions such as Down syndrome (DS), Robertsonian translocation (RT), Klinefelter and Turner syndrome, trisomy X, and disomy. In the control selection of individuals (n = 318), a dozen AcRGs varied at between 119 and 190 copies per diploid genome. In all CA carriers, with the exception of new DS, a dozen AcRGs were not beyond these limits [57]. It was shown earlier that cellular homeostasis and the survival of organisms are only supported when AcRG copy numbers are within these limits, whereas embryos are eliminated when their genomes are characterized by copy numbers outside these limits [56]. It was shown that bearers of structural chromosomal abnormalities can survive only with a relatively high number of AcRGs. These data suggest that the problem of rDNA variability and transcriptional activity correlation with the status of the human body, and this significant observation requires further research for verification.

4. Regulatory Elements of rRNA Transcription

Binding of the rDNA promoter by two Pol I-specific factors, upstream binding factor (UBP) and promoter selectivity factor (SL1), leads to an assembly of the specific multiprotein complex containing Pol I and a number of auxiliary proteins necessary for the initiation of rRNA transcription. UBF activates rRNA transcription by bringing Pol I to the promoter, stabilizing TIF-IB/SL1, and replacing histone H1 [5–7]. UBF can also control promoter release [58] and transcription prolongation [59]. Very often, the rate of cancer cell proliferation correlates with the UBF level [60, 61]. The rate of rRNA transcription is connected with the compatibility between the positive (ERK, mTOR, CBP, c-Myc) and negative (p. 53, Rb, PTEN, ARF, AMPK, GSK3) regulatory pathways of its synthesis [4, 5]. The amount of UBF1 binding to rDNA loci corresponds to the number of transcriptionally active repeats. About 40%–50% of the tandem rDNA repeats are transcribed in normal diploid cells, whereas the rest are present in a state of inactive heterochromatinization. Active and inactive rDNA repeats contain different

histone markers. Inactive rDNA repeats contain repressive markers associated with constitutive heterochromatin. rDNA heterochromatinization is regulated by spacer promoter from the rIGS. The first considerable review devoted to the transcription regulation of ribosomal genes and the assembly of multiprotein complex on rDNA promoter was published in 1995 by Jacob [62]. The number of newly discovered factors in the composition of this multiprotein complex increased markedly, but the essential principles of rRNA transcription regulation have remained unchanged.

Variable rDNA regions can differ according to size, and nucleotide substitutions in both different as well as within the same species. The site of transcription initiation of the 45S pre-rRNA lies within the major core promoter. There is also a spacer promoter upstream of the core promoter (about 2000 bp before), and a spacer terminator (To) adjacent to the core promoter [62–67].

As mentioned above, the joint binding of two Pol I-specific factors with the rDNA promoter, UBF, and SL1 leads to formation of the preinitiation complex [63]. Once more, a group of proteins (TAFI) provides specific binding between the rDNA promoter, UBF, and SL1 that is necessary to support the connection between the Pol I complex and a number of associated proteins (such as actin, myosin, NM1, TIF-IA, PAF53, and TOPOI, as well as IIα, Ku70/80, SIRT7, CK2, and others) [63-71]. These associated proteins can modulate rRNA synthesis in response to various cellular conditions, such as in the case of TIF-IA activity modulation under the action of mTOR. This protein can inactivate TIF-IA, decreasing Ser44 phosphorylation and enhancing Ser199 phosphorylation. The changes in TIF-IA phosphorylation influence transcription complex formation [69-71].

A deficiency of nutrition or growth factors in mammalian cells can decrease significantly (up to 80-90%) rRNA transcription. Various mechanisms are involved to reestablish normal ribosomal biogenesis. Some proteins can modify Pol I to make it incapable of specific initiation [4–13]. One of the proteins involved in this process is Rrn3 [72], which available for reversible association with Pol I. Only 10% of the Pol I molecules in a cell contain Rrn3, which makes connection between Pol I and SL1 [71,72]. Sirtuin 7 (SIRT7) is an NAD-dependent protein deacetylase that is a member of the sirtuin family comprising key mediators of cellular proliferation and oncogenic activity. It influences the rRNA syntesis by monitoring the cell cycle at the control points during diseases and exchange homeostasis, stress tolerance, aging [73,74].

If, in normal cells, rRNA transcription activity is tightly connected with nutrient availability, tumor cells become independent owing to the specific kinase activation, regardless of external signals. It was shown that some protein kinases, such as CK2, ERK, and mTOR, are hyperactivated in carcinogenesis. Pol I-associated CK2 phosphorylates some components of

the Pol I transcription complex, such as TIF-IA, UBF, SL1/TIF-IB, and TOPO I. MAPKs have been observed to activate rRNA synthesis through initiation factors TIF-IA and UBF. Since mTOR inhibition by rapamycin inactivates TIF-IA, it is reasonable that mTOR inhibitors can act as powerful tumor-suppressing substances [70,71]. Rapamycin also affects 18S and 28S rRNA processing, although it remains unknown whether the disruption of rRNA synthesis leads to cell transformation or plays a secondary role in the transformation process.

Analysis of the mouse rIGS region 2000 bp upstream from the transcription start point allowed to detect noncoding a Pol I transcript 150–200 nucleotides, denoted as promoter RNA (pRNA). This molecule binds with TIP5, the large subunit of nucleolar remodeling complex NoRC, suppressing rRNA synthesis [75-77]. Although mammalian rDNA promoters are almost devoid of homology, NoRC-dependent suppression of Pol I transcription was not found to be species-specific. On the contrary, the overexpression of mouse TIP5 suppressed Pol I transcription in mice, as well as in human cells, which was unexpected when considering that NoRC activity is dependent on binding between TIP5 and pRNA complementary to the rDNA promoter [75].

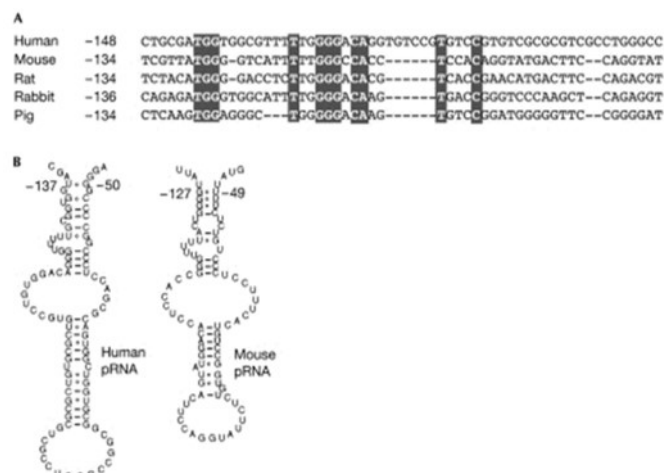**Figure 4** shows a comparison of the promoter and pre-promoter regions of several mammalian ribosomal genes.

Figure 4: (**A**) Alignment of promoter region of various mammalian ribosomal genes. A black background indicates conserved nucleotides. Numbers indicate the positions of nucleotides relative to the transcription start point. The alignment was performed using CLUSTAL W (1.74). (**B**) Secondary structures of human (left) and mouse (right) promoter RNAs (pRNAs) predicted using RNAalifold [75].

5. rDNA Modification and rRNA Transcription

There is a link between the methylation status of the rDNA promoter and rRNA transcriptional activity, which was experimentally verified in various systems [78–82]. What is surprising is that in cells with amplified rDNA, rRNA synthesis activity was not increased, but is elevated upon rDNA demethylation under 5-aza-C action [82]. It was shown that the CpG methylation status in rat rIGS 145 nucleotides upstream of the transcription start point (tsp) can serve as an indicator of gene activity, while CpG methylation in the −133 position in

mouse rIGS impedes it's binding with UBF. It is interesting that in human rIGS, CpG is also present precisely in the positions −145 and −135 [62]. In recent years, age alterations of the ribosomal gene number and the characteristics of their methylation were studied in a number of systems. The age reduction of rDNA quantity in brain and heart tissues was demonstrated using Southern hybridization [83, 84]. The rate of rRNA transcription activity was found to decrease in human fibroblasts in connection with a person's age [85]. This was determined by the calculating the number of Ag-stained NORs. Scientists have shown that cells taken from patients with Werner syndrome grew more slowly and perished, completing only a few divisions, unlike the control [86]. The increased methylation level of rDNA in the cell cultures of patients was considerably higher than in the culture of control cells [87–91]. Thus, rDNA-specific methylation patterns can be used as a marker of a disease or its progression.

The protein coding gene C9ORF72 contains many intronic sequences enriched with microsatellites that are able to expand significantly. The expansion of a GGGGCC repeat in the intronic sequence from 2–22 to 700–1600 copies in transcripts of this gene is associated with 9p-linked amyotrophic lateral sclerosis (ALS) and frontotemporal dementia (FTD) (PMID: 21944778, 21944779). Hexanucleotide expansion resulting in the selective stabilization of repeat-containing pre-mRNA and the accumulation of insoluble dipeptide repeat protein aggregates are most probably pathogenic in FTD/ALS patients [92, 93]. The results obtained suggest that two C9ORF72 gene translation products—GRN from the sense transcript and PRN from the antisense transcript—act to alter information from DNA to mRNA, to protein-poisoning of pre-mRNA splicing, and in the biogenesis of ribosomal RNA. These translation products penetrate cells, bind nucleoli, and kill cells. Exposure of cultured cells to the GR20 and PR20 translation products of C9ORF72 affects both pre-mRNA splicing and the biogenesis of ribosomal RNA. Computational analysis of RNA-seq data also revealed changes in the abundance of a subset of cellular RNAs under the action of the PR20 peptide. Nine PCR primer pairs were designed to study the synthesis and processing of rRNA in detail [92, 93]. Three primer pairs were used to monitor the levels of mature 18S, 5.8S, and 28S rRNAs, and the other six primer pairs were designed to monitor the 45S rRNA precursor. In the cells treated with PR20 peptide, slight reductions in 28S rRNA were observed. Surprisingly, the level of 5.8S rRNA was reduced by 70% under these conditions. These data indicate that peptide treatment of cells presents a severe hazard to ribosomal RNA maturation. Similar results were obtained with brain tissue derived from patients carrying repeat expansions in the C9ORF72 gene. Nucleolar disorders have also been revealed, including delayed processing of the 45S ribosomal RNA precursor. This might mean that these GR20 and PR20 peptides of the hexanucleotide repeats from different disease variants of the C9ORF72 gene behave similarly to cytotoxins that hinder pre-mRNA splicing and the biogenesis of ribosomal RNA [92–94].

6. Disruption of rRNA Biogenesis and Some Human Disorders

We will now discuss the progress made in the latest studies of initiation, mechanisms, and the development of different diseases, and elucidate the participation of ribosomal DNA in these processes.

6.1. Treacher Collins syndrome

Treacher Collins syndrome (TCS) is an autosomal dominant disorder of craniofacial development with a number of features. TCS is caused by mutations in the gene, which encodes the nuclear phosphoprotein treacle. It was detected that a 5 bp deletion in exon 22 of the TCOF1 gene (3469del ACTCT) gives rise to premature stop codon formation [94–96]. Many craniofacial disorders are determined by heterozygous mutations in the regulators of ribosome biogenesis. Genetic perturbations caused by heterozygous mutations in components of the Pol I transcriptional machinery or its cofactor TCOF1 lead to relocalization of nucleolar RNA helicase (DDX21) from the nucleolus to the nucleoplasm, inhibition of rRNA processing, and downregulation of ribosomal protein gene transcription, as well as its loss from chromatin targets. At the molecular level, it was demonstrated that impaired rRNA synthesis occurs as a consequence of the DNA damage response. This means that rDNA damage results in tissue-selective and dose-dependent effects on craniofacial development. The TCOF1 gene product is also involved in pre-rRNA methylation. Defects in craniofacial development result from mutations in the TCOF1 gene. Nucleolar phosphoprotein treacle encoding by the TCOF1 gene interacts with upstream binding factor (UBF) and affects the transcription of rDNA [96]. Treacle participates in $2'$-O-methylation of pre-rRNA. A comparison of rRNA isolated from wild-type mouse embryos and from strains with a lethal phenotype showed significant reduction in $2'$-O-methylation at nucleotide C463 of 18S rRNA. The function of treacle in pre-rRNA methylation is most likely mediated by its immediate interaction with NOP56, a component of the ribonucleoprotein methylation complex. Although treacle co-localizes with UBF throughout mitosis, it also co-localizes with NOP56 and fibrillarin, a putative methyltransferase, only during telophase when rDNA gene transcription and pre-rRNA methylation are known to interact.

6.2. Hodgkin's lymphoma

Hodgkin's lymphoma (HL) is a type of lymphoma in which the cancer originates from lymphocytes. In the last few years, a greater understanding of the peculiarities of different Hodgkin's lymphomas has come to light [97–99]. The morphofunctional characteristics of lymphoma node cells from patients with Hodgkin's disease were obtained by measuring silver-stained nucleolar organizer regions (AgNORs). According to the Rye histological classification of Hodgkin's disease, 3 cases were lymphocyte predominant (LP), the most favorable type, 14 were nodular sclerosing (NS) guarded type, and 15 were mixed cellularity (MC) type [99].

The nucleolar activity of Hodgkin and Reed–Sternberg (HRS) cells was greater in the NS type than in the MC type. The authors explain that the highest expression of interphase rRNA cistrons was found in NS HRS cells by their high proliferative activity and elevated production of transforming growth factor 1, the most effective cytokine present in the NS subtype [97].

6.3. Bloom syndrome

Bloom syndrome [BS] results from mutations in the BLM gene that lead to mutated DNA helicase protein formation [100−102]. The downregulation of cytidine deaminase against the background of genome instability is usually a marker of Bloom syndrome. Synthetic lethal interaction between cytidine deaminase (CDA) and microtubule-associated Tau protein was detected with the use of a genome-wide RNAi screen and transcriptomic profiling [102]. In Tau-deficient HeLa cells, high levels of H2A histone family member X (γ-H2AX) and a large number of induced 53BP1 foci were observed in all cells. Tau downregulation decreases upstream binding factor recruitment and ribosomal RNA synthesis, and affects ribosomal DNA stability. The accompanying depletion of both Tau and CDA proteins intensifies genetic instability and is lethal. This can cause an early cellular response in the induction of double-stranded breaks. Thus, the mechanisms underlying synthetic lethality involve impaired DNA repair and replication processes, and Tau may be regarded as a multifunctional protein whose precise role depends on its localization. As nucleolar regions contain rRNA genes, an important role for Tau in rRNA synthesis was proposed. It was shown that a decrease in Tau expression decreased the level of 45S pre-RNA by attracting UBTF to the rDNA repeats. This allows for the conclusion that Tau binds throughout rDNA loci, with a preference for the promoter and transcriptionally active regions. The high GC content of rDNA loci might make them prone to the formation of G-quadruplex structures, causing arrest or a slowdown in rDNA replication [100]. The mechanisms regulating localization of BLM to the nucleolus are currently under investigation [101,102].

6.4. Senescence

In humans, rDNA instability is caused by a high level of genomic recombination and rearrangements that are involved in premature aging disorders such as Werner and Bloom syndromes [103]. SIRT7 is a member of the mammalian sirtuin family of proteins, acting as a multifunctional chromatin regulator via deacetylation of histone H3K18ac [104]. It can be activated by double-steanded DNA breaks. Nucleolar SIRT7 is implicated in the regulation of rDNA transcription [104−106]. SIRT7-dependent heterochromatin silencing protects against cellular senescence [103].

Transcription of rDNA loci is essential for cell viability in mammals [105], and SIRT7 activates this process. In a new study, Paredes et al. [107] show that SIRT7 can have an opposite effect under the action of SNF2H, a member of the ATP-dependent chromatin remodeling

complex SWI/SNF. This interaction leads to specific silencing of rDNA promoter regions. Cells lost about 50% of their rDNA copies and depletion of SIRT7 led to increased rDNA damage and overall disruption of nucleolar integrity, and more rapid senescence. Subsequent studies have shown that another mammalian sirtuin, SIRT6, also interacts with SNF2H at sites of double-stranded breaks (DSBs), promoting DNA repair [108]. SIRT7 acts on H3K18 and SIRT6 acts on H3K56, influencing their localization. This demonstrates a critical role for SIRT7 in complex with SNF2H in maintaining heterochromatic regions to protect rDNA loci from the rearrangements that are connected with aging and related pathologies. These findings identify rDNA instability as a driver of mammalian cell senescence and implicate SIRT7-dependent heterochromatin silencing in protecting against this process [108,109].

6.5. Cancer

The transcription of rRNA genes and maturation of rRNA are important in the intricate processes of cell growth and proliferation control. It has become clear that changes in rDNA activity can be an important cause of tumorigenesis. This means that cancerous tumors may be attacked using strategies aimed at specific targets. The use of anticancer medicines at the stage of Pol I transcription may become necessary in the immediate future. One increasingly important strategy involves the development of new substances that selectively suppress Pol I transcription in rapidly proliferating cells without injuring healthy tissues.

Recent studies have highlighted the role of ribosomal pathologies in a variety of animal models for diseases associated with cell growth and cell cycle control, and many other diseases. It is now clear that the disruption of ribosome biogenesis causes nucleolar stress that triggers the p53 signaling pathway. Two alternatives have been studied over ca. 20 years regarding the relationship between the priority of cancer transformation and nucleolar function. It is known that protein synthesis consistently increases during cellular neoplastic transformation [62,110–114]; transformed cells produce oncogenic proteins and tumor-suppressor proteins (P53, C-MYC, etc.) [69–71]; and polymerase I transcription of rRNA genes is negatively regulated by tumor oncogenes and suppressor genes [72, 73]. Recently, a number of studies were dedicated to the nucleolar functions in tumors. As long as the majority of cancer cells display a large size and/or increased numbers of nucleoli, nucleolar size can be used for many cancers as a parameter for predicting the prognosis of a tumor, with increasing size corresponding to worse prognosis [62]. rDNA copy number fluctuations and their instability has been shown to result from a disruption in H3.3 deposition and, thus, a failure in heterochromatin formation at rDNA repeats as a result of the absence of ATRX (ATP-dependent helicase ATRX, X-linked helicase II). ATRX-depleted cells have a reduced output of rRNA transcription. Such cells display increased sensitivity to the RNA polymerase I (Pol I) transcription inhibitor CX5461 [112–114]. In addition, human alternative lengthening of telomeres (ALT)-positive cancer cell lines are also more sensitive to CX5461 activity [115-119].

6.6. Neurodegenerative diseases

Several studies performed in the past two decades have indicated that diseases associated with deregulated ribosomal biogenesis result from functional mutations in the nucleolar constituent of the ribosome or factors closely associated with polymerase I (Pol I), collectively named ribosomopathies [31,32]. The most important issue is to identify factors influencing disease onset and progression.

Nucleolar proteins such as nucleolin (Ncl), nucleostemin (NS), nucleophosmin (NPM), and fibrillarin (Fbl) are involved in both cell homeostasis and disease. NS protein, for example, plays a pivotal role in processes such as maintenance of stem cell pluripotency, regulation of telomere length, inhibition of stem cell differentiation, senescence, control of pre-rRNA processing, cell death, and others [120,121]. Neuronal nucleolar stress, a cause of neurodegenerative disorders including Alzheimer's disease (AD), Parkinson's disease, Huntington disease, and many others, has been investigated by numerous researchers [122–127]. In neurodegenerative diseases, nucleolin plays an important role because depriving the rRNA promoter of this histone chaperone downregulates rRNA transcription [128–133]. Abnormal interaction with nucleolin also accounts for oculomotor apraxia type 1, a neurological disorder caused by mutated aprataxin. Abnormalities in the nucleolus are also a cause of spinocerebellar ataxia, an inherited disorder caused by CAG or CTG expansion [134,135]. In these neurodegenerative diseases, nucleolin appears to play a role because rRNA transcription downregulation arises from depriving the rRNA promoter of this histone chaperone by CAG RNAs [136,137]. Several studies have shown that the transcription of rRNA genes is altered in Huntington disease (HD). A protein inhibiting the transcription of both rRNA and ribosomal protein genes (Rrs1) was highly expressed in a presymptomatic HD mouse model [132]. The level of factor UBF1 is tightly connected with RNA polymerase I, and was decreased in cellular and animal HD models [133]. In post-mortem specimens of human HD cases, insoluble aggregates of huntingtin were found in the nucleolus [134].

DNA-damaging response (DDR) proteins, which operate in the nucleus, also play a role in nucleolar repair. The number of studies on nucleolar stress in neurodegenerative diseases is rapidly growing [124]. Silencing of rDNA during the early stage of AD plays a role in AD-related ribosomal deficit with subsequent dementia [122,128]. Differential methylation activity of rDNA is a possible mechanism causing decreased rDNA gene expression in AD patients. A specific methylation pattern could be used as a marker for AD detection and for tracing the course of the disease. Post-mortem brain tissue revealed the disruption of dopaminergic neurons in Parkinson's disease [122,123].

During the passing of neural lineage, there is no direct evidence that rRNA transcription is inhibited, but there is indirect evidence that nucleolar-correlated mechanisms could take

part in this process. For example, in brain and retina, the level of the nucleolar protein nucleostemin-a controller of pre-rRNA processing-is rapidly reduced prior to cell cycle exit and neural differentiation [123]. As far as impaired mitochondrial activity affects nucleolar function, it supports the concept that nucleolar stress may occur at early disease stages, contributing to pathogenesis. It also takes place in the nucleolus in spinocerebellar ataxia, an inherited disorder caused by CAG or CTG expansion [134,135].

Recently, mouse models were developed in which nucleolar function was specifically impaired by genetic removal of TIF-IA, a conserved transcription factor essential for the recruitment of Pol I to rRNA promoters. Since its identification, it became evident that TIF-IA activity is strongly dependent on external signals [138]. Today, it is known that TIF-IA is regulated by a variety of protein kinases at distinct serine residues: ERK and RSK in response to mitogenic signals [139], S6K in response to growth stimuli, JNK2 in response to oxidative stress [140], AMPK in response to cellular energy status, and PERK-dependent phosphorylation in response to endoplasmic reticulum stress [141]. It is also known now that proteasome activity is necessary for pre-rRNA synthesis, and TIF-IA may represent a potential link between proteasomes and rRNA genes.

7. rDNA and Epigenetic Genome Regulation

With a general increase in interest in the organization and functional role of rDNA in the genome, different research groups are focusing on various aspects of this role. Above, we discussed the significance of rDNA representation in genomes in the development of such diseases as Down syndrome, Treacher Collins syndrome, Bloom syndrome, neurodegenerative diseases, cancer, CA abnormalities, to name but a few. Nuclei also perform important functions such as in cell cycle regulation and stress response. In particular, several stress-induced loci localized in the rIGS produce noncoding nucleolar RNAs specific for the state of stress. By mapping the 5′- and 3′-ends of such responsible IGS (srIGS) segments scattered across NOR$^+$ chromosomes, we found that the links in srIGSs most frequently subjected to breaks are adjacent to or overlap with stress-induced loci [3].

Recently, Churikov and co-authors revealed connections between the hotspots of double-stranded breaks (DSBs) in rDNA and gene expression in chromosomal domains [142]. The authors showed that double-stranded DNA breaks are involved in coordinated local gene expression. These 50–150 tbp DNA domains (designated as forum domains) can be visualized by separating nondigested genomic DNA in agarose pulsed-field gel electrophoresis [143] and used for large-scale mapping of DSBs in the genome. Nine DSB hotspots were found in human rDNA genes, which coincided with the binding sites of the CTCF and H3K4me3 markers [144], implying the participation of DSBs in active transcription. In this work, DSBs were mapped in the chromosomes of human HEK293T cells, and a bioinformatics analysis

of the data in Gene Expression Omnibus (number GSE53811) was carried out in accordance with the data from [145]. The findings show that H3K4me3 markers often coincide with DSB hotspots in HEK293T cells and that mapping of these hotspots is important for the research on genomes affected by cancer. Data of 4C analysis of rDNA show that the regions containing DSB hotspots can often bind to specific regions of different chromosomes, including the pericentromeric regions, the binding regions of some histone markers, as well as the binding sites of CTCF, ChIA-PET, and RIP signals. The results suggest a close relationship between chromosome breaks and some mechanisms of epigenetic regulation of gene expression [146-148].

As noted above, eukaryotic cells contain several hundred rRNA genes, some of which are disabled by epigenetic mechanisms. Extensive research has revealed the details of these mechanisms and shown how DNA methyltransferase and histone-modifying enzymes work consistently with chromatin remodeling complexes [149,150]. It was also possible to identify the participation of noncoding RNAs in the mechanism of formation of a specific chromatin structure which determines the transcriptional status of rRNA genes. These studies indicate the existence of complex links between various participants in epigenesis when the chromatin structure changes during the process of activating and deactivating genes. It has become clear that constitutive heterochromatin (GC) is a dynamic and transcriptionally active part of the genome that is important for its stability. In human cells, the main GC clusters are localized at centromeres, telomeres, and rRNA genes. Despite differences in biological function, telomeres, centromeres, and rRNA genes possess characteristic heterochromatic features necessary to maintain nuclear structure and function under normal conditions [151–153].

It has been shown that the switch between active and inactive states of rRNA genes is regulated by NoRC, a chromatin remodeling complex that includes the ATPase SNF2h and the large TIP5 subunit. The direction of NoRC to rDNA establishes de novo histone modifications and DNA methylation, which leads to chromatin compaction and transcriptional silencing of the rDNA repeat fraction. Thus, NoRC combines several enzymatic processes that fix repressive chromatin structures on the rDNA promoter [153]. The consolidation of such chromatin structures at centromeres and telomeres is vital for the integrity of the kinetochore and protection of the ends of the chromosomes; in other words, the protection of chromosome stability. Considering the structural similarity of centromeres, telomeres, and rRNA genes leads to the conclusion that the functions of the NoRC complex are not limited to suppressing the activity of rRNA genes, and that it can play an important role in organizing higher-order chromatin structures at other clusters of repeating sequences. This assumption is confirmed by the results of immunoprecipitation and FISH experiments, which show that, in addition to the nucleoli, NoRC is localized at the ends of the chromosomes and at centromeric repeats. Tip5 knockdown resulted in reduced histone modification in pericentromeres, telomeres, and

subtelomeres, allowing for the definitive conclusion that NoRC has a direct effect on chromatin in these repeating sequences. Although further research is needed to study the mechanism and the results of NoRC function in the regulation of chromatin structure and genomic stability, the fact that NoRC participates in the formation and maintenance of the repressive chromatin conformation in the main genomic clusters of repeating sequences implies its important role in maintaining the structure and function of the genome [149–151].

Noncoding RNAs also play a key role in the formation of functional subcompartments of the nucleus [152]. Using fluorescence microscopy and deep sequencing, it was shown that the nucleolus is enriched with Pol II transcripts of intron *Alu* elements (aluRNA). Inhibition of RNA polymerase II or exhaustion of aluRNA by antisense oligos led to the destruction of nucleolus structure and disrupted the transcription of rRNA genes dependent on RNA polymerase I. On the contrary, overexpression of aluRNA resulted in an increase in the size of the nucleolus and the level of pre-rRNA, which suggests a functional relationship between aluRNA and nucleolus integrity and rRNA synthesis. It is also shown that aluRNAs interact with nucleolin and direct individual segments of the genome to the nucleolus. The obtained results suggest the existence of a mechanism that ensures the interaction of RNA polymerases I and II with the participation of aluRNA and modulates the nucleolus structure and the production of rRNA [152–155].

8. Conclusions

Until 2000, the nucleolus had been considered as an organelle solely involved in ribosome biosynthesis. Ribosomes, the molecular factories that carry out protein synthesis, are essential for every living cell. At the same time, due to the discovery of more nucleolar functional activities, researchers all over the world have provided new insights into the role of the nucleolus as a signaling hub that is important in maintaining cellular homeostasis and lifespan and that may also cause human diseases. The variable rDNA regions differ in size and sequence among organisms and within individual species. A trend has appeared in recent years to develop many novel findings concerning various aspects of ribosome biogenesis in cell growth and cell cycle control. Defects in ribosome biogenesis have also been linked to human diseases. It is now clear that the disruption of ribosome biogenesis causes nucleolar stress that triggers a p53 signaling pathway, thus providing cells with a surveillance mechanism for monitoring ribosomal integrity. The association of nucleolar stress, cellular dysfunction, and human diseases, including cancer; cardiovascular, neurodegenerative, and autoimmune disorders; and infectious and metabolic disorders has become an important research topic. In addition, identifying potentially new risk factors may also help in the development of novel therapeutic lines of attack and new therapeutic approaches for the treatment of diseases.

9. Funding

10. Conflicts of Interest: The authors declare no conflict of interest.

11. References

1. Gonzalez, I.L.; Sylvester, J.E. Human rDNA: Evolutionary patterns within the genes and tandem arrays derived from multiple chromosomes. Genomics 2001, 73, 255–263, doi:10.1006/geno.2001.6540.

2. Warmerdam, D.O.; Wolthuis, R.M. Keeping ribosomal DNA intact: A repeating challenge. Chromosome Res. 2019, 27, 57–72, Doi: 10.1007/s10577-018-9594-z.

3. Kupriyanova, N.S.; Netchvolodov, K.K.; Sadova, A.A.; Cherepanova, M.D., Ryskov, A.P. Non-canonical ribosomal DNA segments in the human genome, and nucleoli functioning. Gene. 2015, 572, 237-242, doi:10.1016/j.gene.2015.07.019.

4. Gonzalez, I.L.; Chambers, C.; Gorski, J.L.; Stambolian, D.; Schmickel, R.D.; Sylvester, J.E. Sequence and structure correlation of human ribosomal transcribed spacers. J. Mol. Boil. 1990, 212, 27–35, doi:10.1016/0022-2836(90)90302-3.

5. Grummt, I. Life on a planet of its own: Regulation of RNA polymerase I transcription in the nucleolus. Genes Dev. 2003, 17, 1691–1702, doi:10.1101/gad.1098503R.

6. Kominami, R.; Muramatsu, M. Amplified ribosomal spacer sequence: Structure and evolutionary origin. J. Mol. Boil. 1987, 193, 217–222.

7. Gonzalez, I.L.; Sylvester, J.E. Beyond ribosomal DNA: On towards the telomere. Chromosoma 1997, 105, 431–437.

8. Sakai, K.L.; Ohta, T.; Minoshima, S.; Kudoh, J.; Wang, Y.; de Jong, P.J.; Shimizu, N. Human ribosomal RNA gene cluster: Identification of the proximal end containing a novel tandem repeat sequence. Genomics 1995, 26, 521–526.

9. Krystal, M.; D'Eustachio, P.; Ruddle, F.H.; Arnheim, N. Human nucleolus organizers on nonhomologous chromosomes can share the same ribosomal gene variants. Proc. Natl. Acad. Sci. USA 1981, 78, 5744–5748, doi:10.1073/pnas.78.9.5744.

10. Long, E.O.; Dawid, I.B. Repeated genes in eukaryotes. Annu. Rev. Biochem. 1980, 49, 727–764.

11. Ranzani, G.N.; Bernini, L.F.; Crippa, M. Inheritance of rDNA spacer length variants in man. Mol. Gen. Genet. 1984, 196, 141–145.

12. Gonzalez, I.L.; Gorski, J.L.; Campen, T.J.; Dorney, D.J.; Erickson, J.M.; Sylvester, J.E.; Schmickel, R.D. Variation among human 28S ribosomal RNA genes. Proc. Natl. Acad. Sci. USA 1985, 82, 7666–7670, doi:10.1073/pnas.82.22.7666.

13. Schmickel, R.D.; Gonzalez, I.L.; Erickson, J.M. Nucleolus organizing genes on chromosome 21: Recombination and nondisjunction. Ann. N. Y. Acad. Sci. 1985, 450, 121–131. doi:10.1073/pnas.82.22.7666.

14. Seperack, P.; Slatkin, M.; Arnheim, N. Linkage disequilibrium in human ribosomal genes: Implications for multigene family evolution. Genetics 1988, 119, 943–949.

15. Garkavtsev, I.V.; Tsvetkova, T.G.; Yegolina, N.A.; Gudkov, A.V. Variability of human rRNA genes: Inheritance and nonrandom chromosomal distribution of structural variants of nontranscribed spacer sequences. Hum. Genet. 1988, 81,

31–37.

16. Wimmer, K.; Thoraval, D.; Kuick, R.; Lamb, B.J.; Hanash, S.M. Identification of amplifications, deletions, and methylation changes in cancer by means of two-dimensional analysis of genomic digests: application to neuroblastoma. Biochem Soc Trans. 1997, 25, 262-267.

17. Kupriyanova, N.S. Conservativity, and Variability of the ribosomal DNA in eukaryotes. Mol. Biol. 2000, 34, 753–765.

18. Kupriyanova, N.S.; Popenko, V.; Eisner, G.; Vengerov, Y.; Timofeeva, M.; Tikhonenko, A.; Skryabin, K.; et al. Organization of loach ribosomal genes (Misgurnus fossilis L.) Mol. Biol. Rep. 1982, 8, 143–148.

19. Arnheim, N.; Calabrese, P. Understanding what determines the frequency and pattern of human germline mutations. Nat Rev Genet. 2009, 10, 478-488, doi: 10.1038/nrg2529.

20. Naylor, SL.; Sakaguchi, A.Y.; Shen, L.P.; Bell, G.I.; Rutter, W.J.; Shows, T.B. Polymorphic human somatostatin gene is located on chromosome 3. Proc. Natl. Acad. Sci. USA 1983, 80, 2686–2689, doi:10.1073/pnas.80.9.2686.

21. Wimmer, K.; Thoraval, D.; Asakawa, J.; Kuick, R.; Kodaira, M.; Lamb, B.; Fawcett, J.; et al. Two-dimensional separation and cloning of chromosome 1 NotI-EcoRV-derived genomic fragments. Genomics. 1996, 38, 124-132.

22. Braga, E.A.; Kapanadze, B.I.; Kupriyanova, N.S.; Ivanova, G.M.; Brodyansky, V.M.; Netchvolodov, K.K.; Shkutov, G.A.; et al. Analysis of distribution of the 7 microsatellite motives entering into cosmids' composition of the ordered clonotec of the human 13 chromosome. Mol. Biol. 1995, 29, 1001–1010.

23. Kupriyanova, N.S.; Netchvolodov, K.K.; Kirilenko, P.M.; Kapanadze, B.I.; Yankovsky, N.K.; Ryskov, A.P. Intragenomic polymorphisms of the ribosomal RNA genes of the human chromosome 13. Molec. Biol. 1996, 30, 51–60.

24. Dvorak, J.; Akhunov, E.D.; Akhunov, A.R.; Deal, K.R.; Luo, M.C. Molecular characterization of a diagnostic DNA marker for domesticated tetraploid wheat provides evidence for gene flow from wild tetraploid wheat to hexaploid wheat. Mol. Biol. Evol. 2006, 23, 1386–1396, doi:10.1093/molbev/msl004.

25. Saintenac, C.; Jiang, D.; Akhunov, E.D. Targeted analysis of nucleotide and copy number variation by exon capture in allotetraploid wheat genome. Genome Biol. 2011, 12, R88, doi: 10.1186/gb-2011-12-9-r88.

26. Kuick, R.; Asakawa, J.; Neel, J.V.; Kodaira, M.; Satoh, C.D.; Gonzalez, I.L.; Hanash, S.M. Studies of the inheritance of human ribosomal DNA variants detected in two-dimensional separations of genomic restriction fragments. Genetics 1996, 144, 307–316.

27. Arnheim, N.; Strange, C.; Erlich, H. Use of pooled DNA samples to detect linkage disequilibrium of polymorphic restriction fragments and human disease: Studies of the HLA class II loci. Proc. Natl. Acad. Sci. USA 1985, 82, 6970–6974, doi:10.1073/pnas.82.20.6970.

28. Wilson, G.N.I.; Mian, A.; de Chadarévian, J.P.; Vekemans, M. Effect of aneuploidy and neoplasia on human ribosomal DNA inheritance. Am. J. Med. Genet Suppl. 1987, 3, 121–132.

29. Kupriyanova, N.S.; Kirilenko, P.M.; Netchvolodov, K.K.; Ryskov, A.P. Preferential cleavage sites for Sau3A restriction endonuclease in human ribosomal DNA. Biochem. Biophys. Res. Commun. 2000, 274, 11–15, doi:10.1006/bbrc.2000.3088.

30. Nedospasov, S.A.; Georgiev, G.P. Non-random cleavage of SV40 DNA in the compact minichromosome and free in solution by micrococcal nuclease. Biochem. Biophys. Res. Commun. 1980, 92, 532–539.

31. Längst, G.; Schätz, T.; Langowski, J.; Grummt, I. Structural analysis of mouse rDNA: Coincidence between nuclease hypersensitive sites, DNA curvature and regulatory elements in the intergenic spacer. Nucleic Acids Res. 1997, 25,

511–517, doi:10.1093/nar/25.3.511.

32. Saikawa, Y.; Kaneda, H.; Yue, L.; Shimura, S.; Toma, T.; Kasahara, Y.; Yachie, A.; et al. Structural evidence of genomic exon-deletion mediated by Alu-Alu recombination in a human case with heme oxygenase-1 deficiency. Hum. Mutat. 2000, 16, 178–179, doi: 10.1002/1098-1004(200008)16:2<178:: AID-HUMU16>3.0.CO;2-X.

33. Alafuzoff, I.; Koivisto, A.M.; Lehtovirta, M.; Pirskanen, M.; Sulkava, R.; Verkkoniemi, A.; Soininen, H. Identification of a novel 4.6-kb genomic deletion in presenilin-1 gene which results in exclusion of exon 9 in a Finnish early onset Alzheimer's disease family: An Alu core sequence-stimulated recombination? Eur. J. Hum. Genet. 2000, 8, 259–266, doi:10.1038/sj.ejhg. 5200423.

34. Kupriyanova, N.S.; Shibalev, D.V.; Voronov, A.S.; Ryskov, A.P. PCR-generated artificial ribosomal DNAs from premature termination at Alu sequences Biomol. Eng. 2004, 21, 21–25.

35. Kirilenko, P.M.; Kupriyanova, N.S.; Ryskov, A.P. Revealing, and characteristic of prolonged deletions in cosmid clones of the ribosomal DNA of human chromosome 13. Dokl. Biochem. Biophys. 2003, 388, 55–59.

36. Kupriyanova, N.S.; Shibalev, D.V.; Voronov, A.S.; Muravenko, O.V.; Zelenin, A.V.; Ryskov, A.P. Segmental duplications in subtelomeric regions of the human chromosome 13. Mol. Biol. 2003, 37, 221–227.

37. Thyagarajan, B.; Lundberg, R.; Rafferty, M.; Campbell, C. Nucleolin promotes homologous DNA pairing in vitro. Somat. Cell Mol. Genet. 1998, 24, 263–272.

38. Hanakahi, L.A.I.; Dempsey, L.A.; Li, M.J.; Maizels, N. Nucleolin is one component of the B cell-specific transcription factor and switch region binding protein, LR1. Proc. Natl. Acad. Sci. USA 1997, 94, 3605–3610, doi:10.1073/ pnas.94.8.3605.

39. Brock, G.J.; Bird, A. Mosaic methylation of the repeat unit of the human ribosomal RNA genes. Hum. Mol. Genet. 1997, 6, 451–456, doi:10.1093/hmg/6.3.451.

40. Shiraishi, M.; Sekiguchi, A.; Chuu, Y.H.; Sekiya, T. Alteration of mosaic methylation of the repeat unit of the human ribosomal RNA genes in lung cancer. Biol. Chem. 1999, 380, 81–84.

41. Monk, M.; Boubelik, M.; Lehnert, S. Temporal and regional changes in DNA methylation in the embryonic, extraembryonic and germ cell lineages during mouse embryo development. Development 1987, 99, 371–382.

42. Jiang, C.; Liao, D. Striking bimodal methylation of the repeat unit of the tandem array encoding human U2 snRNA (the RNU2 locus). Genomics 1999, 62, 508–518, doi:10.1006/geno.1999.6052.

43. Zhang, H.; Wang, J.C.; Liu, L.F. Involvement of DNA topoisomerase I in transcription of human ribosomal RNA genes. Proc. Natl. Acad. Sci. USA 1988, 85, 1060–1064, doi:10.1073/pnas.85.4.1060.

44. Rose, K.M.; Szopa, J.; Han, F.S.; Cheng, Y.C.; Richter, A.; Scheer, U. Association of DNA topoisomerase I and RNA polymerase I: A possible role for topoisomerase I in ribosomal gene transcription. Chromosoma 1988, 96, 411–416.

45. Htun, H.I; Dahlberg, J.E. Topology and formation of triple-stranded H-DNA. Science 1989, 243, 1571–1576.

46. Katzenberg, D.R.; Tilley, S.A.; Birshtein, B.K. Studies of the inheritance of human ribosomal DNA variants detected in two-dimensional separations of genomic restriction fragments. Mol. Cell Biol. 1989, 9, 1324–1326, doi:10.1128/ mcb.9.3.1324.

47. Wahls, W.P.; Wallace, L.J.; Moore, P.D. Hypervariable minisatellite DNA is a hotspot for homologous recombination in human cells. Cell 1990, 60, 95–103.

48. Liao, D.I; Weiner, A.M. Concerted evolution of the tandemly repeated genes encoding primate U2 small nuclear RNA (the RNU2 locus) does not prevent rapid diversification of the (CT) n/ (AG)n microsatellite embedded within the U2 repeat unit. Genomics 1995, 30, 583–593, doi:10.1006/geno.1995.1280.

49. Worton, R.G.; Sutherland, J.; Sylvester, J.E.; Willard, H.F.; Bodrug, S.; Dubé, I.; Duff, C.; et al. Human ribosomal RNA genes: Orientation of the tandem array and conservation of the 5' end. Science 1988, 239, 64–68.

50. Worton, R.G.; Thompson, M.W. Genetics of Duchenne muscular dystrophy. Annu. Rev. Genet. 1988, 22, 601–629, doi:10.1146/annurev.ge.22.120188.003125.

51. Bailey, J.A.; Gu, Z.; Clark, R.A.; Reinert, K.; Samonte, R.V.; Schwartz, S.; Adams, M.D.; et al. Recent segmental duplications in the human genome. Science 2002, 297, 1003–1007, doi:10.1126/science.1072047.

52. Kobayashi, N.; Masuda, J.; Kudoh J.; Shimizu N.; Yoshida T. Binding sites on tau proteins as components for antimicrobial peptides. Biocontrol Sci. 2008, 13(2), 49−56.

53. Wellauer, P.K.; Dawid, I.B. Isolation and sequence organization of human ribosomal DNA. J. Mol. Biol. 1979, 128, 289–303.

54. Bierhoff, H.; Schmitz, K.; Maass, F.; Ye, J.; Grummt, I. Noncoding transcripts in sense and antisense orientation regulate the epigenetic state of ribosomal RNA genes. Cold Spring Harb Symp Quant Biol. 2010, 75, 357−364, doi:10.1101/sqb.2010.75.060.

55. Grummt I. Different epigenetic layers engage in complex crosstalk to define the epigenetic state of mammalian rRNA genes. Hum Mol Genet. 2007, 1(R1), 21-27, doi:10.1093/hmg/ddm020.

56. Safrany, G.; Hidvegi, E.J. New tandem repeat region in the non-transcribed spacer of human ribosomal RNA gene. Nucleic Acids Res. 1989, 17, 3013–3022, doi:10.1093/nar/17.8.3013.

57. Lyapunova, N.A.; Porokhovnik, L.N.; Kosyakova, N.V.; Mandron, I.A.; Tsvetkova, T.G. Effects of the copy number of ribosomal genes (genes for rRNA) on viability of subjects with chromosomal abnormalities. Gene 2017, 611, 47–53, doi:10.1016/j.gene.2017.02.027.

58. Panov, K.I.; Friedrich, J.K.; Russell, J.; Zomerdijk, J.C. UBF activates RNA polymerase I transcription by stimulating promoter escape. EMBO J. 2006, 25, 3310–3322, doi:10.1038/sj.emboj.7601221.

59. Stefanovsky, V.; Langlois, F.; Gagnon-Kugler, T.; Rothblum, L.I.; Moss, T. Growth factor signaling regulates elongation of RNA polymerase I transcription in mammals via UBF phosphorylation and r-Chromatin remodeling. Mol. Cell. 2006, 21, 629–639, doi:10.1016/j.molcel.2006.01.023.

60. Derenzini, M.; Trere, D.; Pession, A.; Montanaro, L.; Sirri, V.; Ochs, R.L. Nucleolar function and size in cancer cells. Am. J. Pathol. 1998, 152, 1291–1299.

61. Hannan, K.M.; Rothblum, L.I.; Jefferson, L.S. Regulation of ribosomal DNA transcription by insulin. Am. J. Physiol. 1998, 275, C130–C138, doi:10.1152/ajpcell.1998.275.1.C130.

62. Jacob, S.T. Regulation of ribosomal gene transcription. Biochem. J. 1995, 306 Pt 3, 617–626, doi: 10.1042/bj3060617.

63. Learned, R.M.; Learned, T.K.; Haltiner, M.M.; Tjian, R.T. Human rRNA transcription is modulated by the coordinate binding of two factors to an upstream control element. Proc. Natl. Acad. Sci. USA 1983, 80, 3558–3562, doi:10.1073/pnas.80.12.3558.

64. Clos, J.; Buttgereit, D.; Grummt, I. A purified transcription factor (TIF-IB) binds to essential sequences of the mouse rDNA. Proc. Natl. Acad. Sci. USA 1986, 83, 604–608, doi:10.1073/pnas.83.3.604.

65. Paule, M.R. Polymerase I transcription, termination, and processing. Gene Expr. 1993, 3, 1–9.

66. Pape, L.K.; Windle, J.J.; Sollner-Webb, B. Half helical turn spacing changes convert a frog into a mouse rDNA promoter: A distant upstream domain determines the helix face of the initiation site. Genes Dev. 1990, 4, 52–62, doi:10.1101/gad.4.1.52.

67. Russell, J.; Zomerdijk, J.C. RNA-polymerase-I directed rDNA transcription, life and works. Trends Biochem. Sci. 2005, 30, 87–96, doi:10.1016/j.tibs.2004.12.008.

68. Dixit, A.; Garg, L.C.; Chao, W.; Jacob, S.T. An enhancer element in the far upstream spacer region of rat ribosomal RNA gene. J. Biol. Chem. 1987, 262, 11616–11622.

69. Mayer, C.; Zhao, J.; Yuan, X.; Grummt, I. MTOR-dependent activation of the transcription factor TIF-IA links rRNA synthesis to nutrient availability. Genes Dev. 2004, 18, 423–434, doi:10.1101/gad.285504.

70. Hidalgo, M.; Rowinsky, E.K. The rapamycin-sensitive signal transduction pathway as a target for cancer therapy. Oncogene 2000, 19, 6680–6686, doi:10.1038/sj.onc.1204091.

71. Rothblum, L.I.; Rothblum, K.; Chang, E. PAF53 is essential in mammalian cells: CRISPR/Cas9 fails to eliminate PAF53 expression. Gene 2017, 612, 55–60, doi:10.1016/j.gene.2016.12.023.

72. Moorefield, B.; Greene, E.A.; Reeder, R.H. RNA polymerase I transcription factor Rrn3 is functionally conserved between yeast and human. Proc. Natl. Acad. Sci. USA 2000, 97, 4724–4729, doi:10.1073/pnas.080063997.

73. Blank, M.F.; Grummt, I. The seven faces of SIRT7. Transcription 2017, 8, 67–74, doi:10.1080/21541264.2016.127 6658.

74. Hannan, K.M.; Sanij, E.; Rothblum, L.I.; Hannan, R.D.; Pearson, R.B. Dysregulation of RNA polymerase I transcription during disease. Biochim. Biophys. Acta 2013, 1829, 342–360, doi:10.1016/j.bbagrm.

75. Mayer, C.I.; Neubert, M.; Grummt, I. The structure of NoRC-associated RNA is crucial for targeting the chromatin remodelling complex NoRC to the nucleolus. EMBO Rep. 2008, 9, 774–780, doi:10.1038/embor.2008.109.

76. Mayer, C.; Schmitz, K.M.; Li, J.; Grummt, I.; Santoro, R. Intergenic transcripts regulate the epigenetic state of rRNA genes. Mol. Cell. 2006, 22, 351–361, doi:10.1016/j.molcel.2006.03.028.

77. Schmitz, K.M.; Mayer, C.; Postepska, A.; Grummt, I. Interaction of noncoding RNA with the rDNA promoter mediates recruitment of DNMT3b and silencing of rRNA genes. Genes Dev. 2010, 24, 2264–2269, doi:10.1101/gad.590910.

78. Hwang, Y.J.; Han, D.; Kim, K.Y.; Min, S.J.; Kowall, N.W.; Yang, L.; Lee, J.; et al. ESET methylates UBF at K232/254 and regulates nucleolar heterochromatin plasticity and rDNA transcription. Nucleic Acids Res. 2014, 42, 1628–1643, doi:10.1093/nar/gkt1041.

79. Arnheim, N.; Krystal, M.; Schmickel, R.; Wilson, G.; Ryder, O.; Zimmer, E. Molecular evidence for genetic exchanges among ribosomal genes on nonhomologous chromosomes in man and apes. Proc. Natl. Acad. Sci. USA 1980, 77, 7323–7327, doi:10.1073/pnas.77.12.7323.

80. Sardana, R.; O'Dell, M.; Flavell, R. Correlation between the size of the intergenic regulatory region, the status of cytosine methylation of rRNA genes and nucleolar expression in wheat. Mol. Gen. Genet. 1993, 236, 155–162.

81. Bird, A.; Taggart, M.; Macleod, D. Loss of rDNA methylation accompanies the onset of ribosomal gene activity in early development of X. laevis. Cell 1981, 26 Pt 1, 381–390.

82. Raval, A.; Sridhar, K.J.; Patel, S.; Turnbull, B.B.; Greenberg, P.L.; Mitchell, B.S. Reduced rRNA expression and increased rDNA promoter methylation in CD34+ cells of patients with myelodysplastic syndromes. Blood 2012, 120, 4812–4818, doi: 10.1182/blood-2012-04-423111.

83. Malinovskaya, E.M.; Ershova, E.S.; Golimbet, V.E.; Porokhovnik, L.N.; Lyapunova, N.A.; Kutsev, S.I.; Veiko, N.N.; et al. Copy Number of Human Ribosomal Genes with Aging: Unchanged Mean, but Narrowed Range and Decreased Variance in Elderly Group. Front. Genet. 2018, 9, 306, doi: 10.3389/fgene. 2018.00306.

84. Zafiropoulos, A.; Tsentelierou, E.; Linardakis, M.; Kafatos, A.; Spandidos, D.A. Preferential loss of 5S and 28S rDNA genes in human adipose tissue during ageing. Int. J. Biochem. Cell Biol. 2005, 37, 409–415, doi:10.1016/j.

biocel.2004.07.007.

85. Halle, J.P.; Müller, S.; Simm, A.; Adam, G. Copy number, epigenetic state and expression of the rRNA genes in young and senescent rat embryo fibroblasts. Eur. J. Cell Biol. 1997, 74, 281–288.

86. Machwe, A.; Orren, D.K.; Bohr, V.A. Accelerated methylation of ribosomal RNA genes during the cellular senescence of Werner syndrome fibroblasts. FASEB J. 2000, 14, 1715–1724, doi:10.1096/fj.99-0926com.

87. Lachapelle, S.; Gagné, J.P.; Garand, C.; Desbiens, M.; Coulombe, Y.; Bohr, V.A.; Hendzel, M.J.; et al. Proteome-wide identification of WRN-interacting proteins in untreated and nuclease-treated samples. J. Proteome Res. 2011, 10, 1216–1227, doi: 10.1021/pr100990s.

88. Lyapunova, N.A.; Veiko, N.N. Ribosomal genes in the human genome: Identification of the four fractions, and their organization in nucleoly, and metaphase chromosoms. Genetika 2010, 46, 1205–1209.

89. Veiko, N.N.I.; Shubaeva, N.O.; Ivanova, S.M.; Speranskii, A.I.; Lyapunova, N.A.; Spitkovskii, D.M. Blood serum DNA in patients with rheumatoid arthritis is considerably enriched with fragments of ribosomal repeats containing immunostimulatory CpG-motifs. Bull. Exp. Biol. Med. 2006, 142, 313–316.

90. Porokhovnik, L.N.; Passekov, V.P.; Gorbachevskaya, N.L.; Sorokin, A.B.; Veiko, N.N.; Lyapunova, N.A. Active ribosomal genes, translational homeostasis and oxidative stress in the pathogenesis of schizophrenia and autism. Psychiatr. Genet. 2015, 25, 79–87, doi:10.1097/YPG.0000000000000076.

91. Chestkov, I.V.; Jestkova, E.M.; Ershova, E.S.; Golimbet, V.E.; Lezheiko, T.V.; Kolesina, N.Y.; Porokhovnik, L.N.; et al. Abundance of ribosomal RNA gene copies in the genomes of schizophrenia patients. Schizophr. Res. 2018, 197, 305–314, doi:10.1016/j.schres.2018.01.001.

92. Kwon, I.; Xiang, S.; Kato, M.; Wu, L.; Theodoropoulos, P.; Wang, T.; Kim, J.; et al. Poly-dipeptides encoded by the C9orf72 repeats bind nucleoli, impede RNA biogenesis, and kill cells. Science 2014, 345, 1139–1145, doi: 10.1126/ science. 1254917.

93. Haeusler, A.R.; Donnelly, C.J.; Periz, G.; Simko, E.A.; Shaw, P.G.; Kim, M.S.; Maragakis, N.J.; et al. C9orf72 nucleotide repeat structures initiate molecular cascades of disease. Nature 2014, 507, 195–200, doi: 10.1038/ nature13124.

94. Su, P.H.; Chen, J.Y.; Chen, S.J.; Yu, J.S. Treacher Collins syndrome with a de Novo 5-bp deletion in the TCOF1 gene. J. Formos. Med. Assoc. 2006, 105, 518–521, doi: 10.1016/S0929-6646(09)60194-60197.

95. Calo, E.; Gu, B.; Bowen, M.E.; Aryan, F.; Zalc, A.; Liang, J.; Flynn, R.A.; et al. Tissue-selective effects of nucleolar stress and rDNA damage in developmental disorders. Nature 2018, 554, 112–117. Doi: 10.1038/nature 25449.

96. Wang, P.; Fan, X.; Fan, Y. The research progress of Treacher Collins syndrome. J. Clin. Otorhinolaryngol. Head Neck Surgery 2016, 30, 333–338.

97. Mamaev, N.N.; Medvedeva, N.V.; Shust, V.F.; Markochev, A.B.; Pasternak, N.D. Nucleoli and AgNORs in Hodgkin's disease. J. Clin. Pathol. Mol. Pathol. 1997, 50, 149–152, doi:10.1136/mp.50.3.149.

98. Eberle, F.C.; Mani, H.; Jaffe, E.S. Histopathology of Hodgkin's lymphoma. Cancer J. 2009, 15, 129–137, doi:10.1097/ PPO.0b013e31819e31cf.

99. Jacob, A.; Thyagarajan, B.; Kumar, M.P.; Shaikh, N.; Sharon, D. Cardiovascular effects of Hodgkin's lymphoma: A review of literature. J. Cancer Res. Clin. Oncol. 2018, 144, 99–107, doi: 10.1007/s00432-017-2560-x.

100. Lebofsky, R.; Bensimon, A. DNA replication origin plasticity and perturbed fork progression in human inverted repeats. Mol. Cell Biol. 2005, 25, 6789–6797, doi:10.1128/MCB.25.15.6789-6797.2005.

101. Tangeman, L.; McIlhatton, M.A.; Grierson, P.; Groden, J.; Acharya, S. Regulation of BLM Nucleolar Localization.

Genes 2016, 7, E69, doi: 10.3390/genes 7090069.

102. Guitton, J.; Onclercq-Delic, R.; Green, M.R.; Alibert, O.; Gazin, C.; Veaute, X.; Amor-Guéret, M. A role for Tau protein in maintaining ribosomal DNA stability and cytidine deaminase-deficient cell survival. Nat. Commun. 2017, 8, 693, doi:10.1038/s41467-017-00633-1.2017; 8(1):693.

103. Etchegaray, J.P.; Mostoslavsky, R. A sirtuin's role in preventing senescence by protecting ribosomal DNA. J. Biol. Chem. 2018, 293, 11251–11252, doi:10.1074/jbc.H118.004040.

104. Barber, M.F.; Michishita-Kioi, E.; Xi, Y.; Tasselli, L.; Kioi, M.; Moqtaderi, Z.; Tennen, R.I.; et al. SIRT7 links H3K18 deacetylation to maintenance of oncogenic transformation. Biochim. Biophys. Acta Mol. Cell Res. 2019, 1866, 1355–1367, doi:10.1016/j.bbamcr.2019.05.001.

105. Sobuz, S.U.; Sato, Y.; Yoshizawa, T.; Karim, F.; Ono, K.; Sawa, T.; Miyamoto, Y.; et al. SIRT7 regulates the nuclear export of NF-κB p65 by deacetylating Ran, and links H3K18 deacetylation to maintenance of oncogenic transformation. Nature 2012, 487, 114–118, doi: 10.1038/nature11043.

106. Ford, E.; Voit, R.; Liszt, G.; Magin, C.; Grummt, I.; Guarente, L. Mammalian Sir2 homolog SIRT7 is an activator of RNA polymerase I transcription. Genes Dev. 2006, 20, 1075–1080, doi: 10.1038/nature11043.

107. Paredes, S.; Angulo-Ibanez, M.; Tasselli, L.; Carlson, S.M.; Zheng, W.; Li, T.-M.; Chua, K.F. The epigenetic regulator SIRT7 guards against mammalian cellular senescence induced by ribosomal DNA instability. J. Biol. Chem. 2018, 293, 11242–11250, doi:10.1074/jbc.AC118.003325.

108. Toiber, D.; Erdel, F.; Bouazoune, K.; Silberman, D.M.; Zhong, L.; Mulligan, P.; Sebastian, C.; et al. SIRT6 recruits SNF2H to DNA break sites, preventing genomic instability through chromatin remodeling. Mol. Cell 2013, 51, 454–468, doi:10.1016/j.molcel.2013.06.018.

109. McStay, B.; Grummt, I. The epigenetics of rRNA genes: From molecular to chromosome biology. Annu. Rev. Cell Dev. Biol. 2008, 24, 131–157, doi:10.1146/annurev.cellbio.24.110707.175259.

110. Bahadori, M.; Azizi, M.H.; Dabiri, S. Recent Advances on Nucleolar Functions in Health and Disease. Arch. Iran. Med. 2018, 21, 600–607.

111. Montanaro, L.; Trere, D.; Derenzini, M. Nucleolus, ribosomes, and cancer. Am. J. Pathol. 2008, 173, 301–310, doi: 10.2353/ ajpath.2008.070752.

112. Andersen, J.S.; Lyon, C.E.; Fox, A.H.; Leung, A.K.; Lam, Y.W.; Steen, H.; Mann, M.; et al. Directed proteomic analysis of the human nucleolus. Curr. Biol. 2002, 12, 1–11, doi:10.1091/mbc.e02-05-0271.

113. Scherl, A.; Couté, Y.; Déon, C.; Callé, A.; Kindbeiter, K.; Sanchez, J.C.; Greco, A.; et al. Functional proteomic analysis of human nucleolus. Mol. Biol. Cell. 2002, 13, 4100–4109, doi:10.1091/mbc.e02- 05-0271.

114. Quin, J.E.; Devlin, J.R.; Cameron, D.; Hannan, K.M.; Pearson, R.B.; Hannan, R.D. Targeting the nucleolus for cancer intervention. Biochim. Biophys. Acta 2014, 1842, 802–816, doi:10.1016/j.bbadis.2013.12.009.

115. Larsen, D.H.; Stucki, M. Nucleolar responses to DNA doublestrand breaks. Nucleic Acids Res. 2016, 44, 538–544, doi:10.1093/nar/gkv1312.

116. Ruggero, D. Revisiting the nucleolus: From marker to dynamic integrator of cancer signaling. Sci. Signal. 2012, 5, 38, doi:10.1126/scisignal.2003477.

117. Orsolic, I.; Jurada, D.; Pullen, N.; Oren, M.; Eliopoulos, A.G.; Volarevic, S. The relationship between the nucleolus and cancer: Current evidence and emerging paradigms. Semin Cancer Biol. 2016, 37-38, 36-50, doi: 10.1016/j. semcancer.2015.12.004.

118. Bahadori, M.; Fayaz-Moghadam, K. Expression of P53 nuclear protein in colorectal adenocarcinoma. An

immunohistochemistry study of 50 cases. Iran. J. Med. Sci. 1995, 20, 24–28.

119. Koh, C.M.; Sabo, A.; Guccione, E. Targeting MYC in cancer therapy: RNA processing offers new opportunities. Bioessays 2016, 38, 266–275, doi:10.1002/bies.201500134.

120. Parlato, R.; Kreiner, G. Nucleolar activity in neurodegenerative diseases: A missing piece of the puzzle? J. Mol. Med. 2013, 91, 541–547, doi: 10.1007/s00109-012-0981-1.

121. Hetman, M.; Pietrzak, M. Emerging roles of the neuronal nucleolus. Trends Neurosci. 2012, 35, 305–314, doi:10.1016/j.tins.2012.01.002.

122. Rieker, C.; Engblom, D.; Kreiner, G.; Domanskyi, A.; Schober, A.; Stotz, S.; Neumann, M.; et al. Nucleolar disruption in dopaminergic neurons leads to oxidative damage and parkinsonism through repression of mammalian target of rapamycin signaling. J. Neurosci. 2011, 31, 453–460, doi:10.1523/JNEUROSCI.0590-10.2011.

123. Sia, P.I.; Wood, J.P.; Chid, G.; Sharma, S.; Craig, J.; Casson, R.J. Role of the nucleolus in neurodegenerative diseases with particular reference to the retina: A review. Clin. Exp. Ophthalmol. 2016, 44, 188–195, doi:10.1111/ceo.12661.

124. Boulon, S.; Westman, B.J.; Hutten, S.; Boisvert, F.M.; Lamond, A.I. The nucleolus under stress. Mol. Cell. 2010, 40, 216–227, doi:10.1016/j.molcel.2010.09.024.

125. Paridaen, J.T.; Janson, E.; Utami, K.H.; Pereboom, T.C.; Essers, P.B.; van Rooijen, C.; Zivkovic, D.; et al. The nucleolar GTP binding proteins Gnl2 and nucleostemin are required for retinal neurogenesis in developing zebrafish. Dev. Biol. 2011, 355, 286–301, doi:10.1016/j.ydbio.2011.04.028.

126. Lo, D.; Lu, H. Nucleostemin: Another nucleolar "Twister" of the p53-MDM2 loops. Cell Cycle 2010, 9, 3227–3232, doi:10.4161/cc.9.16.12605.

127. Mazon, J.N.; de Mello, A.H.; Ferreira, G.K.; Rezin, G.T. The impact of obesity on neurodegenerative diseases. Life Sci. 2017, 182, 22–28, doi:10.1016/j.lfs.2017.06.002.

128. Pietrzak, M.; Rempala, G.; Nelson, P.T.; Zheng, J.J.; Hetman, M. Epigenetic silencing of nucleolar rRNA genes in Alzheimer's disease. PLoS ONE 2011, 6, e22585, doi:1371/journal.pone.0022585.

129. Cong, R.; Das, S.; Ugrinova, I.; Kumar, S.; Mongelard, F.; Wong, J.; Bouvet, P. Interaction of nucleolin with ribosomal RNA genes and its role in RNA polymerase I transcription. Nucleic Acids Res. 2012, 40, 9441–9454, doi:10.1093/nar/gks720.

130. Abdelmohsen, K.; Gorospe, M. RNA-binding protein nucleolin in disease. RNA Biol. 2012, 9, 799–808, doi:10.4161/rna.19718.

131. Carnemolla, A.; Fossale, E.; Agostoni, E.; Michelazzi, S.; Calligaris, R.; De Maso, L.; Del Sal, G.; et al. Rrs1 is involved in endoplasmic reticulum stress response in Huntington disease. J. Biol. Chem. 2009, 284, 18167–18173, doi: 10.1074/jbc. M109.018325.

132. Lee, J.; Hwang, Y.J.; Boo, J.H.; Han, D.; Kwon, O.K.; Todorova, K.; Kowall, N.W.; et al. Dysregulation of upstream binding factor-1 acetylation at K352 is linked to impaired ribosomal DNA transcription in Huntington's disease. Cell Death Differ. 2011, 18, 1726–1735, doi:10.1038/cdd.2011.38.

133. Latonen, L. Nucleolar aggresomes as counterparts of cytoplasmic aggresomes in proteotoxic stress. Proteasome inhibitors induce nuclear ribonucleoprotein inclusions that accumulate several key factors of neurodegenerative diseases and cancer. Bioessays 2011, 33, 386–395, doi:10.1002/bies.201100008.

134. Baltanas, F.C.; Casafont, I.; Weruaga, E.; Alonso, J.R.; Berciano, M.T.; Lafarga, M. Nucleolar disruption and cajal body disassembly are nuclear hallmarks of DNA damage-induced neurodegeneration in purkinje cells. Brain Pathol. 2011, 21, 374–388, doi: 10.1111/j. 1750-3639.2010.00461.x.

135. Tsoi, H.; Lau, T.C.; Tsang, S.Y.; Lau, K.F.; Chan, H.Y. CAG expansion induces nucleolar stress in polyglutamine diseases. Proc. Natl. Acad. Sci. USA 2012, 109, 13428–13433, doi:10.1073/pnas.1204089109.

136. Becherel, O.J.; Gueven, N.; Birrell, G.W.; Schreiber, V.; Suraweera, A.; Jakob, B.; Taucher-Scholz, G.; et al. Nucleolar localization of aprataxin is dependent on interaction with nucleolin and on active ribosomal DNA transcription. Hum. Mol. Genet. 2006, 15, 2239–2249.

137. Bodem, J.; Dobreva, G.; Hoffmann-Rohrer, U.; Iben, S.; Zentgraf, H.; Delius, H.; Vingron, M.; et al. TIF-IA, the factor mediating growth-dependent control of ribosomal RNA synthesis, is the mammalian homolog of yeast Rrn3p. EMBO Rep. 2000, 1, 171–175, doi:10.1038/sj.embor.embor605.

138. Zhao, J.; Yuan, X.; Frodin, M.; Grummt, I. ERK-dependent phosphorylation of the transcription initiation factor TIF-IA is required for RNA polymerase I transcription and cell growth. Mol. Cell. 2003, 11, 405–413.

139. Mayer, C.; Bierhoff, H.; Grummt, I. The nucleolus as a stress sensor: JNK2 inactivates the transcription factor TIF-IA and downregulates rRNA synthesis. Genes Dev. 2005, 19, 933–941.

140. DuRose, J.B.; Scheuner, D.; Kaufman, R.J.; Rothblum, L.I.; Niwa, M. Phosphorylation of eukaryotic translation initiation factor 2alpha coordinates rRNA transcription and translation inhibition during endoplasmic reticulum stress. Mol. Cell Biol. 2009, 29, 4295–4307, doi:10.1128/MCB.00260-09.

141. Fatyol, K.; Grummt, I. Proteasomal ATPases are associated with rDNA: The ubiquitin proteasome system plays a direct role in RNA polymerase I transcription. Biochim. Biophys. Acta 2008, 1779, 850–859, doi:10.1016/j.bbagrm.2008.08.010.

142. Tchurikov, N.A.; Kretova, O.V.; Fedoseeva, V.R.; Chechetkin, M.A.; Gorbacheva, M.A.; Snezhkina, A.V.; Alembekov, I.R.; et al. Genome-wide mapping of hot spots of DNA double-strand breaks in human cells as a tool for epigenetic studies and cancer genomics. Mol. Genet. Metab. Rep. 2017, 13, 89–93, doi:10.1016/j.ymgmr.2017.07.005.

143. Tchurikov, N.A.; Fedoseeva, D.M.; Sosin, D.V.; Snezhkina, A.V.; Melnikova, N.V.; Kudryavtseva, A.V.; Kravatsky, Y.V.; et al. Hot spots of DNA double-strand breaks and genomic contacts of human rDNA units are involved in epigenetic regulation. J. Mol. Cell Biol. 2015, 7, 366–382, doi:10.1093/jmcb/mju038.

144. Tchurikov, N.A.; Ponomarenko, N.A. Detection of DNA domains in Drosophila, human, and plant chromosomes possessing mainly 50- to 150-kilobase stretches of DNA. Proc. Natl. Acad. Sci. USA 1992, 89, 6751–6755, doi:10.1073/pnas.89.15.6751.

145. Tchurikov, N.A.; Kretova, O.V.; Fedoseeva, D.M.; Chechetkin, V.R.; Gorbacheva, M.A.; Karnaukhov, A.A.; Kravatskaya, G.I.; et al. Mapping of genomic double-strand breaks by ligation of biotinylated oligonucleotides to forum domains: Analysis of the data obtained for human rDNA units. Genom. Data 2014, 3, 15–18, doi:10.1016/j.gdata.2014.10.024.

146. Tchurikov, N.A.; Kretova, O.V.; Fedoseeva, D.M.; Sosin, D.V.; Grachev, S.A.; Serebraykova, M.V.; Romanenko, S.A.; et al. DNA double-strand breaks coupled with PARP1 and HNRNPA2B1 binding sites flank coordinately expressed domains in human chromosomes. PLoS Genet. 2013, 9, e1003429, doi:10.1371/journal.pgen.1003429.

147. Kravatsky, Y.V.; Chechetkin, V.R.; Tchurikov, N.A.; Kravatskaya, G.I. Genome-wide study of correlations between genomic features and their relationship with the regulation of gene expression. DNA Res. 2015, 22, 109–119, doi:10.1093/dnares/dsu044.

148. Wong, K.K.; Lawrie, C.H.; Green, T.M. Oncogenic Roles and Inhibitors of DNMT1, DNMT3A, and DNMT3B in Acute Myeloid Leukaemia. Biomark. Insights 2019, 14, 1177271919846454, doi: 10.1177/1177271919846454.

149. Santoro, R.; Grummt, I. Epigenetic mechanism of rRNA gene silencing: Temporal order of NoRC-mediated histone modification, chromatin remodeling, and DNA methylation. Mol. Cell Biol. 2005, 25, 2539–2546, doi:10.1128/MCB.25.7.2539-2546.2005.

150. Guetg, C.; Santoro, R. Formation of nuclear heterochromatin: The nucleolar point of view. Epigenetics 2012, 7, 811–814, doi:10.4161/epi.21072.

151. Postepska-Igielska, A.; Grummt, I. NoRC silences rRNA genes, telomeres, and centromeres. Cell Cycle 2014, 13, 493–494, doi:10.4161/cc.27783.

152. Caudron-Herger, M.; Pankert, T.; Seiler, J.; Németh, A.; Voit, R.; Grummt, I.; Rippe, K. Alu element-containing RNAs maintain nucleolar structure and function. EMBO J. 2015, 34, 2758–2774, doi:10.15252/embj.201591458.

153. Postepska-Igielska, A.; Krunic, D.; Schmitt, N.; Greulich-Bode, K.M.; Boukamp, P.; Grummt, I. The chromatin remodelling complex NoRC safeguards genome stability by heterochromatin formation at telomeres and centromeres. EMBO Rep. 2013, 14, 704-710, doi:10.1038/embor.2013.87.

154. Bierhoff, H.; Postepska-Igielska, A.; Grummt, I. Noisy silence: Non-coding RNA and heterochromatin formation at repetitive elements. Epigenetics 2014, 9, 53–61, doi:10.4161/epi.26485.

155. Sheng, J.; Yu, W.; GAO, X.; Xu, Z.; Hu, G.F. Angiogenin stimulates ribosomal RNA transcription by epigenetic activation of the ribosomal DNA promoter. J. Cell Physiol. 2014, 229, 521–529, doi:10.1002/jcp.24477.

Advances in Biotechnology

Chapter 3

A Comprehensive Review on the Physical and Chemical Properties of the Three Generations of Biofuels

Mehdi Ardjmand[1]* and Farid Jafarihaghighi[1], Mohammad Salar Hassani[1], Neda Bazel[1], Hasanali Bahrami[2]

[1]*Department of Chemical Engineering, South Tehran Branch, Islamic Azad University, Tehran, Iran.*

[2]*Department of Mechatronics, Arak University, Iran*

****Correspondense to: Mehdi Ardjmand,** Head of Department of Chemical Engineering, South Tehran Branch, Islamic Azad University, Tehran, Iran.*

Tel: +989121513117; Email: m_arjmand@azad.ac.ir

Abstract

The shortage of fossil fuel resources and the dramatic increase in population have raised many concerns about fuel supply in the years ahead. Researchers are now focusing on renewable fuels, and biodiesel is one of those renewables. Four generations of biodiesel have been reported today and many studies have been done to optimize and enhance their performance. The present review article examines the physical and chemical properties of three generations of biodiesel. It was observed that the physical and chemical properties of the biodiesel vary based on the feed stocks and have a significant effect on the dynamic characteristics of emission level and performance of engine. All properties have the highest and lowest ranges for each feed. All the oils that have been studied for three generations to date have been fully reported, and these properties have been studied and compared for each of the three generations.

Keywords: Biodiesel; First Generation; Second Generation; Third Generation; Physical and Chemical Properties

1. Introduction

Ardjmand M

policies and dramatic fuel price changes in fuel-producing countries have caused many crises in the world. Lack of adequate resources and fossil fuel contamination in the world are other causes of global energy issues. (**Figure 1**) shows the increase of the demanding for the crude oil and the price changes in the world. These reasons have made the need for alternative fuel in the world completely necessary. Nowadays, biofuels have attracted a lot of attention as an alternative to fossil fuels [1-5]. Biofuels are included several advantages and the most important of them are related to the environmental benefits. Biodiesel can diminish emissions that cause environmental difficulties such as acid rain and global warming. Also, health issues as a consequence of emissions exposure are significantly declined by the cleaner emissions of biodiesel [5, 6]. Biodiesel is the non-petroleum based diesel fuel. It is contained of the mono-alkyl esters of the long-chain fatty acids derived from the renewable lipid sources [7-9]. Quality of biofuels is always dependent on many factors. Some of them are included the feedstock, fatty acid composition, production process, handling and storage, and postproduction parameters [10].

The close similarities between the properties of biodiesel and diesel fuels make that biodiesel is a good alternative to diesel fuels. The viscosity of biodiesel is so close to the diesel fuel. The conversion of triglycerides into ethyl or methyl esters via the transesterification procedure diminishes the molecular weight and viscosity and rises the volatility gradually. The cetane number is around 50-60 for biodiesel and it's higher than diesel fuels, however, the heating value of the diesel fuel is greater than biodiesel. The flashpoint and density of biodiesel are much higher than diesel fuels, while the cloud point for diesel fuels normally is better than biodiesel fuel. The sulfur compounds in petrodiesel provide much of the lubricity, however, Biodiesel comprises virtually no sulfur and this is frequently applied as the additive to ultra-low-sulfur diesel (ULSD) fuel to help with lubrication [11-13].
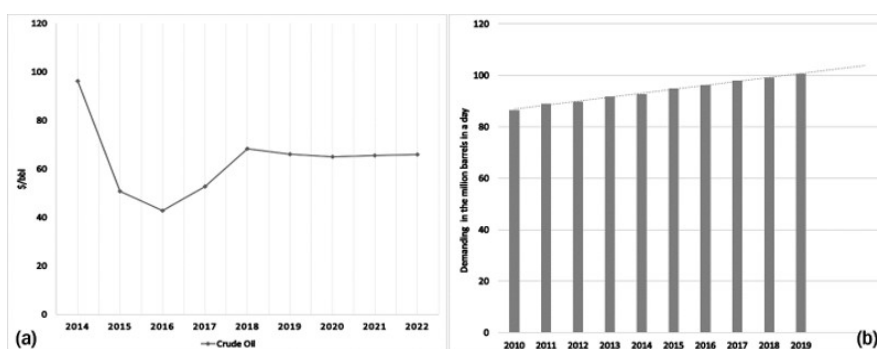
Figure 1: World Bank: average crude oil prices (a) and daily demand for crude oil worldwide (b)

1.1. Biodiesel feedstocks

The different types of feedstocks are used for the production of biodiesel. The choice of feedstocks relies on the economic aspects and availability of the concerned country. The major biodiesel feedstocks for different regions of the world are shown in (**Figure 2**). Four genera-

tions of biodiesel fuels are applied worldwide.

Figure 2: Main biofuel producers by region

The first generation of biodiesel is edible oils such as palm, soybeans, rapeseed, and sunflower oil. Some of the main advantages of the first generation of biodiesel are shown in Fig 3. However, the use of edible oil sources as biodiesel fuel has caused great concern in the world. These concerns include the possibility of food shortages in the world and rising food prices. This generation has also required arable land for the production and it creates serious ecological imbalances due to that countries start cutting down forests for plantation purposes. Therefore, the demand for biodiesel increases, it will cause severe damage to the environment and wildlife, due to the greater need for arable land and larger scale deforestation [3, 5].

The second generation of biodiesel is non-edible oils. The mahua, jatropha, tobacco seed, jojoba oil are examples of second-generation biodiesel. This generation of biodiesel has many advantages, as shown in Fig 3. This generation also has some limitations for worldwide using. They may not be abundant enough to substitute transportation fuels. The performance of this generation has some restriction in cold temperatures [14].

The third generation of biodiesel are included microalgae, animal fats, and waste cooking oils. Some advantages of this generation are shown in (Figure 3) [3]. While, this generation requires huge amount of money for producing. According to research, the production of algae biofuel still requires a lot of work, mainly in the process of the oil extraction and low yields as well as it emits captured carbon dioxide.

Figure 3: The advantages of the first, second, and third generation

Limited information is available on fourth generation biodiesel. This has led to a complete lack of scrutiny in this area. The Synthetic Genomics Company is applied genetic engineering in produ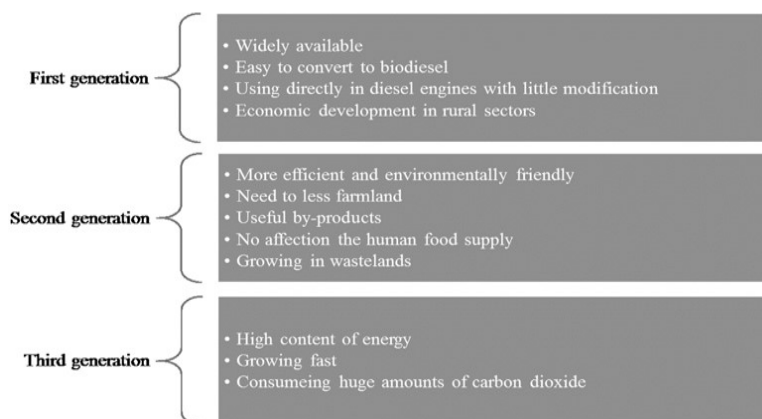ction of biofuel. The genetically modified microorganisms is used to generate fuel directly from the carbon dioxide on the industrial scale. Furthermore, the fourth generation biofuels are gained from genetically modified crops in which they spend more carbon dioxide from the atmosphere than they release over combustion which makes it a carbon negative fuel.

1.2. The standards of biodiesel in the worldwide

Several studies indicated that the physical properties of biodiesel have a huge effect on emission and combustion. The physical and chemical properties of the produced biodiesel must reach the standard value defined in the different regions for using. Some of the standards are included EN 14213/EN 14214, SANS 1935, JASO M360, ASTM D 6751, ANP 42, and IS 15607 which used in EU, South Africa, Japan, U.S, Brazil, and India, respectively [10]. Some of the most important physical characteristics of biodiesel are included density, cetane number, kinematic viscosity, flash point, pour point and cloud point, calorific value, acid value, copper strip corrosion, ash content, sulfur content, glycerine, and oxidation stability [12, 15]. Standards set guidelines for testing the biodiesel fuels and propose the proper ranges for different physical and chemical properties of the fuel.

There have been limited studies of the physical properties of biodiesel, but no reports to date have examined the physical properties of all three generations of biodiesel and comparing them to one another. A recent study has surveyed all the physical properties of three-generations of biodiesel from all oil sources which effect on the engine performance and emission features and also shown comparisons between them. The report also mentioned the lowest highest values of properties and shows the range for all biodiesels.

1.3. Characteristics and properties of three generations of biodiesel

The important physical properties of three-generation biodiesels are summarized in Table 1, 2, and 3. The Physicochemical property ranges are illustrated for pure biodiesels. All tables show the most important properties of biodiesels such as Density (kg/m^3), Kinematic Viscosity 40°C (mm^2/s), Calorific Value (Mj/Kg), Higher (gross) Heating Value (Mj/Kg), Lower (net) Heating Value (Mj/Kg), Acid Value (Neutralization number) (mg KOH/g), Flash Point (°C), Cetane Number, Oxidation Stability (h), Cloud Point (°C), and Pour Point (°C).

There have been numerous reports on the types of vegetable oils and different amounts have been reported. About 69 first generation oils that have been the most researched are shown in (**Table 1**).

Oil											
Taramira (Eruca sativa)	at 15°C: 881.1 [183] at 40°C: 871±0.15 [184]	5.71±0.21, 5.9 [184] [183]	...	...	0.40 [183]	197.3±2.1 [184]	48, 59.08±1.34 [183] [184]	6 [183]	1.5±0.7 [184]	-2.97±0.17 [184]	
Tea seed (Camellia)	at 20°C: 884 [185]	4.95 [185]	37.512 [185]	...	...	120 [185]	52 [185]	...	...	...	
Thistle (Silybum marianum)	at 20°C: 863 [186] at 15.6°C: 0.8788 ± 0.0012 [187] at 40°C: 899 [188]	4.46, 6.32 [186] [188]	16.984 [188]	...	0.10 ± 0.01, 0.44 [187] [186]	115.0 ± 0.50, 153 [187] [186]	44, 51 [188] [186]	2.1 [186]	-1, 7 [186] [188]	-6, 10 ± 1.0 [188] [187]	
Tobacco seed (Nicotiana tabacum)	at 15°C: 886.8, 888.5 [189] [137] at 25°C: 870 [190] at 20°C: 882 [191]	3.5, 5.2 [189] [191]	38, 39.811 [190] [189]	...	0.3 , 0.66 [137] [191]	165.4 [137]	51, 52 [189] [190]	0.8 [137]	...	...	
Tomato seed	at 40°C: 915.1 [192]	28 [192]	...	35.9 [192]	...	189 [192]	54.71 [192]	...	...	...	
Castor	at 20°C: 917 [90]	13.5, 14.4 [43] [90]	...	...	0.42, 3.9 [43] [90]	165 to 186.5 [193]	...	...	...	...	
Colza (Brassica rapa)	at 20°C: 882±25 [30]	4.02±0.12 [30]	...	...	0.22±0.03 [30]	185±3 [30]	...	11.2±0.1 [30]	...	...	
Radish	...	4.6 [37]	...	...	...	...	53 [37]	...	...	...	
Tigernut (Nutsedge , Cyperus esculentus)	at 30°C: 866 [194]	2.34 [194]	...	...	...	186 [194]	...	...	...	...	

Niger seed (Asteraceae, Guizotia abyssinica)	at 15°C: 890 [163]	4.10, 4.30 [163] [164]	...	...	...		128, 157 [163] [164]	57 [164]	1.02 [164]	3, 4 [163] [164]	2.5 [163]
Okra seed (Abelmoschus esculentus)	at 15°C: 870 [104]	4.1 [104]	...	...	...	0.22 [104]	126 [104]	...	1.6 [104]	6 [104]	6 [104]
Papaya seed	at 40°C: 840, 900 [165] [166] at 15°C: 895 [134]	3.53, 6 [165] [167]	42.085 [41]	38.49, 38.97319 [165] [134]	...	0.35, 0.72 [167] [166]	112, 147 [165] [134]	77.3, 48.29 [168] [165]		1, 2 [167] [168]	-1, 1 [167] [168]
Pequi (Caryocar brasiliense)	at 20°C: 69.69 ± 0.07, 866.3 [169] [170]	4.27 ± 0.03, 5.64 [169] [170]	...	...	...	0.7909 [170]	...	...	4.5±0.3, 5.85 [169] [170]	...	...
Pomegranate seed (Punica granatum)	at 40°C: 892 [171] at 20°C: 895.2 [135]	3.31, 5.65 [135] [171]	39.49, 40.048 [135] [171]	...	...		130 [171]	26.1, 45.02 [135] [171]	...	...	...
Poppyseed	893 [41]	3.5, 4.63 [49] [41]	42.085 [41]		...		...	...	...	...	...
Pracaxi (Pentaclethra macroloba)	at 20°C: 869±6 [172]	5.8 ±0.03 [172]	...	...	...		...	...	3.2±0.2 [172]	...	...
Rice bran	at 40°C: 868.1 [26] at 15°C: 876±15.7, 892 [173] [174]	4.14, 5.37 [175] [114]	39.957, 42.2 [26] [176]	39.5, 43.10±0.98 [114] [173]	...	0.09, 0.586 [175] [26]	174.5, 183 [26] [176]	73.6, 51 [26] [114]	1.61, 1.63±0.12 [86] [173]	-10, 9 [174] [176]	-11, -2.00±0.14 [174] [173]
Sacha inchi	...	4.66 [177]	...	...	...	0.39 [177]	...	...	...	...	...
Sapote	at 40°C: 864 [178]	4.5, 5.43 [179] [178]	37.12 [178]	37.12 [179]	...	0.16 [179]	174 [178]	52 [178]	...	...	-6 [179]
Shea butter	At 5°C: 877, 883 [180] [181]	4.42, 5.93 [180] [181]	...	37.93, 37.98 [180] [182]	38.9 [182]	0.16, 0.28 [181] [180]	130, 171 [181] [180]	47, 58 [181] [180]	...	3,12 [182] [181]	3, 10 [180] [181]

Cocklebur (Xanthium)	at 15°C: 896.89 [148]	6.877 [148]	38.527 [148]	...	...	...	166 [148]	42.3 [148]	...	-1 [148]	-19 [148]
Coriander seed	...	4.21 [92]	...	40.1 [92]	37.5 [92]	0.1 [92]	...	...	14.6 [92]	...	-19 [92]
Date seed	at 15°C: 870 to 890 [149]	3.7 to 4.2 [149]	...	...	...	...	122 to 131 [149]	53.56 [149]	...	3 to 7 [149]	...
Dika (Irvingia gabonensis)	...	3.2 [150]	39 [150]	...	39 [151]	0.01 [150]	140 [150]	...	...	-14 [151]	-6 [151]
False flax (Camelina sativa)	...	2.9 to 3.15, 4.37 [152] [51]	45.05 to 46.15 [152]	...	...	0.04 [51]	179 [51]	41.26 to 51.17 [152]	...	4.1 [51]	-11 to -8, 0 [152] [51]
Grape seed	at 20°C: 882 [135] at 32°C: 890 [126]	4.04, 4.1 [135] [38]	39.73 [135]	...	...	0.27, 0.31 [38] [126]	175 [38]	48, 48.6 [38] [135]	0.5 [38]	...	-22 [126]
Hemp	at 15°C: 884, 891.5 [153] [154] at 40°C: 858, 872 [155] [156]	3.48, 4.23 [155] [156]	39.81 [155]	...	...	0.01, 0.67 [156] [153]	120, 175 [154] [157]	...	...	-5, -2.5 [153] [154]	-17, -4 [155] [154]
Kapok seed (Ceiba pentandra)	at 15°C: 876.9, 890 [158] [104] at 40°C: 875 [159]	4.2, 5.4 [104] [159]	40.493 [158]	36.292 [159]	...	0.24, 0.38 [104] [158]	156, 167 [159] [104]	57.2 [158]	0.8, 4.42 [104] [158]	2, 3 [104] [158]	1, 2.8 [104] [158]
Kenaf seed (Hibiscus cannabinus)	at 15°C: 879.5 [160]	4.8 [160]	...	...	...	0 [160]	...	54 [160]	0.35 [160]	3.8 [160]	1.7 [160]
Marula (Sclerocarya birrea)	at 25°C: 877 [161]	4.12 [161]	...	...	...	...	171 [161]	...	...	6 [161]	3 [161]
Meadowfoam seed	...	6.18, 6.22 [162] [51]	...	40.591 [162]	38.499 [162]	0.02, 0.06 [162] [51]	205 [51]	...	...	-6.6, -6 [51] [162]	-10 [162]
Mustard	at 40°C: 866 [36]	4.1 [36]	...	41.3 [36]	...	...	169 [36]	...	...	...	...

Seed	Density										
Açaí (Euterpe oleracea)	...	4.5 [138]	...	...	...	...	200 [138]	...	1.5 [138]	...	...
Black seed (Nigella sativa)	at 15°C: 886.1 [139] at 40°C: 867.7 [139]	4.5026 [139]	39.967 [139]	...	...	0.26 [139]	172.5 [139]	...	1.32 [139]	-1 [139]	-1 [139]
Blackcurrant seed (Ribes nigrum)	at 15°C: 892.6 [140]	3.84 [140]	...	...	...	0 [140]	...	40.5 [140]	1.67 [140]	-2.2 [140]	-12 [140]
Borage seed (Borago officinalis)	at 15°C: 887.09 [140]	4 [140]	...	...	...	0 [140]	...	45.6 [140]	1.67 [140]	4.5 [140]	-2 [140]
Evening promise (Oenothera biennis)	at 15°C: 878 [141]	5.68 [141]	...	...	...	0.37 [141]	196 [141]	51 [141]	...	7 [141]	4 [141]
Flaxseed (linseed, Linum usitatissimum)	at 40°C:870, 888.2 [32][142]	2.8, 4.07 [32][25]	...	40.84, 41.82 [32][142]	37.267 [25]	...	142, 184 [36][138]	41, 55 [37][142]	2.2 [138]	...	...
Apricot	at 15°C: 884.3 [143]	4.92 [143]	39.95 [143]	...	...	...	111 [143]	...	...	...	...
Apple seed	at 20°C: 881 [135] at 40°C: 865 [144]	4.12,5.9 [135][144]	37.51, 40.48 [145][144]	...	...	0.34 [144]	150, 161 [145][144]	50.4 [135]	...	2 [145]	5 [145]
Avocado	at 15°C: 877.68 [146]	4.9581 [146]	41.33 [146]	...	...	...	184 [146]	...	...	...	-7 [146]
Babassu (Attalea speciousa)	...	3.18 [147]	...	...	...	0.0778 [147]	112 [147]	...	...	...	...
Ben (Moringa oleifera)	at 40°C: 859.6, 869.6 [22][63] at 15°C: 869.6, 885.8 [56][86]	4.1264, 5.0735 [86][27]	40.05 [22]	39.888, 40.115 [86][27]		0.05, 0.185 [56][26]	150.5, 180.5 [63][56]	56, 67.07 [56][26]	4.45, 26.2 [56][63]	0, 19 [86][56]	19 [27]

Macadamia	at 15°C: 859.2, 868 [114] [115]	4.4, 4.57 [37] [115]	39.88 [115]	39.9 [114]	...	0.08 & 0.055, 0.15 [116] [115]	135, 178.5 [115] [114]	55, 59.5 & 57.5 [37] [116]	1.97 & 2.06, 3.35 [116] [114]	-1, 8 [117] [114]	-3, 5 & 1 [115] [116]
Mongongo nut (Manketti, Schinziophyton rautaneuii)	at 15°C: 876, 878 [118] [119] at 25°C: 869 [120]	3.72, 4.43 [120] [118]	36.97, 37.82 [118] [119]	41.2 [120]	...	0.08, 0.35 [118] [120]	150, 165 [119] [120]	49.1, 51 [118] [120]	4.75 [119]	-3.8, 1.2 [119] [118]	-6.2, -4.1 [119] [118]
Pistachio	at 15°C: 860, 880 [121] [122]	3.44, 4.71 [121] [122]	...	...	...	0.16, 0.187 [122] [121]	148, 168 [122] [121]	52, 53.94 [122] [121]	8.3 [122]	-2 [122]	-1 [122]
Walnut	at 40°C: 864 [36] at 15°C: 864 [89]	3.88, 4.11 [68] [89]	39.47, 41.18 [68] [89]	41.32 [36]	...	0.03 [68]	170 [36]	...	2.9 [68]	-6.1 [68]	-10 [68]
Lemon	at 40°C: 853 [123]	1.06 [123]	41.510 [123]	...	...	...	...	...	...	...	...
Orange	at 40°C: 812, 876 [124] [125] at 32°C: 892 [126] at 15°C: 852 [127]	1.04, 5.6 [127] [126]	38.158, 42.8 [125] [124]	...	...	0.25 [126]	29, 78.5 [127] [125]	37, 49 [125] [124]	...	...	-25, -10 [126] [125]
Bitter ground (Momordica charantia)	at 15°C: 889 ± 10.50 [128]	4.48 ± 1.02 [128]	...	...	...	0.40 ± 0.39 [128]	162 ± 11.20 [128]	64.0 ± 4.80 [128]	1.99 ± 0.85 [128]	9.00 ± 2.12 [128]	15.00 ± 1.82 [128]
Egusi seed (Cucumeropsis mannii naudin)	at 15°C: 883, 884±8.75 [129] [99]	3.83, 3.91±0.014 [129] [99]	...	39.97, 42±1.2 [129] [99]	...	0.11±0.01, 0.19 [99] [129]	142±2.82 [99]	53.66, 55 [99] [108]	1.32±0.1, 1.41 [99] [129]	0.5±0.1 [99]	...
Pumpkin seed	at 15°C: 883.7 [130]	4.1, 4.41 [37] [130]	40.21 [131]	38.08, 40.84 [130] [132]	...	0.48 [130]	120, 175 [130] [131]	47, 60.01 [37] [132]	7.2 [131]	-18 [131]	-32 [131]
Watermelon seed (Citrullus vulgaris)	at 15°C: 800, 893 [133] [134] at 20°C: 880.6 [135]	1.05, 5.33 [133] [134]	39.74, 39.85 [135] [136]	39.36195 [134]	...	1.387, 3.66 [136] [137]	107, 143 [133] [134]	44.47, 54.682 [133] [136]	...	-1 [133]	-3 [133]

Soybean	at 40°C: 855, 877 [33] [32] at 20°C: 871±20, 885 [30] [90] at 15°C: 881.1, 887 [53] [41]	3.5, 5.75 [32] [91]	39.72 to 40.08, 40.297 [44] [41]	39.85, 45.07 [92] [53]	37.38, 37.75 [92] [33]	0.04±0.01, 0.45 [44] [91]	152, 202.5 [41] [27]	58.1, 46 [93] [37]	1.3, 6±0.3 [38] [30]	-2, 4 [33] [93]	-6, 1 [33] [27]
Sunflower	at 40°C: 863, 874 [36] [32] at 20°C: 832±4 [30] at 15°C: 880, 888.4, [41] [94]	3.2, 5.241 [49] [95]	38.1 to 38.472, 42.02 [44] [96]	41.03, 41.33 [32] [36]	37.532 [25]	0.04±0.01, 1.3 [44] [95]	125, 192±2 [41] [30]	47, 54 to 58 [37] [44]	0.5, 1.73 [95] [93]	-14, 5±1 [96] [44]	-16, -2±1 [44] [96]
Almond	at 25°C: 881 [58] at 15°C: 882±0.011, 887 [97] [98]	4.2, 4.726 [38] [58]	41.761 [58]	...	...	0.10±0.02, 0.44 [97] [98]	145, 173 [58] [98]	44.6, 58 [98] [99]	3, 3.1 [38] [99]	-3, 11 [99] [88]	-9±0.5, -2 [97] [88]
Beech nut (Fagus sylvatica)	at 15°C: 876 [100]	3.8 to 4 [100]	...	...	...	...	173 [100]	49 [100]	...	...	...
Brazilnut (Bertholletia excelsa)	...	4.3, 4.56 [37] [101]	...	...	...	0.15 [101]	170.3 [101]	53 [37]	...	...	...
Cashew	at 40°C: 863.6, 909.3 [102] [103] at 15°C: 880, 884 [104] [105] at 18°C: 882, 883.5 [106] [107] at 20°C: 890 [19]	37.51, 39.52 [105] [54]	34.3 [103]	...	...	0.25, 3.69 [104] [103]	113, 170 [104] [103]	51, 63 [37] [108]	5.6 [104]	-5, 10 [103] [107]	-1, 7.9 [103] [107]
Hazelnut	at 40°C: 875 [36] at 15°C: 863, 884.8 [109] [110]	3.097, 5.48 [109] [110]	37.23, 41.172 [111] [110]	39.889, 41.12 [112] [36]	39.75 [109]	0.05, 0.23 [68] [96]	152, 183 [36] [89]	52.6, 55 [109] [111]	7.6 [68]	-14.7±0.5, -9.3 [113] [68]	-17, -13 [96] [68]

Oil	Density										
Olive	at 40°C: 860 [36]	4.18, 6.18 [36] [54]	39.92 [54]	41.35 [36]	...	0.13 [38]	178, 204 [38] [36]	57, 61.72 [38] [27]	3.3 [38]	...	...
Palm	at 40°C: 858.9, 875 [22] [55] at 15°C: 858.9, 879.7 [56] [57] at 25°C: 884 [58]	2.8, 5.64 [23] [25]	36.5, 40.322 [23] [58]	38.3, 41.3 [59] [60]	37.13, 37.92 [61] [57]	0.01±0.01, 0.4 [44] [21]	125, 214.5 [23] [27]	44, 72.09 [59] [25]	2.41, 23.56 [22] [27]	3, 17±1 [62] [44]	3, 15±1 [63] [44]
Peanut (Arachis hypogea, Ground nut)	at 40°C: 861.1, 992 [39] [64] at 15°C: 848.5, 884 [65] [41] at 20°C: 877.1±2, 877.3 [66] [67]	4.29, 5.908 [39] [64]	39.98, 40.297 [68] [41]	...		0.08, 0.28 [68] [65]	156, 192 [67] [64]	53, 58.9±4.1 [38] [66]	2, 21.1 [38] [68]	0, 17.8 [65] [68]	-8, 15 [65] [68]
Rapeseed	at 40°C: 857, 872 [36] [32] at 20°C: 879.35 [29] at 15°C: 884, 880 [69] [70]	3.3, 5.51 [49] [71]	37.23, 38.7 [69] [72]	41.31, 41.55 [32] [36]	38.177, 39 [71] [73]	0.03, 0.33 [69] [74]	130, 180 [74] [36]	51, 55 [71] [38]	2, 8.1 [38] [74]	-5 [70]	-13, -10 [70] [69]
Safflower	at 40°C: 866 [36] at 15°C: 860, 890.73 [75] [76] at 20°C: 888, 891 [77] [78]	2.9, 5.8 [49] [79]	38.122, 40.71 [80] [41]	40.604, 45.21±1.58 [81] [82]	38.122, 39.322 [77] [79]	0.06, 0.39 [83] [75]	129, 187 [84] [85]	42.07, 53.16 [76] [75]	0.9, 2.66 [70] [81]	-5, -2±0.05 [76] [82]	-24, -7 [85] [81]
Sesame	at 40°C: 866.9, 884.8 [86] [26] at15°C: 867.2, 884.8 [87] [88]	3.04, 4.3998 [36] [26]	39.996, 40.7 [26] [89]	39.996, 40.9 [86] [32]	...	0.3 [87]	145, 208.5 [36] [26]	50.48 [87]	1.135, 1.14 [86] [26]	-6 to 1 [26]	-14 to 1 [26]

Table 1: Properties of the first generations of biodiesel.

Biodiesels	Physicochemical property ranges										
	Density (kg/m^3)	Kin. Viscosity 40°C (mm^2/s)	Calorific Value (Mj/Kg)	Higher (gross) Heating Value (Mj/Kg)	Lower (net) Heating Value (Mj/Kg)	Acid Value (Neutralization number) (mg KOH/g)	Flash Point (°C)	Cetane Number	Oxidation Stability (h)	Cloud Point (°C)	Pour Point (°C)
Coconut (Coconut pulm, Copra)	at 40°C: 800, 869.5 [16] [17] at 15°C: 873.3 [18] at 20°C: 870 [19]	2.61, 4.0927 [20] [21]	38, 41.9 [22] [23]	37.26, 39.95 [24] [16]	57.743 [25]	0.106, 0.35 [26] [21]	108, 120.5 [25] [22]	37, 63.73 [24] [19]	5.12, 9.2 [22] [18]	-3, 1 [18] [27]	-12, -4 [18] [22]
Corn (Maize)	at 15°C: 864.2, 879.65 [28] [29] at 20°C: 865±12, 890 [30] [31] at 40°C: 868, 880 [32] [33]	2.45 to 2.56, 4.89 [34] [29]	39.12, 44.92 to 45.06 [31] [34]	39.93, 41.14 [35] [32]	37.679, 38.48 [25] [33]	0.03±0.002, 0.3 [30] [28]	154, 188±4 [36] [30]	46, 58.37 to 59 [37] [34]	1.2, 6.5±0.3 [38] [30]	-15, -3 [28] [33]	-5 to -2 [34]
Canola	at 40°C: 853.6, 875±0.6 [39, 40] at 15°C: 883, 883.2 [41] [42]	2.56 to 2.84, 4.6 [34] [43]	44.65 to 44.93, 37.3 to 39.87 [34] [44]	25.11±0.29, 40.195 [40] [27]	…	0.01±0.01, 0.35 [44] [43]	105, 186.5 [41] [27]	48 to 56 [44]	7.08, 12 [27] [42]	-3, 1 to 2 [27] [40]	-4 to -1, -8 to -10 [34] [40]
Cotton seed	at 40°C: 871 [36] at 20°C: 878±9, 882±1 [30] [45] at 15°C: 850, 887 [46] [47] at 25°C: 875±15.7 [48]	3.1, 6 [49] [46]	39.19, 39.524 [47] [41]	41.68, 48.18 [46] [36]	36.896 [50]	0.02, 0.58 [51] [47]	150±3, 200 [48] [50]	48, 57.1 [52] [53]	1.83±0.12, 4.9±0.8 [48] [45]	-5, 7±0.11 [52] [48]	-4, 6±0.15 [46] [48]

Nerium oleander(Thevetia peruviana)	at 15°C: 875,880 [240] [241]	4.3, 4.33 [241] [240]	42.4, 44.986 [241] [240]	42.279 [240]	...	0.057, 0.66 [240] [241]	75, 178 [240] [241]	61.5, 71.5 [240] [241]	6.5 [241]	-3, 15 [241] [240]	-7, 3 [241] [240]
cebera odollam(sea mango)	at 15°C: 880 [242]	4.5 [242]	39.095 [242]	...	...	...	138 [242]	...	...	...	...
nagchampa	at 40°C: 876.8,877 [243] [244]	2.64, 4.72 [244] [243]	39.882 [243]	...	...	0.41, 0.76 [244] [243]	151, 159 [243] [244]	51.9 [243]	...	13 [243]	10 [243]
Croton megalocarpus	at 40°C: 867.2, 870.4 [22] [27] at 15°C: 883 [245]	4.05, 4.78 [22] [245]	37.24, 39.53 [245] [22]	39.786 [27]	...	0.16 & 0.2 [26]	164, 192 [27] [245]	46.6, 47.52 [26] [245]	0.71, 2.88 [27] [245]	-6, -3 [245] [27]	-3, -2 [22] [27]
Patchouli (Pogostemon cablin)	at 40°C: 922.1 [27]	6.0567 [27]	...	44.18 [27]	...	...	118.5 [27]	...	0.022 [27]	-33 [27]	-33 [27]
Sterculia foetida	at 40°C: 877.6 [27]	6.3717 [27]	...	40.001 [27]	...	...	130.5 [27]	...	1.46 [27]	1 [27]	2 [27]
greenseed	at 40°C: 877±1 [40]	...	...	20.95±0.2 [40]	...	0.162±0.021 [40]	...	...	...	1 to 3 [40]	-12 to -10 [40]
Aphanamixis polystachya	at 40°C: 873.5 [26]	4.7177 [26]	39.960 [26]	...	...	0.448 [26]	188.5 [26]	...	0.16 [26]	8 [26]	8 [26]

Feedstock											
Honesty (Lunaria annua)	at 15°C: 877±2 [223]	6.815±0.034 [223]	...	...	...	0,42±0.02 [223]	...	78.9±0.8 [223]	...	...	...
Mango	at 40°C: 873, 882 [224] [225]	4.3, 4.73 [224] [225]	40.453 [225]	...	...	0.78 [224]	135, 178 [225] [224]	54 [225]	...	...	...
Neem (Azadirachta indica)	at 40°C: 868,895.2±0.59 [26] [226]	3.58, 5.53 [227] [228]	39.810 [26]	...		0.42, 0.649 [227] [26]	76 to 120, 175 [26] [227]	48 to 53, 57 [26] [229]	7.1 [26]	2,10 [26] [227]	9 to 14.4, 6 [26] [228]
Passion fruit (Passiflora edulis)	...	4.1 [138]	...	...	...	...	172 [138]	...	3.1 [138]	...	...
Rubber seed (Hevea brasiliensis)	at 15°C: 877.3 [230]	5.77 [230]	...	40.3 [230]	37.15 [230]	0.448 [230]	141 [230]	52.56 [230]	8 [230]	7 [230]	9 [230]
Sea buckthorn (Hippophae rhamnoides)	at 20°C:886.5 [135]	3.79,[135]	39.64 [135]	...	...	...	...	40.9 [135]	...	...	...
Tall	at 15°C: 878 to 885, 922 [231] [232]	4.1 to 5.3, 7.1 [231] [232]	40.023 [232]	...	...	...	89 [232]	54 [232]	...	...	1 [232]
Tamanu (Polanga, Foraha, Calophyllum tacamahaca)	at 40°C: 869, 894 & 892 & 893 [197] [233], at 15°C: 868.7, 873 [56] [234], at 32°C: 905 [235]	5.74, 3.99 [22] [197]	38.33, 41.397 [234] [197]	39.38, 41.5 [56] [235]	...	0.3, 0.88 & 1 & 0.76 [120] [233]	93.5, 162.5 [22] [27]	56.53 & 58.42 & 58.39, 50 [233] [235]	3.58, 9.42 [56] [22]	4.3, 13 [234]	7, 13.2 [56] [234]
Tucumã butter (Astrocaryum vulgare)	at 40°C: 877 [236]	3.7, 4.54 [237] [236]	...	...	...	0.23 [237]	124 [237]	...	...	...	...
sapindus mukorossi (soapnut)	at 15°C: 875, 876 [238] [239] at 20°C: 870 [238]	4.63 [239]	40.02 [239]	...	...	0.14 [239]	140 [239]	56 [239]	...	-4 [239]	-1 [239]

Stillingia (Chinese vegetable tallow, Sapium sebiferum)	at 15°C: 892, 900 [209] [210]	3.698, 4.81 [209] [210]	...	...	...	...	0.007, 0.15 [211] [209]	137, 180 [211] [209],	40.2, 50 [209] [210]	0.6, 0.8 [211] [209]	-13 [211]	...
Artichoke	at 25°C: 880 [212] at 15°C: 889 [213]	3.56, 5.101 [212] [213]	...	...	39.8 [212]	...		175, 182 [212] [213]	59 [213]	...	-4, -1 [213] [212]	...
Astrocaryum murumuru butter	at 20°C: 877.9 ± 1.6 [172]	3.1 ± 0.03 [214]	...	...	...	...	0.6±0.1 [214]	...	...	40 [172]	...	...
Balanos (Balanites aegyptiaca)	at 40°C: 860, 874.8 [215] [216]	3.98, 4.46 [215] [216]	...	42.5 [216]	39.65 [215]	...	0.34, 1.26 [215] [216]	75, 160 [215] [216]	42 [216]	...	-2.5, 0 [215] [216]	...
Brucea javanica	at 40°C: 871 [217]	3.556 [217]	...	...	...	...	0.027 [217]	164 [217]	...	3 [217]	2 [217]	1 [217]
Buriti (Mauritia flexuosa)	at 40°C: 877.3 ± 6 [172]	5.22 [218]	...	...	...	...	...	190 [218]	...	16.5 [218]	...	...
Candlenut (Kukui nut)	at 40°C: 886.9 [219] at 20°C: 885.7 [220]	4.8, 4.819 [220] [219]	...	40.33 [220]	...	...	0.4 [220]	160, 161 [219] [220]	...	5.9 [220]	6 [220]	6.667, 6.84 [219] [220]
Chaulmoogra (Hydnocarpus wightiana)	at 40°C: 893 [221]	5.4 [221]	...	40.7 [221]	...	...	...	163 [221]	...	...	...	2 [221]
Crambe (Crambe abyssinica)	at 40°C: 848 [32]	5.1, 5.12 [32] [36]	...	...	41.98, 42.26 [36] [32]	...	...	190 [36]	...	...	...	...
Croton (tiglium , Croton tiglium)	at 40°C: 865 [16]	4.78 [16]	...	...	39.95 [16]	...	...	...	46.6 [16]	...	...	...
Cuphea	...	2.38 & 2.4 [222]	...	...	...	...	...	...	56.07 & 55.06 [222]	3.09 & 3.57 [222]	-9.1 & -10.1 [222]	-21.5 & -22.5 [222]
Cupuaçu butter	...	4.8 [138]	...	...	...	...	...	176 [138]	...	72.7 [138]	...	...

A wide range of second-generation oils, all of which are non-edible, are reported in the table. Table 2 shows the second generation oils that have been the most researched. The limitations of second generation oils compared to first generation oils are quite evident and 39 oils have been studied to date.

Table 2: Properties of the second generations of biodiesel.

| Biodiesels | Physicochemical property ranges | | | | | | | | | | |
	Density (kg/m^3)	Kin. Viscosity 40°C (mm^2/s)	Calorific Value (Mj/Kg)	Higher (gross) Heating Value (Mj/Kg)	Lower (net) Heating Value (Mj/Kg)	Acid Value (Neutralization number) (mg KOH/g)	Flash Point (°C)	Cetane Number	Oxidation Stability (h)	Cloud Point (°C)	Pour Point (°C)
Tung	at 15°C: 883, 903 [195] [196]	4.64, 7.84 [195] [196]	38.8 [195]	...	...	0.124 [196]	197 [195]	39 [196]	0.3 [196]	...	...
Jatropha	at 40°C: 864.2, 873 [27] [197] at 20°C: 784, 875.9 [198] [199] at 15°C: 865.7, 880 [56] [104]	2.35 to 2.47, 6.1 to 6.7 [34] [200]	39.56, 42.673 [200] [152]	39.738, 39.84 [27] [16]	...	0.05, 1.05 [56] [104]	108, 194 [199] [124]	49, 60.74 to 63.27 [26] [34]	3.02, 13.51 [56] [199]	1, 10.2 [104] [197]	-6 to 2, 10 [34] [27]
Jojoba (Simmondsia chinensis)	at 40°C: 830 [201]	2.2, 5.86 [201] [202]	35.66 [202]	...	...	0.22 to 0.45 [202]	100, 150 [201] [202]	...	...	7 [201]	5 [201]
Nahor (Mesua ferrea)	at 40°C: 873 [203]	4.1, 5.525 [204] [203]	35 [203]	...	...	1.8 [203]	113, 142 [203] [204]	...	...	6.1 [204]	-1.2 [204]
Paradise (Simarouba glauca)	at 40°C: 875.2 [205] at 15°C: 865 [206]	4.68, 5.4 [206] [205]	...	...	...	0.1, 0.7 [205] [207]	141.2, 165 [205] [206]	64 [205]	...	19 [206]	14.5 [206]
Pongamia (Karanja , Honge, Millettia pinnata)	at 15°C: 880, 890 [208] [104] at 40°C: 883 [197]	3.99, 5.52 to 5.79 [208] [34]	37.8 to 39.69, 42.133 [34] [197]	...	...	0.1, 0.72 to 0.76 [93] [34]	141, 163 [93] [197]	55.1, 59.68 to 60.9 [93] [34]	2.35, 4.5 [93] [104]	-1, 14.6 [104] [197]	-3, 5.1 [104] [197]

	Density										
Mutton fat	at 40°C: 856 [270]	...	...	...	...	0.65 [270]	...	59 [270]	...	-4 [270]	-5 [270]
Poultry fat	...	4.32, 4.71 [271] [278]	...	...	...	0.298 [279]	...	...	0.52 [271]	7 [278]	1, 3 [278] [280]
Waste cooking oil	at 15°C: 874.9, 880 [281] [282] at 40°C: 863.7, 890 [283] [284]	2.72, 6.1 [284] [285]	37.2, 37.9 [286] [285]	35.401, 41.2 [284] [282]	...	0.6, 0.71 [286] [283]	134, 186 [281] [284]	51.48, 64.2 [286] [281]	15.9 [281]	10.5 [286]	-1, 1 [282] [286]
Waste fat oil	...	...	...	...	...	10.91 [287]	...	...	...	...	...
Waste fried oil	at 25°C: 855 [288] at 15°C: 888 [289]	4.318, 4.57 [289] [288]	...	...	39.55, 40.5 [289] [288]	1.31±0.06 [287]	126, 156 [288] [289]	52 [289]	...	-8.3, 3 [288] [289]	-2.5 [289]
Waste frying palm oil	at 15°C: 875 [290]	4.401 [290]	38.73 [290]	...	...	0.15 [290]	70.6 [290]	60.4 [290]	...	...	...
Waste mixed vegetable oil	at 15°C: 878.9 [280]	4.83 [280]	...	...	...	...	...	59.7 [280]	14.12 [280]	...	...
Waste sunflower oil	at 15°C: 887.5 [280]	4.42 [280]	...	...	...	...	...	51.5 [280]	0.43 [280]	...	...
Trout oil	at 15°C: 885 [291]	4.25 [291]	37.8 [291]	...	...	...	...	51.3 [291]	...	...	...
Larvae grease (housefly)	at 15°C: 881 [292]	5.64 [292]	...	...	...	0.63 [292]	145 [292]	52 [292]	...	...	...
Plastic pyrolysis oil	at 15°C: 981 [293]	1.918 [293]	...	...	38.3 [293]	41 [293]	13 [293]	...	...	...	...
Sludge pyrolysis oil	at 22°C: 890 [294]	8.2 [294]	...	39.29 [294]	36.49 [294]	0.489 [294]	170 [294]	...	...	...	...
Neem seed pyrolysis oil	at 40°C: 982 [295]	9.38 [295]	...	20.8 [295]	...	...	...	...	...	...	...

Schizochytrium mangrovei	...	5.22 [259]	...	...	...	7.59 [259]	186.53 [259]	68.80 [259]	0.05 [259]	19.12 [259]	...
Spirulina	at 40°C: 860 [258]	5.66 [258]	41.36 [258]	...	...	0.45 [258]	130 [258]	...	...	...	-18 [258]
Spirulina platensis	at 15°C: 863.7 [260]	12.4 [260]	45.63 [260]	...	...	0.75 [260]	189 [260]	70 [260]	...	-3 [260]	-9 [260]
Animal fat	at 15°C: 871, 877 [261] [262]	4.03, 4.42 [261, 262]	...	36.73 [263]	36.83, 89.49 [261] [262]	0.38 [263]	161.5 [261]	57,49, 65.6 [261] [262]	13.03 [263]	...	
Animal fat traps	at 15°C: 870 [264]	4.7 [264]	...	...	37 [264]	0.3 [264]	128 [264]	53 [264]	...	...	...
Beef tallow	at 17°C: 877 [265] at 20°C: 832 266] at 40°C: 0.890 [267]	4.89, 5.47±0.005 [266] [268]	39.858 [265]	39.931 [267]		0.495±0.007 [268]	152, 210 [266] [268]	58.8, 64.8 [267] [267]	1.99 [268]	...	0 [265]
Camelus dromedaries fat (Camel fat)	at 15°C: 871 [269]	3.39 [269]	...	39.52 [269]	...	...	158 [269]	58.7 [269]	...	12.7 [269]	15.5 [269]
Chicken fat	at 40°C: 867, 881.6 [270] [267] at 15°C: 869, 889.7 [271] [272]	5.3 [272]	...	39.911 [267]	...	0.25, 0.43 [270] [272]	169 [272]	57, 61 [267] [270]	...	-5 [270]	-6 [270]
Fish oil	at 40°C: 880,885 [273] [274]	4, 4.96 [273] [275]	37.8, 42.241 [275] [273]	...	...	...	114, 176 [274] [273]	51, 52.4 [275] [276]	...	-5 [275]	-14,4 [275, 276]
Fleshing oil	at 15°C: 876.7 [272]	4.7 [272]	...	...	...	0.28 [272]	168 [272]	58.8 [272]	...	...	...
inedible animal tallow	at 17°C: 877 [265]	5.072 [265]	39.858 [265]	...	...	...	...	...	...	...	...
Lard	at 40°C: 879.5 [267]	4.64 to 7.73 [277]	...	39.932 [267]	...	1.13 [277]	...	57.8 [267]	...	...	...

The third generation of biofuels, which has done less to date than the previous two generations. The values are reported in Table 3.33 oils in the third generation have been studied to date and the incidence rate is lower than the previous two generations due to the novelty.

Table 3: Properties of the third generations of biodiesel.

| Biodiesels obtained from | Physicochemical property ranges | | | | | | | | | | |
	Density (kg/m^3)	Kin. Viscosity 40°C (mm^2/s)	Calorific Value (Mj/Kg)	Higher (gross) Heating Value (Mj/Kg)	Lower (net) Heating Value (Mj/Kg)	Acid Value (Neutralization number) (mg KOH/g)	Flash Point (°C)	Cetane Number	Oxidation Stability (h)	Cloud Point (°C)	Pour Point (°C)
Ankistrodesmus braunii and Nannochloropsis	at 40°C: 869 [246]	4.19 [246]	40.72 [246]	…	…		144 [246]	…	…	7 [246]	-6 [246]
Auxenochorella protothecoides	at 15°C: 876.9 [247]	4.354 [247]	…	…	…	0.2 [247]	…	52.6 [247]	1.2 [247]	…	…
Chlorella protothecoides	at 15°C: 882 [248] at 40°C: 864 [249]	4.41, 5.2 [249] [250]	39.01, 41 [249, 250]	…	…	0.29, 0.374 [248] [249]	115 [249]	…	4.52 [248]	…	…
Chlorella variabilis	at 15°C: 867 [251]	4.85 [251]	38.78 [251]	…	…	…	157 [251]	58.6 [251]	…	…	…
Chlorella vulgaris	at 40°C: 860, 895 [252] [253]	4.1, 5.2 [253] [252]	42.7 [253]	…	…	0.51 [253]	115 [252]	…	…	…	-7 [253]
Euglena sanguinea	at 15°C: 861, 868 [254] [255]	4.483, 4.545 [254, 255]	…	…	…	0.29, 0.32 [255] [254]	169, 172 [254] [255]	65 [255]	6.20 [255]	15 [255]	13 [255]
Heterotrophic microalgae (Sugar plant)	at 15°C: 778 [256]	2.748 [256]	…	…	44 [256]	…	…	75 [256]	…	…	…
Melanothamnus afaqhusainii	at 40°C: 870 [257]	3.67 [257]	…	…	…	0.75 [257]	…	…	…	-1 [257]	-2 [257]
Pond water algae	at 40°C: 872 [258]	5.82 [258]	40.80 [258]	…	…	0.40 [258]	…	…	…	…	-16 [258]

2. Density

Density is one of the most important factors in biodiesels. Most studies have reported temperatures of density between 15 and 40 ˚C for all three generations because the temperature has a direct effect on density. Also, the free fatty acid content, molar mass, temperature, the water content can effect on the density of esters. The cetane number, viscosity, heating value, fuel performance, and the quality of combustion and atomization are strongly connected to the density. The density of diesel fuel is lower than biodiesels. The unit quantity of all reports is converted to kg/m^3.

The maximum density of the first generation of biodiesel is reported for Castor biodiesel (at 20°C: around 917). Peanut sample also showed the highest density of about 992 and 884 at 40 and 15°C. The minimum density of the biodiesel was stated for the Watermelon seed around 800 and 880.6 at 15 and 20°C.

Patchouli and Tall biodiesels (second generation of biodiesel) could show the highest amount of density at 15 and 40°C around 922 and 922.1. The minimum of this generation was shown by the jojoba and jatropha at 40, 20 and 15°C (830, 865.7, and 874).

Plastic pyrolysis and neem seed pyrolysis were shown the highest amount of density at 15 and 40°C around 981 and 982. The majority of reports were done at 15 and 40°C, however, some reports were performed at 22, 17, and 25°C (Table 3). The lowest of the density for the third generation of biodiesels were shown by the heterotrophic microalgae at 15°C (778).

Comparison between three generations of biodiesel shows that the highest of density was reported by Peanut biodiesel (first generation) and it was higher than second and third generation of biodiesel around 8 and 2 % and heterotrophic microalgae (third-generation) had the lowest density compared to other generation to approximately 3 and 8%.

2.1. Viscosity

The viscosity plays a leading role in the engine performance of biodiesels. It can affect the size of the particles, spray quality, starting the engine, the quality of the fuel-air mixture combustion, and penetration of the injected jet. Also, the viscosity can affect the lubricity. The amount viscosity has a limitation due to several reasons. The high viscosity makes the formation of too big drops, the increase of combustion chamber deposits, the increase of needed fuel pumping energy and wear of the pump and the injector elements. Also, the high viscosity causes operational issues at the low temperatures due to that the viscosity enhances with reducing the temperature. The low viscosity makes the inadequate penetration and the formation of the black smoke specific to combustion (during the absence of oxygen). Biodiesel is more polar compared to the diesel fuel, so, the viscosity of biodiesel is greater than diesel

fuel. Table 1, 2, and 3 show the viscosity of different feedstocks. The viscosity was measured at 40°C for three generations of biodiesel.

The unit quantity of all reports is converted to mm^2/s.

The maximum viscosity was reported for castor biodiesel around 14.4 for the first generation of biodiesel. Orange and watermelon seed biodiesels also showed the lowest amount of viscosity to roughly 1.04 and 1.05.

The highest amount of viscosity for the second generation of biodiesel was shown by tung. It could show the viscosity around 7.84. The minimum of the viscosity was displayed by the jatropha and jojoba biodiesel. It was only around 2.35 and 2.2.

Spirulina platensis and neem seed pyrolysis were shown the highest amount of viscosity for the third generation of biodiesel. They were around 12.4 and 9.38. On the other hand, the lowest amount of viscosity was reported for plastic pyrolysis and it was about 1.91.

The comparison between all generations could show that the maximum viscosity was shown by the castor and it was higher than the second and third generation of biodiesels to approximately 46 and 14%. The minimum of viscosity also reported by the first generation of biodiesels and it was 52 and 45% lower than the second and third generation of biodiesels.

2.2. Calorific Value

The heating value or calorific value of the fuel is defined as the amount of energy released through the combustion of the unit value of the fuel. The unit quantity of all reports is converted to Mj/Kg. The upper heating value is gained while all products of the combustion are cooled down to the temperature before the water vapor combustion formed over combustion is condensed. The lower heating value is achieved by subtracting the latent heat of vaporization of the water vapor formed with the combustion from the upper heating value. Some of the reports indicated only to the calorific value and others referred to higher and lower heating values.

The highest calorific value for the first generation was gained by the false flax biodiesel. It was from 45.05 to 46.15. The maximum higher heating value was shown by the cottonseed and it was about 48.18. Also, the greatest amount of the lower heating values reported by the coconut biodiesel (57.74). On the other hand, the minimum of calorific value was displayed by the thistle biodiesel (36.5). The lowest amount of the higher and lower heating values were gained by the canola and cottonseed biodiesels (25.11±0.29 and 36.89).

Nerium oleander had the highest amount of calorific value between all second generations of the biodiesel (44.98) and the lowest heating value was shown by the nahor biodiesel [35].

The higher heating value of the patchouli was greater than other second generations (44.18). The lowest higher heating value was shown by the green seed biodiesel and it was only around 20.95±0.2.

Spirulina platensis showed the maximum of calorific value between all third generations of biodiesel (45.63). The lowest calorific value was gained by waste cooking and it was around 37.2. Lard biodiesel showed the highest higher heating values around 39.93 and neem seed pyrolysis was gained 20.8. The greatest lower heating value of the third generation of biodiesels was gained by the heterotrophic microalgae. It was around 44. The minimum lower heating value was reported sludge pyrolysis biodiesel (36.49).

Comparison between all biodiesel generations could display that the spirulina platensis could achieve the maximum of calorific value and it was higher than nerium oleander and false flax to approximately 3 and 2%. Also, the highest higher heating value of the first generation of biodiesel (cottonseed) was higher than the second and third generation of biodiesel around 9 and 18%.

2.3. Acid Value

The acidic value (acid number or neutralization number) in chemistry is the amount of mg of potassium hydroxide needed to neutralize one gram of a substance. An acidic number is a measure of the number of carboxylic acid groups in a compound, such as a fatty acid or a mixture of compounds. The upper amount of free fatty acid contributes to the elevated acid value which in turn causes severe corrosion in fuel supply lines of the engine. Besides, the acid value can be observed as the indication of the level of lubrication in fuel lines. The unit quantity of all reports is mg KOH/g.

The castor biodiesel showed the highest acid value between all biodiesels of the first generation (3.9). The lowest acid value was displayed by the dika biodiesel and it was merely around 0.01.

The maximum of acid value for the second generation of biodiesel was gained by the nahor (1.8) and the minimum of the acid value was shown by the stillingia (0.007).

Plastic pyrolysis biodiesel from the third generation could display the highest amount of the acid value (41) and the lowest of acid value was gained by the waste frying palm (0.15).

The third generation of the biodiesel could show the much higher acid value compared to other generations and the second generation of biodiesel could gain the minimum of the acid value compared to others.

2.4. Flash Point

Flashpoint is the smallest temperature at which the fuel will ignite on the application of the ignition source under particular situations. Every liquid has a vapor pressure which is a function of its temperature. As the temperature rises, the vapor pressure increases. As the vapor pressure increases, the density of flammable liquid vapor increases. Therefore, temperature determines the amount of combustible liquid vapor in the air. Flashpoint measurement is done in two main ways: open cup and closed cup. The diesel fuel has a flashpoint around 50-65°C. Mostly, the flashpoint of the biodiesel is much higher than diesel fuel. The high flash point of biodiesel increases the security of fuel storage and transportation. The unit quantity of all reports is Celsius (centigrade).

The palm biodiesel had the maximum of the flashpoint between all first generation of biodiesel (214.5°C). On the other hand, the minimum of the flashpoint was gained by the orange biodiesel (29°C) and it was lower than diesel fuel.

Tung biodiesel (second generation of biodiesel) had the highest amount of the flashpoint around 197°C. However, the flashpoint of the nerium oleander was merely about 73°C.

In the third generation of biodiesel, the beef tallow had the greatest flashpoint between all samples (around 210°C) while the plastic pyrolysis biodiesel was only around 13°C.

The flashpoint of palm biodiesel was higher than tung and beef tallow around 8 and 3% and the plastic pyrolysis biodiesel was lower than the nerium oleander and orange biodiesel around 82 and 55%

2.5. Cetane Number

The cetane number represents the delay between the start of the injection into the combustion chamber and the start of the fuel combustion. During this delay, the fuel accumulates and then ignites and the combustion explodes to produce a powerful effect. Reducing the delay time makes the combustion more uniform. The increase of the cetane number causes the quick ignition of the fuel and it makes less non-ignited fuels building up in the combustion chamber and also further complete fuel combustion. The low cetane number affect the incomplete combustion and it causes the enhancement of the exhaust emissions and extreme deposits in the engine. Normally, biodiesels have a higher cetane number due to greater oxygen content compared to the diesel fuel.

Papaya seed biodiesel (first generation) showed the highest amount of the cetane number compared to other biodiesels. The value of the cetane number was around 77.3. On the contrary, pomegranate seed biodiesel had the lowest cetane number around (26.1).

Honesty biodiesel (second generation) displayed the highest amount of cetane number around 78.9±0.8 compared to other biodiesels in this generation, while tung biodiesel could

reach only around 39.

Heterotrophic microalgae were shown the maximum of the cetane number in the third generation of biodiesel (almost 75). However, the cetane number of the fish biodiesel was around 51.

The highest cetane number between all generations was shown by the honesty biodiesel and it was 3 and 6 % higher than the maximum of the other generations. Pomegranate seed biodiesel was shown the lowest amount of cetane number compared to other generations and it was 33 and 48% than the minimum of the other generations.

2.6. Oxidation Stability

The oxidation can affect the quality of the biodiesel over storage in contact with air. The storage stability is extremely important for the biodiesel and it indicates the ability of the fuel to stand chemical changes over the long term storage due to the connection with the oxygen from the air. The oxidation stability of biodiesel is subject to the number of bis-allylic sites in unsaturated compounds. The primitive oxidation is started by the radical formation at bis-allylic sites and it forms peroxides. Then, the secondary oxidation generates the aldehydes, volatile organic compounds, and ketones with ruing the methyl ester which polymerizes to form waste sludge that can detriment the engine fuel injection system.

This feature is not mentioned in all reports but Ben biodiesel had the highest in first-generation biodiesel (26.2 h). On the contrary, the kenaf seed biodiesel had the lowest oxidation stability and it was around 0.35 h.

The honesty biodiesel showed the maximum of the oxidation stability between all second generations of biodiesel (72 h). Sterculia foetida biodiesel displayed the minimum of the oxidation stability around 0.022 h.

The waste mixed vegetable biodiesel presented the greatest amount of oxidation stability in the third generation of biodiesel about 14.12 h. However, the lowest of the oxidation stability was shown by the waste sunflower biodiesel (around 0.43 h).

Comparing between all generations, the honesty biodiesel was higher than the maximum of the first and third generation of biodiesel around 63 and 80%. Also, Sterculia foetida biodiesel (second generation of biodiesel) was lower than the minimum of the first and third generation of biodiesel to approximately 93 and 94%.

2.7. Cloud and Pour Point

The minimum temperature at which a cloud of paraffin crystals appears inside the oil product is called the cloud point. At this temperature, the sample does not lose its fluidity and

is usable. The pour point of a hydrocarbon material is when it cools under certain conditions and is defined as the lowest temperature at which the hydrocarbon flows. This temperature is somewhat higher than the solidification point temperature. It is difficult to define precisely the pour or solidification point since the transition from the liquid phase to the solid phase is gradual. The unit quantity of all reports is Celsius (centigrade).

Ben biodiesel showed the highest could and pour point between all first generations of biodiesel (19°C). However, pumpkin seed had the minimum of could point around -18°C. Also, it had the lowest pour point between all biodiesel samples around -32°C.

The maximum of could and pour point was shown by the paradise biodiesel between the second generation of biodiesel (19 and 14.5°C). On the other hand, the minimum of could and pour point was reported by the patchouli biodiesel (-33°C).

Euglena sanguinea biodiesel had the greatest could and pour point between all third generations of biodiesel and it was around 15 and 13°C. Waste fried oil and Spirulina showed the lowest cloud and pour point to roughly -8.3 and -18°C.

Paradise and ben biodiesel had the highest cloud point and it was 21% higher than Euglena sanguinea biodiesel. However, the ben biodiesel had the maximum pour point compared to the all second and third generation of biodiesel. It was 23 and 31% higher than the maximum of other generations. The patchouli biodiesel indicated the minimum of the cloud and pour point between all generations and it was lower than the lowest cloud and pour point of other generations between 4-74%.

3. Conclusion and Future Trend

This review article attempts to provide comprehensive information on the physical properties of the majority of biodiesel used in all three generations and propose the best biodiesel concerning their physical properties. Biodiesel has many advantages over fossil fuels. One of the most important reasons for choosing biodiesel is its impact on the economy, environment and energy security in the world. Some of the most important benefits of biodiesel on the economy can be sustainability, job opportunities in the rural area, fuel diversity, more income taxes, development of agriculture, International competitiveness, decreasing the dependency on the imported petroleum, and improving investments in equipment and plant. Reducing air contamination, Biodegradability, Greenhouse gas reductions, better combustion efficiency, and carbon sequestration are some of the environmental impacts of biodiesel. One of the most important impacts of biodiesel on energy security can also be addressed renewability, ready availability, domestic distribution, supply reliability, domestic targets, and decreasing use of fossil fuels [296].

Although biodiesel has superior properties over fossil fuels, choosing the right biodiesel has many difficulties. Choosing the right biodiesel depends on various factors including standards set in different countries, raw material production policies, weather conditions, engine biodiesel performance, initial production costs, and physical properties of biodiesel available in that region and so on. Therefore, choosing the best option among all the studied biofuels is almost impossible, and choosing the best feedstock has to take into account all the physical, chemical and product conditions, and so on.

4. Acknowledgments

5. Conflict Of Interest Statement

The authors have confirmed that there is no conflict of interest.

6. References

1. Armas, O., J.J. Hernández, and M.D. Cárdenas, Reduction of diesel smoke opacity from vegetable oil methyl esters during transient operation. Fuel, 2006. 85(17-18): p. 2427-2438.

2. Atadashi, I., M. Aroua, and A.A. Aziz, High quality biodiesel and its diesel engine application: a review. Renewable and sustainable energy reviews, 2010. 14(7): p. 1999-2008.

3. Baskar, G., et al., Microalgae A Source for Third-Generation Biofuels. Bioprocess Engineering for a Green Environment, 2018: p. 297-306.

4. Klass, D.L., Biomass for renewable energy, fuels, and chemicals. 1998: Elsevier.

5. Ahmad, A., et al., Microalgae as a sustainable energy source for biodiesel production: a review. Renewable and Sustainable Energy Reviews, 2011. 15(1): p. 584-593.

6. Zhu, L., C. Cheung, and Z. Huang, Impact of chemical structure of individual fatty acid esters on combustion and emission characteristics of diesel engine. Energy, 2016. 107: p. 305-320.

7. Knothe, G., J. Krahl, and J. Van Gerpen, The biodiesel handbook. 2015: Elsevier.

8. Knothe, G., C.A. Sharp, and T.W. Ryan, Exhaust emissions of biodiesel, petrodiesel, neat methyl esters, and alkanes in a new technology engine. Energy & Fuels, 2006. 20(1): p. 403-408.

9. Ranganathan, S.V., S.L. Narasimhan, and K. Muthukumar, An overview of enzymatic production of biodiesel. Bioresource technology, 2008. 99(10): p. 3975-3981.

10. Barabás, I. and I.-A. Todoruţ, Biodiesel quality, standards and properties. Biodiesel-quality, emissions and by-products, 2011: p. 3-28.

11. Casanave, D., J.-L. Duplan, and E. Freund, Diesel fuels from biomass. Pure and Applied Chemistry, 2007. 79(11): p. 2071-2081.

12. Erdmann, M., M. Böhning, and U. Niebergall, Physical and chemical effects of biodiesel storage on high-density polyethylene: Evidence of co-oxidation. Polymer Degradation and Stability, 2019. 161: p. 139-149.

13. Hoekman, S.K., et al., Review of biodiesel composition, properties, and specifications. Renewable and sustainable energy reviews, 2012. 16(1): p. 143-169.

14. Naik, S.N., et al., Production of first and second generation biofuels: a comprehensive review. Renewable and sustainable energy reviews, 2010. 14(2): p. 578-597.

15. Ramírez-Verduzco, L.F., J.E. Rodríguez-Rodríguez, and A. del Rayo Jaramillo-Jacob, Predicting cetane number, kinematic viscosity, density and higher heating value of biodiesel from its fatty acid methyl ester composition. Fuel, 2012. 91(1): p. 102-111.

16. Lujaji, F., et al., Cetane number and thermal properties of vegetable oil, biodiesel, 1-butanol and diesel blends. Journal of Thermal Analysis and Calorimetry, 2010. 102(3): p. 1175-1181.

17. Khot, M., et al., Fungal production of single cell oil using untreated copra cake and evaluation of its fuel properties for biodiesel. J Microbiol Biotechnol, 2015. 25(4): p. 459-63.

18. Kumar, G., et al., Continuous Low Cost Transesterification Process for the Production of Coconut Biodiesel. Energies, 2010. 3(1): p. 43-56.

19. Lafont, J.J., A.A. Espitia, and J.R. Sodré, Potential vegetable sources for biodiesel production: cashew, coconut and cotton. Materials for Renewable and Sustainable Energy, 2015. 4(1).

20. Duncan, A.M., et al., High-Pressure Viscosity of Biodiesel from Soybean, Canola, and Coconut Oils. Energy & Fuels, 2010. 24(10): p. 5708-5716.

21. Habibullah, M., et al., Biodiesel production and performance evaluation of coconut, palm and their combined blend with diesel in a single-cylinder diesel engine. Energy Conversion and Management, 2014. 87: p. 250-257.

22. Atabani, A.E., et al., Effect of Croton megalocarpus, Calophyllum inophyllum, Moringa oleifera, palm and coconut biodiesel–diesel blending on their physico-chemical properties. Industrial Crops and Products, 2014. 60: p. 130-137.

23. Benjapornkulaphong, S., C. Ngamcharussrivichai, and K. Bunyakiat, Al2O3-supported alkali and alkali earth metal oxides for transesterification of palm kernel oil and coconut oil. Chemical Engineering Journal, 2009. 145(3): p. 468-474.

24. Kalam, M.A., M. Husnawan, and H.H. Masjuki, Exhaust emission and combustion evaluation of coconut oil-powered indirect injection diesel engine. Renewable Energy, 2003. 28(15): p. 2405-2415.

25. Pinzi, S., et al., Multiple response optimization of vegetable oils fatty acid composition to improve biodiesel physical properties. Bioresour Technol, 2011. 102(15): p. 7280-8.

26. Wakil, M.A., et al., Influence of biodiesel blending on physicochemical properties and importance of mathematical model for predicting the properties of biodiesel blend. Energy Conversion and Management, 2015. 94: p. 51-67.

27. Atabani, A.E., et al., A comparative evaluation of physical and chemical properties of biodiesel synthesized from edible and non-edible oils and study on the effect of biodiesel blending. Energy, 2013. 58: p. 296-304.

28. Aydin, F., et al., The Basic Properties of Transesterified Corn Oil and Biodiesel-Diesel Blends. Energy Sources, Part A: Recovery, Utilization, and Environmental Effects, 2011. 33(8): p. 745-751.

29. Tesfa, B., et al., Prediction models for density and viscosity of biodiesel and their effects on fuel supply system in CI engines. Renewable Energy, 2010. 35(12): p. 2752-2760.

30. Serqueira, D.S., et al., Influence of blending soybean, sunflower, colza, corn, cottonseed, and residual cooking oil methyl biodiesels on the oxidation stability. Fuel, 2014. 118: p. 16-20.

31. Hazar, H. and U. Ozturk, The effects of Al2O3–TiO2 coating in a diesel engine on performance and emission of corn oil methyl ester. Renewable Energy, 2010. 35(10): p. 2211-2216.

32. Demirbas, A., Prediction of Higher Heating Values for Biodiesels from Their Physical Properties. Energy Sources, Part A: Recovery, Utilization, and Environmental Effects, 2009. 31(8): p. 633-638.

33. Shehata, M.S., A.M.A. Attia, and S.M. Abdel Razek, Corn and soybean biodiesel blends as alternative fuels for diesel engine at different injection pressures. Fuel, 2015. 161: p. 49-58.

34. Patil, P.D. and S. Deng, Optimization of biodiesel production from edible and non-edible vegetable oils. Fuel, 2009. 88(7): p. 1302-1306.

35. Gülüm, M. and A. Bilgin, Density, flash point and heating value variations of corn oil biodiesel–diesel fuel blends. Fuel Processing Technology, 2015. 134: p. 456-464.

36. Demirbas, A., Relationships derived from physical properties of vegetable oil and biodiesel fuels. Fuel, 2008. 87(8-9): p. 1743-1748.

37. Prestes, R.A., et al., A rapid and automated low resolution NMR method to analyze oil quality in intact oilseeds. Anal Chim Acta, 2007. 596(2): p. 325-9.

38. Ramos, M.J., et al., Influence of fatty acid composition of raw materials on biodiesel properties. Bioresour Technol, 2009. 100(1): p. 261-8.

39. Ahmed, M., et al., Effect of biodiesel fuel properties and its blends on atomization. 2006, SAE Technical Paper.

40. Dmytryshyn, S.L., et al., Synthesis and characterization of vegetable oil derived esters: evaluation for their diesel additive properties. Bioresource Technology, 2004. 92(1): p. 55-64.

41. Eryilmaz, T., et al., Biodiesel production potential from oil seeds in Turkey. Renewable and Sustainable Energy Reviews, 2016. 58: p. 842-851.

42. Ozsezen, A.N., et al., Performance and combustion characteristics of a DI diesel engine fueled with waste palm oil and canola oil methyl esters. Fuel, 2009. 88(4): p. 629-636.

43. Albuquerque, M.C.G., et al., Properties of biodiesel oils formulated using different biomass sources and their blends. Renewable Energy, 2009. 34(3): p. 857-859.

44. Moser, B.R., Influence of blending canola, palm, soybean, and sunflower oil methyl esters on fuel properties of biodiesel. Energy & fuels, 2008. 22(6): p. 4301-4306.

45. Fernandes, D.M., et al., Preparation and characterization of methylic and ethylic biodiesel from cottonseed oil and effect of tert-butylhydroquinone on its oxidative stability. Fuel, 2012. 97: p. 658-661.

46. Nabi, M.N., M.M. Rahman, and M.S. Akhter, Biodiesel from cotton seed oil and its effect on engine performance and exhaust emissions. Applied thermal engineering, 2009. 29(11-12): p. 2265-2270.

47. Alhassan, Y., et al., Co-solvents transesterification of cotton seed oil into biodiesel: Effects of reaction conditions on quality of fatty acids methyl esters. Energy Conversion and Management, 2014. 84: p. 640-648.

48. Rashid, U., F. Anwar, and G. Knothe, Evaluation of biodiesel obtained from cottonseed oil. Fuel Processing Technology, 2009. 90(9): p. 1157-1163.

49. Demirbaş, A., Biodiesel from vegetable oils via transesterification in supercritical methanol. Energy conversion and management, 2002. 43(17): p. 2349-2356.

50. Karabektas, M., G. Ergen, and M. Hosoz, The effects of preheated cottonseed oil methyl ester on the performance and exhaust emissions of a diesel engine. Applied Thermal Engineering, 2008. 28(17-18): p. 2136-2143.

51. Moser, B.R., Fuel property enhancement of biodiesel fuels from common and alternative feedstocks via complementary blending. Renewable Energy, 2016. 85: p. 819-825.

52. Lingfeng, C., et al., Transesterification of cottonseed oil to biodiesel by using heterogeneous solid basic catalysts. Energy & Fuels, 2007. 21(6): p. 3740-3743.

53. Keera, S.T., S.M. El Sabagh, and A.R. Taman, Transesterification of vegetable oil to biodiesel fuel using alkaline catalyst. Fuel, 2011. 90(1): p. 42-47.

54. Okoro, L.N., et al., Thermodynamic and viscometric evaluation of biodiesel and blends from olive oil and cashew nut oil. Research journal of chemical sciences, 2011. 1(4): p. 90-97.

55. Rizwanul Fattah, I.M., et al., Effect of antioxidant on the performance and emission characteristics of a diesel engine fueled with palm biodiesel blends. Energy Conversion and Management, 2014. 79: p. 265-272.

56. Mofijur, M., et al., Assessment of Physical, Chemical, and Tribological Properties of Different Biodiesel Fuels, in Clean Energy for Sustainable Development. 2017. p. 441-463.

57. Salamanca, M., et al., Influence of palm oil biodiesel on the chemical and morphological characteristics of particulate matter emitted by a diesel engine. Atmospheric Environment, 2012. 62: p. 220-227.

58. Abu-Hamdeh, N.H. and K.A. Alnefaie, A comparative study of almond and palm oils as two bio-diesel fuels for diesel engine in terms of emissions and performance. Fuel, 2015. 150: p. 318-324.

59. Bunyakiat, K., et al., Continuous production of biodiesel via transesterification from vegetable oils in supercritical methanol. Energy & Fuels, 2006. 20(2): p. 812-817.

60. Kalam, M. and H. Masjuki, Biodiesel from palmoil—an analysis of its properties and potential. Biomass and Bioenergy, 2002. 23(6): p. 471-479.

61. Benjumea, P., J. Agudelo, and A. Agudelo, Effect of altitude and palm oil biodiesel fuelling on the performance and combustion characteristics of a HSDI diesel engine. Fuel, 2009. 88(4): p. 725-731.

62. Trakarnpruk, W. and S. Porntangjitlikit, Palm oil biodiesel synthesized with potassium loaded calcined hydrotalcite and effect of biodiesel blend on elastomer properties. Renewable Energy, 2008. 33(7): p. 1558-1563.

63. Mofijur, M., et al., Comparative evaluation of performance and emission characteristics of Moringa oleifera and Palm oil based biodiesel in a diesel engine. Industrial Crops and Products, 2014. 53: p. 78-84.

64. Ahmad, M., et al., Optimization of base catalyzed transesterification of peanut oil biodiesel. African Journal of Biotechnology, 2009. 8(3).

65. Kaya, C., et al., Methyl ester of peanut (Arachis hypogea L.) seed oil as a potential feedstock for biodiesel production. Renewable Energy, 2009. 34(5): p. 1257-1260.

66. Silveira Junior, E.G., et al., Potential of Virginia-type peanut (Arachis hypogaea L.) as feedstock for biodiesel production. Industrial Crops and Products, 2016. 89: p. 448-454.

67. Pinto, L.M., et al., Comparative evaluation of the effect of antioxidants added into peanut (arachis hypogae l.) oil biodiesel by P-DSC and rancimat. Journal of Thermal Analysis and Calorimetry, 2014. 120(1): p. 277-282.

68. Moser, B.R., Preparation of fatty acid methyl esters from hazelnut, high-oleic peanut and walnut oils and evaluation as biodiesel. Fuel, 2012. 92(1): p. 231-238.

69. Labeckas, G. and S. Slavinskas, The effect of rapeseed oil methyl ester on direct injection Diesel engine performance and exhaust emissions. Energy Conversion and Management, 2006. 47(13-14): p. 1954-1967.

70. Xin, J., H. Imahara, and S. Saka, Oxidation stability of biodiesel fuel as prepared by supercritical methanol. Fuel, 2008. 87(10-11): p. 1807-1813.

71. Kegl, B. and A. Hribernik, Experimental analysis of injection characteristics using biodiesel fuel. Energy & fuels,

2006. 20(5): p. 2239-2248.

72. Azcan, N. and A. Danisman, Microwave assisted transesterification of rapeseed oil. Fuel, 2008. 87(10-11): p. 1781-1788.

73. Tsolakis, A., et al., Engine performance and emissions of a diesel engine operating on diesel-RME (rapeseed methyl ester) blends with EGR (exhaust gas recirculation). Energy, 2007. 32(11): p. 2072-2080.

74. Dzida, M. and P. Prusakiewicz, The effect of temperature and pressure on the physicochemical properties of petroleum diesel oil and biodiesel fuel. Fuel, 2008. 87(10-11): p. 1941-1948.

75. Duz, M.Z., A. Saydut, and G. Ozturk, Alkali catalyzed transesterification of safflower seed oil assisted by microwave irradiation. Fuel Processing Technology, 2011. 92(3): p. 308-313.

76. Eryilmaz, T. and M.K. Yesilyurt, Influence of blending ratio on the physicochemical properties of safflower oil methyl ester-safflower oil, safflower oil methyl ester-diesel and safflower oil-diesel. Renewable Energy, 2016. 95: p. 233-247.

77. Çelebi, Y. and H. Aydın, Investigation of the effects of butanol addition on safflower biodiesel usage as fuel in a generator diesel engine. Fuel, 2018. 222: p. 385-393.

78. Işık, M.Z. and H. Aydın, Analysis of ethanol RCCI application with safflower biodiesel blends in a high load diesel power generator. Fuel, 2016. 184: p. 248-260.

79. Aydın, H., Scrutinizing the combustion, performance and emissions of safflower biodiesel–kerosene fueled diesel engine used as power source for a generator. Energy Conversion and Management, 2016. 117: p. 400-409.

80. Ilkılıç, C., et al., Biodiesel from safflower oil and its application in a diesel engine. Fuel Processing Technology, 2011. 92(3): p. 356-362.

81. Al-Samaraae, R., et al., Perspective of safflower (Carthamus tinctorius) as a potential biodiesel feedstock in Turkey: characterization, engine performance and emissions analyses of butanol–biodiesel–diesel blends. Biofuels, 2017: p. 1-17.

82. Rashid, U. and F. Anwar, Production of biodiesel through base-catalyzed transesterification of safflower oil using an optimized protocol. Energy & Fuels, 2008. 22(2): p. 1306-1312.

83. Karabas, H., Application of the Taguchi Method for the Optimization of Effective Parameters on the Safflower Seed Oil Methyl Ester Production. International Journal of Green Energy, 2014. 11(9): p. 1002-1012.

84. Özçelik, A.E. Determination of the Effects of Safflower Biodiesel and Its Blends with Diesel Fuel on Engine Performance and Emissions in a Single Cylinder Diesel Engine. in International Conference on Software Technology and Engineering, 3rd (ICSTE 2011). 2011. ASME Press.

85. Hamamci, C., et al., Biodiesel Production via Transesterification from Safflower (Carthamus tinctoriusL.) Seed Oil. Energy Sources, Part A: Recovery, Utilization, and Environmental Effects, 2011. 33(6): p. 512-520.

86. Wakil, M.A., et al., Evaluation of rice bran, sesame and moringa oils as feasible sources of biodiesel and the effect of blending on their physicochemical properties. RSC Adv., 2014. 4(100): p. 56984-56991.

87. Saydut, A., et al., Transesterified sesame (Sesamum indicum L.) seed oil as a biodiesel fuel. Bioresour Technol, 2008. 99(14): p. 6656-60.

88. Atapour, M. and H.-R. Kariminia, Optimization of Biodiesel Production from Iranian Bitter Almond Oil Using Statistical Approach. Waste and Biomass Valorization, 2013. 4(3): p. 467-474.

89. Rao, G.L.N., et al., Relationships among the physical properties of biodiesel and engine fuel system design requirement. International journal of energy and environment, 2010. 1(5): p. 919-926.

90. Valente, O.S., et al., Fuel consumption and emissions from a diesel power generator fuelled with castor oil and soybean biodiesel. Fuel, 2010. 89(12): p. 3637-3642.

91. Candeia, R.A., et al., Influence of soybean biodiesel content on basic properties of biodiesel–diesel blends. Fuel, 2009. 88(4): p. 738-743.

92. Moser, B.R. and S.F. Vaughn, Coriander seed oil methyl esters as biodiesel fuel: Unique fatty acid composition and excellent oxidative stability. Biomass and Bioenergy, 2010. 34(4): p. 550-558.

93. Sarin, R., et al., Jatropha–Palm biodiesel blends: An optimum mix for Asia. Fuel, 2007. 86(10-11): p. 1365-1371.

94. Vujicic, D., et al., Kinetics of biodiesel synthesis from sunflower oil over CaO heterogeneous catalyst. Fuel, 2010. 89(8): p. 2054-2061.

95. Porte, A.F., et al., Sunflower biodiesel production and application in family farms in Brazil. Fuel, 2010. 89(12): p. 3718-3724.

96. Saydut, A., et al., Process optimization for production of biodiesel from hazelnut oil, sunflower oil and their hybrid feedstock. Fuel, 2016. 183: p. 512-517.

97. Fadhil, A.B., A.M. Aziz, and M.H. Altamer, Potassium acetate supported on activated carbon for transesterification of new non-edible oil, bitter almond oil. Fuel, 2016. 170: p. 130-140.

98. Atapour, M. and H.-R. Kariminia, Characterization and transesterification of Iranian bitter almond oil for biodiesel production. Applied Energy, 2011. 88(7): p. 2377-2381.

99. Giwa, S.O., L.A. Chuah, and N.M. Adam, Fuel properties and rheological behavior of biodiesel from egusi (Colocynthis citrullus L.) seed kernel oil. Fuel Processing Technology, 2014. 122: p. 42-48.

100. Aburas, H. and A. Demirbas, Evaluation of beech for production of bio-char, bio-oil and gaseous materials. Process Safety and Environmental Protection, 2015. 94: p. 29-36.

101. Gonçalves, J.D., M. Aznar, and G.R. Santos, Liquid–liquid equilibrium data for systems containing Brazil nut biodiesel+methanol+glycerin at 303.15K and 323.15K. Fuel, 2014. 133: p. 292-298.

102. Latinwo, G.K., D.S. Aribike, and S.A. Kareem, Comparative study of biodiesels produced from unrefined vegetable oils. Nature and Science, 2010. 8(9): p. 102-106.

103. Vedharaj, S., et al., Experimental and finite element analysis of a coated diesel engine fueled by cashew nut shell liquid biodiesel. Experimental Thermal and Fluid Science, 2014. 53: p. 259-268.

104. Phoo, Z.W.M.M., et al., Physico-Chemical Properties of Biodiesel from Various Feedstocks, in Zero-Carbon Energy Kyoto 2012. 2013. p. 113-121.

105. Radhakrishnan, S., et al., Effect of nanoparticle on emission and performance characteristics of a diesel engine fueled with cashew nut shell biodiesel. Energy Sources, Part A: Recovery, Utilization, and Environmental Effects, 2018. 40(20): p. 2485-2493.

106. Devarajan, Y., D.B. Munuswamy, and B. Nagappan, Emissions analysis on diesel engine fuelled with cashew nut shell biodiesel and pentanol blends. Environ Sci Pollut Res Int, 2017. 24(14): p. 13136-13141.

107. Senthilkumar, G., et al., Evaluation of emission, performance and combustion characteristics of dual fuelled research diesel engine. Environ Technol, 2018: p. 1-8.

108. Bello, E., F. Out, and A. Osasona, Cetane number of three vegetable oils, their biodiesels and blends with diesel fuel. Journal of Petroleum Technology and Alternative Fuels, 2012. 3(5): p. 52-57.

109. Koçak, M.S., E. Ileri, and Z. Utlu, Experimental study of emission parameters of biodiesel fuels obtained from

canola, hazelnut, and waste cooking oils. Energy & fuels, 2007. 21(6): p. 3622-3626.

110. Çelikten, İ., E. Mutlu, and H. Solmaz, Variation of performance and emission characteristics of a diesel engine fueled with diesel, rapeseed oil and hazelnut oil methyl ester blends. Renewable Energy, 2012. 48: p. 122-126.

111. Gumus, M., Evaluation of hazelnut kernel oil of Turkish origin as alternative fuel in diesel engines. Renewable Energy, 2008. 33(11): p. 2448-2457.

112. Gülüm, M. and A. Bilgin, Measurements and empirical correlations in predicting biodiesel-diesel blends' viscosity and density. Fuel, 2017. 199: p. 567-577.

113. Xu, Y.X. and M.A. Hanna, Synthesis and characterization of hazelnut oil-based biodiesel. Industrial Crops and Products, 2009. 29(2-3): p. 473-479.

114. Rahman, M.M., et al., Effect of small proportion of butanol additive on the performance, emission, and combustion of Australian native first- and second-generation biodiesel in a diesel engine. Environ Sci Pollut Res Int, 2017. 24(28): p. 22402-22413.

115. Azad, A.K., et al., Biodiesel From Queensland Bush Nut (Macadamia integrifolia), in Clean Energy for Sustainable Development. 2017. p. 419-439.

116. Knothe, G., Biodiesel Derived from a Model Oil Enriched in Palmitoleic Acid, Macadamia Nut Oil. Energy & Fuels, 2010. 24(3): p. 2098-2103.

117. Azad, A.K., et al., Macadamia Biodiesel as a Sustainable and Alternative Transport Fuel in Australia. Energy Procedia, 2017. 110: p. 543-548.

118. Kivevele, T.T. and M.M. Mbarawa, Experimental Investigations of Oxidation Stability of Biodiesel Produced from Manketti Seeds Oil (Schinziophyton rautanenii). Energy & Fuels, 2011. 25(5): p. 2341-2346.

119. Kivevele, T.T. and Z. Huan, An Analysis of Fuel Properties of Fatty Acid Methyl Ester from Manketti Seeds Oil. International Journal of Green Energy, 2014. 12(4): p. 291-296.

120. Rutto, H.L. and C.C. Enweremadu, Optimization of Production Variables of Biodiesel from Manketti Using Response Surface Methodology. International Journal of Green Energy, 2011. 8(7): p. 768-779.

121. Khiari, K., et al., Experimental investigation of pistacia lentiscus biodiesel as a fuel for direct injection diesel engine. Energy Conversion and Management, 2016. 108: p. 392-399.

122. Samani, B.H., et al., Ultrasonic-assisted production of biodiesel from Pistacia atlantica Desf. oil. Fuel, 2016. 168: p. 22-26.

123. Ashok, B., et al., Lemon peel oil – A novel renewable alternative energy source for diesel engine. Energy Conversion and Management, 2017. 139: p. 110-121.

124. Kumar, P. and N. Kumar, Comparative study of biodiesel from Jatropha and orange peel oils as pilot fuels in a dual-fuel engine. Energy Sources, Part A: Recovery, Utilization, and Environmental Effects, 2016. 38(23): p. 3491-3496.

125. Tüccar, G., et al., Diesel engine emissions and performance from blends of citrus sinensis biodiesel and diesel fuel. Fuel, 2014. 132: p. 7-11.

126. Agarry, S., et al., Alkali-catalysed production of biodiesel fuel from Nigerian Citrus seeds oil. International Journal of Engineering Science and Technology, 2013. 5(9): p. 1682.

127. Deep, A., et al., Potential Utilization of the Blend of Orange Peel Oil Methyl Ester and Isopropyl Alcohol in CI Engine, in SAE Technical Paper Series. 2014.

128. Rashid, U., et al., Momordica CharantiaSeed Oil Methyl Esters: A Kinetic Study And Fuel Properties. International

Journal of Green Energy, 2014. 11(7): p. 727-740.

129. Giwa, S., L.C. Abdullah, and N.M. Adam, Investigating "Egusi" (Citrullus Colocynthis L.) Seed Oil as Potential Biodiesel Feedstock. Energies, 2010. 3(4): p. 607-618.

130. Schinas, P., et al., Pumpkin (Cucurbita pepo L.) seed oil as an alternative feedstock for the production of biodiesel in Greece. Biomass and Bioenergy, 2009. 33(1): p. 44-49.

131. Bello, E., S. Anjorin, and M. Agge, Production of biodiesel from fluted pumpkin (Telfairia occidentalis Hook F.) seeds oil. International Journal of Mechanical Engineering, 2011. 1(2).

132. Sokoto, M., et al., Influence of fatty acid methyl esters on fuel properties of biodiesel produced from the seeds oil of Curcubita pepo. Nigerian Journal of Basic and Applied Sciences, 2011. 19(1).

133. Ogunwole, O.A., Production of biodiesel from watermelon (Citrullus lanatus) seed oil. Leonardo J. Sci, 2015. 27: p. 63-74.

134. Asokan, M.A., et al., Performance, combustion and emission characteristics of diesel engine fuelled with papaya and watermelon seed oil bio-diesel/diesel blends. Energy, 2018. 145: p. 238-245.

135. Górnaś, P. and M. Rudzińska, Seeds recovered from industry by-products of nine fruit species with a high potential utility as a source of unconventional oil for biodiesel and cosmetic and pharmaceutical sectors. Industrial Crops and Products, 2016. 83: p. 329-338.

136. Panneerselvam, N., et al., Performance, emissions and combustion characteristics of CI engine fuel with watermelon (Citrullus vulgaris) methyl esters. International Journal of Ambient Energy, 2015. 38(3): p. 308-313.

137. Usta, N., et al., Properties and quality verification of biodiesel produced from tobacco seed oil. Energy Conversion and Management, 2011. 52(5): p. 2031-2039.

138. Pantoja, S.S., et al., Oxidative stability of biodiesels produced from vegetable oils having different degrees of unsaturation. Energy Conversion and Management, 2013. 74: p. 293-298.

139. Yunus Khan, T.M., et al., Ceiba pentandra , Nigella sativa and their blend as prospective feedstocks for biodiesel. Industrial Crops and Products, 2015. 65: p. 367-373.

140. Knothe, G., Fuel properties of methyl esters of borage and black currant oils containing methyl γ-linolenate. European Journal of Lipid Science and Technology, 2013. 115(8): p. 901-908.

141. Hoseini, S.S., et al., Characterization of biodiesel production (ultrasonic-assisted) from evening-primroses (Oenothera lamarckiana) as novel feedstock and its effect on CI engine parameters. Renewable Energy, 2019. 130: p. 50-60.

142. Demirbas, A., Production of biodiesel fuels from linseed oil using methanol and ethanol in non-catalytic SCF conditions. Biomass and Bioenergy, 2009. 33(1): p. 113-118.

143. Gumus, M. and S. Kasifoglu, Performance and emission evaluation of a compression ignition engine using a biodiesel (apricot seed kernel oil methyl ester) and its blends with diesel fuel. Biomass and Bioenergy, 2010. 34(1): p. 134-139.

144. Hotti, S.R. and O.D. Hebbal, Biodiesel Production Process Optimization from Sugar Apple Seed Oil (Annona squamosa) and Its Characterization. Journal of Renewable Energy, 2015. 2015: p. 1-6.

145. Sriram, V., J. Jeevahan, and A. Poovannan, Comparative study of performance of the DI diesel engine using custard apple biodiesel. International Journal of Ambient Energy, 2017. 40(1): p. 54-56.

146. Rachimoellah, H., et al., Production of biodiesel through transesterification of avocado (Persea gratissima) seed oil using base catalyst. Jurnal Teknik Mesin, 2010. 11(2): p. 85-90.

147. Nogueira Jr, C.A., et al., Densities and viscosities of binary mixtures of babassu biodiesel+ cotton seed or soybean biodiesel at different temperatures. Journal of Chemical & Engineering Data, 2010. 55(11): p. 5305-5310.

148. Cesur, C., et al., Cocklebur (Xanthium strumarium L.) seed oil andits properties as an alternative biodiesel source. Turkish Journal of Agriculture and Forestry, 2018. 42: p. 29-37.

149. Chapagain, B.P., Y. Yehoshua, and Z. Wiesman, Desert date (Balanites aegyptiaca) as an arid lands sustainable bioresource for biodiesel. Bioresour Technol, 2009. 100(3): p. 1221-6.

150. Bello, E., et al., Characterization and evaluation of African bush mango Nut (Dika nut)(Irvingia gabonensis) oil biodiesel as alternative fuel for diesel engines. Journal of Petroleum Technology and Alternative Fuels, 2011. 2(9): p. 176-180.

151. Nwufo, O.C., Effect of temperature on the biodiesel yield from Nigerian physic nut, castor bean, dika nut and sandbox seed oils. International Journal of Ambient Energy, 2013. 37(1): p. 16-19.

152. Patil, P.D., V.G. Gude, and S. Deng, Biodiesel production from Jatropha curcas, waste cooking, and Camelina sativa oils. Industrial & Engineering Chemistry Research, 2009. 48(24): p. 10850-10856.

153. Li, S.Y., et al., The feasibility of converting Cannabis sativa L. oil into biodiesel. Bioresour Technol, 2010. 101(21): p. 8457-60.

154. Ahmad, M., et al., Physicochemical Analysis of Hemp Oil Biodiesel: A Promising Non Edible New Source for Bioenergy. Energy Sources, Part A: Recovery, Utilization, and Environmental Effects, 2011. 33(14): p. 1365-1374.

155. Ragit, S.S., et al., Brown hemp methyl ester: Transesterification process and evaluation of fuel properties. Biomass and Bioenergy, 2012. 41: p. 14-20.

156. Yang, R., et al., One-pot process combining transesterification and selective hydrogenation for biodiesel production from starting material of high degree of unsaturation. Bioresour Technol, 2010. 101(15): p. 5903-9.

157. Stamenković, O.S., et al., Optimization of KOH-catalyzed methanolysis of hempseed oil. Energy Conversion and Management, 2015. 103: p. 235-243.

158. Silitonga, A.S., et al., Experimental study on performance and exhaust emissions of a diesel engine fuelled with Ceiba pentandra biodiesel blends. Energy Conversion and Management, 2013. 76: p. 828-836.

159. Vallinayagam, R., et al., Pine oil–biodiesel blends: A double biofuel strategy to completely eliminate the use of diesel in a diesel engine. Applied Energy, 2014. 130: p. 466-473.

160. Knothe, G., L.F. Razon, and F.T. Bacani, Kenaf oil methyl esters. Industrial Crops and Products, 2013. 49: p. 568-572.

161. Modiba, E., P. Osifo, and H. Rutto, The use of impregnated perlite as a heterogeneous catalyst for biodiesel production from marula oil. Chemical Papers, 2014. 68(10).

162. Moser, B.R., G. Knothe, and S.C. Cermak, Biodiesel from meadowfoam (Limnanthes alba L.) seed oil: oxidative stability and unusual fatty acid composition. Energy & Environmental Science, 2010. 3(3): p. 318-327.

163. Yerranguntla, R., et al., Production of Biodiesel from Guizotia abyssinica seed oil using crystalline Manganese carbonate (MnCO3) a Green catalyst. Catalysis for Sustainable Energy, 2012. 1.

164. Sarin, R., M. Sharma, and A.A. Khan, Studies on Guizotia abyssinica L. oil: biodiesel synthesis and process optimization. Bioresour Technol, 2009. 100(18): p. 4187-92.

165. Anwar, M., M.G. Rasul, and N. Ashwath, Production optimization and quality assessment of papaya (Carica papaya) biodiesel with response surface methodology. Energy Conversion and Management, 2018. 156: p. 103-112.

166. Wong, C. and R. Othman, Biodiesel production by enzymatic transesterification of papaya seed oil and rambutan seed oil. Int. J. Eng. Technol, 2014. 6: p. 2773-2777.

167. De Melo, M.L.S., et al., Use of thermal analysis techniques for evaluation of the stability and chemical properties of papaya biodiesel (Carica Papaya L.) at low temperatures. Journal of Thermal Analysis and Calorimetry, 2011. 106(3): p. 831-836.

168. Agunbiade, F.O. and T.A. Adewole, Methanolysis ofCarica papayaSeed Oil for Production of Biodiesel. Journal of Fuels, 2014. 2014: p. 1-6.

169. Silva, T.A., et al., Methylic and ethylic biodiesels from pequi oil (Caryocar brasiliense Camb.): Production and thermogravimetric studies. Fuel, 2014. 136: p. 10-18.

170. Borges, K.A., et al., Production of methyl and ethyl biodiesel fuel from pequi oil (Caryocar brasiliensis Camb.). Chemistry and Technology of Fuels and Oils, 2012. 48(2): p. 83-89.

171. Tüccar, G. and E. Uludamar, Emission and engine performance analysis of a diesel engine using hydrogen enriched pomegranate seed oil biodiesel. International Journal of Hydrogen Energy, 2018. 43(38): p. 18014-18019.

172. Lima, R.P., et al., Murumuru (Astrocaryum murumuru Mart.) butter and oils of buriti (Mauritia flexuosa Mart.) and pracaxi (Pentaclethra macroloba (Willd.) Kuntze) can be used for biodiesel production: Physico-chemical properties and thermal and kinetic studies. Industrial crops and products, 2017. 97: p. 536-544.

173. Rashid, U., et al., Optimization of alkaline transesterification of rice bran oil for biodiesel production using response surface methodology. Journal of Chemical Technology & Biotechnology, 2009. 84(9): p. 1364-1370.

174. Ahmad, M., et al., Physicochemical Characterization of Eco-friendly Rice Bran Oil Biodiesel. Energy Sources, Part A: Recovery, Utilization, and Environmental Effects, 2011. 33(14): p. 1386-1397.

175. El Boulifi, N., et al., Optimization and oxidative stability of biodiesel production from rice bran oil. Renewable Energy, 2013. 53: p. 141-147.

176. Sinha, S., A.K. Agarwal, and S. Garg, Biodiesel development from rice bran oil: Transesterification process optimization and fuel characterization. Energy Conversion and Management, 2008. 49(5): p. 1248-1257.

177. Zuleta, E.C., L.A. Rios, and P.N. Benjumea, Oxidative stability and cold flow behavior of palm, sacha-inchi, jatropha and castor oil biodiesel blends. Fuel Processing Technology, 2012. 102: p. 96-101.

178. Pochareddy, Y.K., et al., Performance and emission characteristics of a stationary direct injection compression ignition engine fuelled with diethyl ether–sapote seed oil methyl ester–diesel blends. Biofuels, 2016. 8(2): p. 297-305.

179. Kumar, A.R., G.J. Raju, and K.H. Reddy, Biodiesel production by alkaline transesterification of Mamey Sapote oil. International Journal for Research in Applied Science and Engineering Technology, 2016. 4(2): p. 391-396.

180. Enweremadu, C., H. Rutto, and J. Oladeji, Investigation of the relationship between some basic flow properties of shea butter biodiesel and their blends with diesel fuel. International Journal of Physical Sciences, 2011. 6(4): p. 758-767.

181. Ajala, E.O., et al., Optimization of a two stage process for biodiesel production from shea butter using response surface methodology. Egyptian Journal of Petroleum, 2017. 26(4): p. 943-955.

182. Bello, E.I. and A. Mamman, Shea Butter (Vitellaria paradoxa) Biodiesel. Journal: JOURNAL OF ADVANCES IN BIOTECHNOLOGY, 2015. 4(3).

183. Chakrabarti, M.H. and R. Ahmad, Investigating possibility of using least desirable edible oil of Eruca sativa L., in biodiesel production. Pakistan Journal of Botany, 2009. 41(1): p. 481-7.

184. Mumtaz, M.W., et al., Biodiesel production using Eruca sativa oil: optimization and characterization. Pakistan journal of botany, 2012. 44(3): p. 1111-1120.

185. Serin, H. and Ş. Yıldızhan, Hydrogen addition to tea seed oil biodiesel: Performance and emission characteristics. International Journal of Hydrogen Energy, 2018. 43(38): p. 18020-18027.

186. Takase, M., et al., Silybum marianum oil as a new potential non-edible feedstock for biodiesel: A comparison of its production using conventional and ultrasonic assisted method. Fuel Processing Technology, 2014. 123: p. 19-26.

187. Fadhil, A.B., A.M. Aziz, and M.H. Al-Tamer, Biodiesel production from Silybum marianum L. seed oil with high FFA content using sulfonated carbon catalyst for esterification and base catalyst for transesterification. Energy Conversion and Management, 2016. 108: p. 255-265.

188. Ahmad, M., et al., The Optimization of Biodiesel Production from a Novel Source of Wild Non-Edible Oil Yielding Plant Silybum Marianum. International Journal of Green Energy, 2013. 11(6): p. 589-594.

189. Usta, N., Use of tobacco seed oil methyl ester in a turbocharged indirect injection diesel engine. Biomass and Bioenergy, 2005. 28(1): p. 77-86.

190. Rao, B.S., et al., Studies on exhaust emissions and combustion characteristics of tobacco seed oil in crude form and biodiesel from a high grade low heat rejection diesel engine. International Journal of Industrial Engineering and Technology, 2013. 3(1): p. 27-36.

191. Veljkovic, V., et al., Biodiesel production from tobacco (Nicotiana tabacum L.) seed oil with a high content of free fatty acids. Fuel, 2006. 85(17-18): p. 2671-2675.

192. Sivasubramanian, H., et al., Investigation of biodiesel obtained from tomato seed as a potential fuel alternative in a CI engine. Biofuels, 2017: p. 1-9.

193. Dias, J.M., et al., Biodiesel production from raw castor oil. Energy, 2013. 53: p. 58-66.

194. Barminas, J., et al., A preliminary investigation into the biofuel characteristics of tigernut (Cyperus esculentus) oil. Bioresource technology, 2001. 79(1): p. 87-89.

195. Kaur, A., M. Roy, and K. Kundu, Transesterification process optimization for tung oil methyl ester (Aleurites fordii) and characterization of fuel as a substitute for diesel. IJCS, 2017. 5(6): p. 632-638.

196. Chen, Y.H., et al., Biodiesel production from tung (Vernicia montana) oil and its blending properties in different fatty acid compositions. Bioresour Technol, 2010. 101(24): p. 9521-6.

197. Sahoo, P.K. and L.M. Das, Process optimization for biodiesel production from Jatropha, Karanja and Polanga oils. Fuel, 2009. 88(9): p. 1588-1594.

198. Balan, K.N., et al., Investigation on emission characteristics of alcohol biodiesel blended diesel engine. Energy Sources, Part A: Recovery, Utilization, and Environmental Effects, 2018. 41(15): p. 1879-1889.

199. Diana da Silva Araújo, F., et al., Study of degumming process and evaluation of oxidative stability of methyl and ethyl biodiesel of Jatropha curcas L. oil from three different Brazilian states. Renewable Energy, 2014. 71: p. 495-501.

200. Mazumdar, P., et al., Physico-chemical characteristics of Jatropha curcas L. of North East India for exploration of biodiesel. Biomass and Bioenergy, 2012. 46: p. 546-554.

201. Shah, M., et al., Catalytic conversion of jojoba oil into biodiesel by organotin catalysts, spectroscopic and chromatographic characterization. Fuel, 2014. 118: p. 392-397.

202. Al-Hamamre, Z. and A. Al-Salaymeh, Physical properties of (jojoba oil+biodiesel), (jojoba oil+diesel) and (biodiesel+diesel) blends. Fuel, 2014. 123: p. 175-188.

203. Aslam, M., P. Saxena, and A.K. Sarma, Green Technology for Biodiesel Production From Mesua Ferrea L. Seed Oil. Energy and Environment Research, 2014. 4(2).

204. De, B. and D. Bhattacharyya, Biodiesel from minor vegetable oils like karanja oil and nahor oil. Lipid/Fett, 1999. 101(10): p. 404-406.

205. Devan, P.K. and N.V. Mahalakshmi, Utilization of unattended methyl ester of paradise oil as fuel in diesel engine. Fuel, 2009. 88(10): p. 1828-1833.

206. Mishra, S., et al., Production of bio-diesel (Methyl Ester) from Simarouba glauca oil. Research Journal of Chemical Sciences ISSN, 2012. 2231: p. 606X.

207. Mishra, S.R., et al., Optimisation of base-catalysed transesterification ofSimarouba glaucaoil for biodiesel production. International Journal of Sustainable Energy, 2013. 33(6): p. 1033-1040.

208. Baiju, B., M.K. Naik, and L.M. Das, A comparative evaluation of compression ignition engine characteristics using methyl and ethyl esters of Karanja oil. Renewable Energy, 2009. 34(6): p. 1616-1621.

209. Wang, R., et al., Production and selected fuel properties of biodiesel from promising non-edible oils: Euphorbia lathyris L., Sapium sebiferum L. and Jatropha curcas L. Bioresour Technol, 2011. 102(2): p. 1194-9.

210. Li, Q. and Y. Yan, Production of biodiesel catalyzed by immobilized Pseudomonas cepacia lipase from Sapium sebiferum oil in micro-aqueous phase. Applied Energy, 2010. 87(10): p. 3148-3154.

211. Liu, Y., H.-l. Xin, and Y.-j. Yan, Physicochemical properties of stillingia oil: Feasibility for biodiesel production by enzyme transesterification. Industrial Crops and Products, 2009. 30(3): p. 431-436.

212. Encinar, J.M., et al., Preparation and properties of biodiesel from Cynara C ardunculus L. oil. Industrial & Engineering Chemistry Research, 1999. 38(8): p. 2927-2931.

213. Fernández, J., M.D. Curt, and P.L. Aguado, Industrial applications of Cynara cardunculus L. for energy and other uses. Industrial Crops and Products, 2006. 24(3): p. 222-229.

214. Pereira Lima, R., et al., Murumuru (Astrocaryum murumuru Mart.) butter and oils of buriti (Mauritia flexuosa Mart.) and pracaxi (Pentaclethra macroloba (Willd.) Kuntze) can be used for biodiesel production: Physico-chemical properties and thermal and kinetic studies. Industrial Crops and Products, 2017. 97: p. 536-544.

215. Deshmukh, S.J. and L.B. Bhuyar, Transesterified Hingan (Balanites) oil as a fuel for compression ignition engines. Biomass and Bioenergy, 2009. 33(1): p. 108-112.

216. Naik, N.S. and B. Balakrishna, Experimental evaluation of a diesel engine fueled with Balanites aegyptiaca (L.) Del biodiesel blends. Biofuels, 2016. 7(6): p. 603-609.

217. Hasni, K., et al., Optimization of biodiesel production from Brucea javanica seeds oil as novel non-edible feedstock using response surface methodology. Energy Conversion and Management, 2017. 149: p. 392-400.

218. Pantoja, S.S., et al., High-Quality Biodiesel Production from Buriti (Mauritia flexuosa) Oil Soapstock. Molecules, 2018. 24(1).

219. Sulistyo, H., et al., Biodiesel production from high iodine number candlenut oil. World Acad. Sci. Eng. Technol, 2008. 48: p. 485-488.

220. Imdadul, H.K., et al., Experimental assessment of non-edible candlenut biodiesel and its blend characteristics as diesel engine fuel. Environ Sci Pollut Res Int, 2017. 24(3): p. 2350-2363.

221. Math, M.C. and H.L. Hegde, Experimental studies on performance and combustion characteristics of a compression ignition engine fuelled with Hydnocarpus wightiana methyl ester and its blends with conventional diesel and domestic kerosene. Biofuels, 2017. 9(6): p. 677-684.

222. Knothe, G., S.C. Cermak, and R.L. Evangelista, Cuphea oil as source of biodiesel with improved fuel properties caused by high content of methyl decanoate. Energy & fuels, 2009. 23(3): p. 1743-1747.

223. Dodos, G.S., et al., Renewable fuels and lubricants from Lunaria annua L. Industrial Crops and Products, 2015. 75: p. 43-50.

224. Ogunsuyi, H., Acid and base catalysed transesterification of mango (mangifera indica) seed oil to biodiesel. IOSR Journal of Applied Chemistry, 2012. 2(2): p. 18-22.

225. Velmurugan, K. and A.P. Sathiyagnanam, Impact of antioxidants on NO x emissions from a mango seed biodiesel powered DI diesel engine. Alexandria Engineering Journal, 2016. 55(1): p. 715-722.

226. Pillay, A.E., et al., A comparison of trace metal profiles of neem biodiesel and commercial biofuels using high performance ICP-MS. Fuel, 2012. 97: p. 385-389.

227. Anya, U.A., N.N. Chioma, and O. Obinna, Optimized reduction of free fatty acid content on neem seed oil, for biodiesel production. Journal of Basic and Applied Chemistry, 2012. 2(4): p. 21-28.

228. Aransiola, E.F., Production of biodiesel from crude neem oil feedstock and its emissions from internal combustion engines. African Journal of Biotechnology, 2012. 11(22).

229. Muthu, H., et al., Synthesis of biodiesel from neem oil using sulfated zirconia via tranesterification. Brazilian Journal of Chemical Engineering, 2010. 27(4): p. 601-608.

230. Bello, E.I., F. Otu, and S. Rao, Physicochemical Properties of Rubber (Hevea brasiliensis) Seed Oil, Its Biodiesel and Blends with Diesel. British Journal of Applied Science & Technology, 2015. 6(3): p. 261-275.

231. Demirbas, A., Production of Biodiesel from Tall Oil. Energy Sources, Part A: Recovery, Utilization, and Environmental Effects, 2008. 30(20): p. 1896-1902.

232. Altiparmak, D., et al., Alternative fuel properties of tall oil fatty acid methyl ester-diesel fuel blends. Bioresour Technol, 2007. 98(2): p. 241-6.

233. Jahirul, M.I., et al., Physio-chemical assessment of beauty leaf (Calophyllum inophyllum) as second-generation biodiesel feedstock. Energy Reports, 2015. 1: p. 204-215.

234. Peer, M.S., et al., Experimental evaluation on oxidation stability of biodiesel/diesel blends with alcohol addition by rancimat instrument and FTIR spectroscopy. Journal of Mechanical Science and Technology, 2017. 31(1): p. 455-463.

235. Mohanraj, T. and K.M. Mohan Kumar, Operating Characteristics of a Variable Compression Ratio Engine Using Esterified Tamanu Oil. International Journal of Green Energy, 2013. 10(3): p. 285-301.

236. Lima, J.R.d.O., et al. Indian-Nut (Aleurites Moluccana) and Tucum (Astrocaryum Vulgare); Non Agricultural Sources for Niodiesel Production Using Ethanol: Composition; Characterization and Optimization of the Reactional Production Conditions. in World Renewable Energy Congress-Sweden; 8-13 May; 2011; Linköping; Sweden. 2011. Linköping University Electronic Press.

237. Lima, J.R.d.O., et al., Biodiesel of tucum oil, synthesized by methanolic and ethanolic routes. Fuel, 2008. 87(8-9): p. 1718-1723.

238. Pelegrini, B.L., et al., Thermal and rheological properties of soapberry Sapindus saponaria L. (Sapindaceae) oil biodiesel and its blends with petrodiesel. Fuel, 2017. 199: p. 627-640.

239. Chakraborty, M. and D.C. Baruah, Production and characterization of biodiesel obtained from Sapindus mukorossi kernel oil. Energy, 2013. 60: p. 159-167.

240. Deka, D.C. and S. Basumatary, High quality biodiesel from yellow oleander (Thevetia peruviana) seed oil. Biomass and Bioenergy, 2011. 35(5): p. 1797-1803.

241. Yadav, A.K., et al., Biodiesel production from Nerium oleander (Thevetia peruviana) oil through conventional and ultrasonic irradiation methods. Energy Sources, Part A: Recovery, Utilization, and Environmental Effects, 2016. 38(23): p. 3447-3452.

242. Ang, G.T., et al., Optimization and kinetic studies of sea mango (Cerbera odollam) oil for biodiesel production via supercritical reaction. Energy Conversion and Management, 2015. 99: p. 242-251.

243. Nayak, S.K. and P.C. Mishra, Application of Nagchampa biodiesel and rice husk gas as fuel. Energy Sources, Part A: Recovery, Utilization, and Environmental Effects, 2016. 38(14): p. 2024-2030.

244. Gole, V.L. and P.R. Gogate, Intensification of Synthesis of Biodiesel from Nonedible Oils Using Sonochemical Reactors. Industrial & Engineering Chemistry Research, 2012. 51(37): p. 11866-11874.

245. Kivevele, T.T. and M.M. Mbarawa, Comprehensive Analysis of Fuel Properties of Biodiesel from Croton megalocarpus Oil. Energy & Fuels, 2010. 24(11): p. 6151-6155.

246. Haik, Y., M.Y.E. Selim, and T. Abdulrehman, Combustion of algae oil methyl ester in an indirect injection diesel engine. Energy, 2011. 36(3): p. 1827-1835.

247. Xiao, Y., et al., Industrial Fermentation of Auxenochlorella protothecoides for Production of Biodiesel and Its Application in Vehicle Diesel Engines. Front Bioeng Biotechnol, 2015. 3: p. 164.

248. Chen, Y.-H., et al., Fuel properties of microalgae (Chlorella protothecoides) oil biodiesel and its blends with petroleum diesel. Fuel, 2012. 94: p. 270-273.

249. Satputaley, S.S., D.B. Zodpe, and N.V. Deshpande, Performance, combustion and emission study on CI engine using microalgae oil and microalgae oil methyl esters. Journal of the Energy Institute, 2017. 90(4): p. 513-521.

250. Xu, H., X. Miao, and Q. Wu, High quality biodiesel production from a microalga Chlorella protothecoides by heterotrophic growth in fermenters. J Biotechnol, 2006. 126(4): p. 499-507.

251. Singh, D., et al., Transient performance and emission characteristics of a heavy-duty diesel engine fuelled with microalga Chlorella variabilis and Jatropha curcas biodiesels. Energy Conversion and Management, 2015. 106: p. 892-900.

252. Kalhor, A.X., et al., Biodiesel production in crude oil contaminated environment using Chlorella vulgaris. Bioresource technology, 2016. 222: p. 190-194.

253. Mathimani, T., L. Uma, and D. Prabaharan, Homogeneous acid catalysed transesterification of marine microalga Chlorella sp. BDUG 91771 lipid – An efficient biodiesel yield and its characterization. Renewable Energy, 2015. 81: p. 523-533.

254. Arunachalam Sivagurulingam, A.P., et al., Optimization and kinetic studies on biodiesel production from microalgae (Euglena sanguinea) using calcium methoxide as catalyst. Energy Sources, Part A: Recovery, Utilization, and Environmental Effects, 2018. 41(12): p. 1497-1507.

255. Kings, A.J., et al., Cultivation, extraction and optimization of biodiesel production from potential microalgae Euglena sanguinea using eco-friendly natural catalyst. Energy Conversion and Management, 2017. 141: p. 224-235.

256. Petersen, J., et al., Combustion Characterization and Ignition Delay Modeling of Low- and High-Cetane Alternative Diesel Fuels in a Marine Diesel Engine. Energy & Fuels, 2014. 28(8): p. 5463-5471.

257. Khan, A.M. and N. Fatima, Biodiesel synthesis via metal oxides and metal chlorides catalysis from marine alga Melanothamnus afaqhusainii. Chinese Journal of Chemical Engineering, 2016. 24(3): p. 388-393.

258. Nautiyal, P., K.A. Subramanian, and M.G. Dastidar, Production and characterization of biodiesel from algae. Fuel Processing Technology, 2014. 120: p. 79-88.

259. Hong, D.D., et al., Biodiesel production from Vietnam heterotrophic marine microalga Schizochytrium mangrovei PQ6. J Biosci Bioeng, 2013. 116(2): p. 180-5.

260. Mostafa, S.S.M. and N.S. El-Gendy, Evaluation of fuel properties for microalgae Spirulina platensis bio-diesel and its blends with Egyptian petro-diesel. Arabian Journal of Chemistry, 2017. 10: p. S2040-S2050.

261. Barrios, C.C., et al., Effects of animal fat based biodiesel on a TDI diesel engine performance, combustion characteristics and particle number and size distribution emissions. Fuel, 2014. 117: p. 618-623.

262. Armas, O., A. Gómez, and Á. Ramos, Comparative study of pollutant emissions from engine starting with animal fat biodiesel and GTL fuels. Fuel, 2013. 113: p. 560-570.

263. Ballesteros, R., E. Monedero, and J. Guillén-Flores, Determination of aldehydes and ketones with high atmospheric reactivity on diesel exhaust using a biofuel from animal fats. Atmospheric Environment, 2011. 45(16): p. 2690-2698.

264. Awad, S., K. Loubar, and M. Tazerout, Experimental investigation on the combustion, performance and pollutant emissions of biodiesel from animal fat residues on a direct injection diesel engine. Energy, 2014. 69: p. 826-836.

265. Öner, C. and Ş. Altun, Biodiesel production from inedible animal tallow and an experimental investigation of its use as alternative fuel in a direct injection diesel engine. Applied Energy, 2009. 86(10): p. 2114-2120.

266. Teixeira, L.S.G., et al., Comparison between conventional and ultrasonic preparation of beef tallow biodiesel. Fuel Processing Technology, 2009. 90(9): p. 1164-1166.

267. Sander, A., et al., The influence of animal fat type and purification conditions on biodiesel quality. Renewable Energy, 2018. 118: p. 752-760.

268. Araújo, B.Q., et al., Synthesis and Characterization of Beef Tallow Biodiesel. Energy & Fuels, 2010. 24(8): p. 4476-4480.

269. Sbihi, H.M., et al., Production and characterization of biodiesel from Camelus dromedarius (Hachi) fat. Energy Conversion and Management, 2014. 78: p. 50-57.

270. Bhatti, H., et al., Biodiesel production from waste tallow. Fuel, 2008. 87(13-14): p. 2961-2966.

271. de Guzman, R., et al., Synergistic Effects of Antioxidants on the Oxidative Stability of Soybean Oil- and Poultry Fat-Based Biodiesel. Journal of the American Oil Chemists' Society, 2009. 86(5): p. 459-467.

272. Alptekin, E., et al., Using waste animal fat based biodiesels–bioethanol–diesel fuel blends in a DI diesel engine. Fuel, 2015. 157: p. 245-254.

273. Godiganur, S., C. Suryanarayana Murthy, and R.P. Reddy, Performance and emission characteristics of a Kirloskar HA394 diesel engine operated on fish oil methyl esters. Renewable Energy, 2010. 35(2): p. 355-359.

274. Gnanasekaran, S., N. Saravanan, and M. Ilangkumaran, Influence of injection timing on performance, emission and combustion characteristics of a DI diesel engine running on fish oil biodiesel. Energy, 2016. 116: p. 1218-1229.

275. Swaminathan, C. and J. Sarangan, Performance and exhaust emission characteristics of a CI engine fueled with biodiesel (fish oil) with DEE as additive. Biomass and Bioenergy, 2012. 39: p. 168-174.

276. Behçet, R., Performance and emission study of waste anchovy fish biodiesel in a diesel engine. Fuel Processing Technology, 2011. 92(6): p. 1187-1194.

277. Dias, J.M., M.C. Alvim-Ferraz, and M.F. Almeida, Production of biodiesel from acid waste lard. Bioresour Technol, 2009. 100(24): p. 6355-61.

278. Ramalho, E.F.S.M., et al., Low temperature behavior of poultry fat biodiesel:diesel blends. Fuel, 2012. 93: p. 601-605.

279. Tang, H., S.O. Salley, and K.S. Ng, Fuel properties and precipitate formation at low temperature in soy-, cottonseed-, and poultry fat-based biodiesel blends. Fuel, 2008. 87(13-14): p. 3006-3017.

280. Can, Ö., Combustion characteristics, performance and exhaust emissions of a diesel engine fueled with a waste cooking oil biodiesel mixture. Energy Conversion and Management, 2014. 87: p. 676-686.

281. Cai, Z.-Z., et al., A two-step biodiesel production process from waste cooking oil via recycling crude glycerol esterification catalyzed by alkali catalyst. Fuel Processing Technology, 2015. 137: p. 186-193.

282. Lin, Y.-C., K.-H. Hsu, and C.-B. Chen, Experimental investigation of the performance and emissions of a heavy-duty diesel engine fueled with waste cooking oil biodiesel/ultra-low sulfur diesel blends. Energy, 2011. 36(1): p. 241-248.

283. Maddikeri, G.L., P.R. Gogate, and A.B. Pandit, Intensified synthesis of biodiesel using hydrodynamic cavitation reactors based on the interesterification of waste cooking oil. Fuel, 2014. 137: p. 285-292.

284. Muralidharan, K. and D. Vasudevan, Performance, emission and combustion characteristics of a variable compression ratio engine using methyl esters of waste cooking oil and diesel blends. Applied Energy, 2011. 88(11): p. 3959-3968.

285. Lin, Y.-S. and H.-P. Lin, Study on the spray characteristics of methyl esters from waste cooking oil at elevated temperature. Renewable Energy, 2010. 35(9): p. 1900-1907.

286. Sahar, et al., Biodiesel production from waste cooking oil: An efficient technique to convert waste into biodiesel. Sustainable Cities and Society, 2018. 41: p. 220-226.

287. Sanek, L., et al., Pilot-scale production of biodiesel from waste fats and oils using tetramethylammonium hydroxide. Waste Manag, 2016. 48: p. 630-637.

288. Atmanli, A., Comparative analyses of diesel–waste oil biodiesel and propanol, n-butanol or 1-pentanol blends in a diesel engine. Fuel, 2016. 176: p. 209-215.

289. Utlu, Z. and M.S. Koçak, The effect of biodiesel fuel obtained from waste frying oil on direct injection diesel engine performance and exhaust emissions. Renewable Energy, 2008. 33(8): p. 1936-1941.

290. Ozsezen, A.N. and M. Canakci, The emission analysis of an IDI diesel engine fueled with methyl ester of waste frying palm oil and its blends. Biomass and Bioenergy, 2010. 34(12): p. 1870-1878.

291. Buyukkaya, E., et al., Effects of trout-oil methyl ester on a diesel engine performance and emission characteristics. Energy Conversion and Management, 2013. 69: p. 41-48.

292. Yang, S., et al., Biodiesel production from swine manure via housefly larvae (Musca domestica L.). Renewable Energy, 2014. 66: p. 222-227.

293. Kalargaris, I., G. Tian, and S. Gu, Combustion, performance and emission analysis of a DI diesel engine using plastic pyrolysis oil. Fuel Processing Technology, 2017. 157: p. 108-115.

294. Hossain, A.K., et al., Experimental investigation of performance, emission and combustion characteristics of an indirect injection multi-cylinder CI engine fuelled by blends of de-inking sludge pyrolysis oil with biodiesel. Fuel, 2013. 105: p. 135-142.

295. Alagu, R.M. and E. Ganapathy Sundaram, Preparation and characterization of pyrolytic oil through pyrolysis of neem seed and study of performance, combustion and emission characteristics in CI engine. Journal of the Energy Institute, 2018. 91(1): p. 100-109.

296. Demirbas, A., Political, economic and environmental impacts of biofuels: A review. Applied energy, 2009. 86: p. S108-S117.

Advances in Biotechnology

Chapter 5

Molecular Regulation of Preimplantation Development of Farm Animals

Nasser Ghanem[1,]; Romysa Samy[1]; MD Fakruzzamana[2]; Ibrahim Abdalla Hassan Barakat[3,4]; Kong IK[5]*

[1]*Animal Production Department, Faculty of Agriculture, Cairo University Research Park, Cairo University, Egypt.*

[2]*Department of Genetics and Animal Breeding, Faculty of Animal Science and Veterinary Medicine, Patuakhali Science and Technology University, Out Campus, Khanpura, Babuganj, Barishal-8210, Bangladesh.*

[3]*Zoology Department, College of Science, King Saud University, Riyadh, Saudi Arabia.*

[4]*Cell Biology Department, National Research Center, Dokki, Giza, Egypt.*

[5]*Division of Applied Life Science (BK21), Graduate School of Gyeongsang National University, Jinju 660-701, Republic of Korea.*

***Correspondence to: Nasser Ghanem (Ph.D),** Animal Production Department, Faculty of Agriculture, Cairo University Research Park, Cairo University, Egypt.*

Email: nassergo@agr.cu.edu.eg

Background

Preimplantation period is the early series of events required to establish pregnancy. Therefore, it is one of the main research focus all over the world. The early classic studies was based on *in vivo* model to monitor the success of fertilization based on superovulation and embryo flushing at different time points. However, application of *in vitro* embryo production has advanced our understanding on the molecular regulation of the events encompass this crucial period. Indeed, different approaches and molecular techniques have been performed to get deep insights into the molecular mechanisms controlling early events of preimplantation embryo development of several mammalian species. Semi- and quantitative real-time polymerase chain reaction was first introduced as gene-by-gene approach to study spatiotemporal regulation of well-known candidate genes and their involvement in determining the quality of oocytes and embryos. Another interesting focus of research was to identify the alterations of transcript abundance of candidate genes in response to various biological conditions like *in vivo* and *in vitro* culture conditions. The polyadenylation pattern during oocyte maturation and

embryonic development was the key molecular mechanism that was investigated deeply in many laboratories. Recently, genome-wide assessment strategies of omics approaches (transcriptomics, miRNAomics, proteomics, lipidomics and metabolomics) have been applied to profile all detailed structural and functional changes of the whole genome in attempt to use this knowledge in downstream applications and practices. Although, the great efforts have been done in this field during the last decades, the applications are still in the infancy stage. In this chapter, more highlights will be focused on all attempts has been made in this field.

1. Introduction

The reproductive performance of a herd is the biggest factor affecting production and product quality of livestock. Thus, a decline of either the female or the male fertility represents a dramatic economic loss in beef and dairy industries. Therefore, it would be of great importance to define and manage the biological factors contributing to livestock fertility. In large animal farm management, individual male could serve thousands of females worldwide through application of artificial insemination. Therefore, a genetic mutation related to certain phenotypic trait(s) of one male will transmitted to have a global economic impact. Thus, a single male has a larger impact on herd productivity than fertility of a single female. Additionally, sperm viability is a determinant factor, which affects success rate of fertilization, and embryo production [1]. Subsequently, the expression of compromised genetic information from the spermatozoa can impair embryo quality [2]. A study done in bovine bulls has detected novel genetic loci harboring ITGB5 gene, which associated with the bull reproductive performance by controlling sperm-oocyte interaction, and resulted embryo development [3]. Expression profile of selected genes was used as a good indicator for the physiochemical parameters of semen collected from farm animals' males of different species [4, 5 and 6]. This confirms the involvement of sperm genes in various reproductive processes such as spermatogenesis, sperm motion [7]. fertilization of ova and subsequent preimplantation development [8].

On the female side, animal breeders normally select dairy cows based on milk record as the main phenotypic (productive) trait, which resulted in fertility decline of their progeny during next generations [9]. This attitude has resulted in compromising fertility of highly milk producing which was measured by the reduction of first service conception rate from approximately 65% in 1951 to 40% in 1996 [10]. Buffalo breeding is faced with the low fertility rate, which leads to high economic loss under heat stress conditions [11]. In this regard, cumulus-oocytes complexes are highly affected when the female is exposed to environmental heat stress during follicular development, ovulation and in vivo events of oocyte maturation [12, 13, 14]. Buffalo cumulus-oocyte complexes that were collected during hot season had a high percentage of arrested oocytes in metaphase I stage of nuclear progression after in vitro maturation [15]. Interestingly, bovine oocytes that have been exposed to increased temperatures at 40.0°C and 41.0°C recorded lower rates of nuclear and cytoplasmic maturation that was

linked with reduced in vitro embryo development [16]. In support to previous observation, experimental exposure of COCs to heat shock during the maturation has revealed reduced cleavage rate as well as blastocyst development [17]. In vivo experiments have reported reduced pregnancy rate by 25% for each °C elevation in body temperature, which is due to the negative impact of heat stress on preimplantation development embryos [18]. The expression of stress indictor gene known as HSP70 was increased in buffalo oocytes collected under heat stress condition compared to those collected in cold season [19]. [20] have reported greater expression profile of genes related to thermal stress (HSP 70.1 and HSP 70.2) and cell death inducing genes (CASPASE-3, BID and BAX) in buffalo embryos (8-16-cell and blastocyst stages) exposed to 39.5°C and 40.5°C than that in control group. This implicates that exposure of buffalo preimplantation stages of development to heat stress even for short duration reduced embryo development rate and this was regulated by increase cell death genes and embryo try to resist this negative effect by upregulation of heat shock genes.

The key biological factor that is behind the reduced fertility either in high milk producing cows and under heat stress is the poor oocyte, which compromise embryonic development qualities [21, 18]. It was established that the molecular mechanisms linked with low developmental potential of bovine oocytes is highly complex and may be reliant on many small changes in the RNA levels of many genes [22,23]. There is a clear relationship between altered transcript abundance patterns and some aspects of embryo quality (i.e. cryotolerance), which render the embryo capable of establishing a pregnancy, if transferred fresh, but incapable of withstanding cryopreservation [24,25]. The main factors implicated in embryo and fetal loss can be categorized as those of intrinsic genetic problems, environmental factors like heat stress, failures in maternal physiological environment, and endocrine related problems like unsuccessful embryo-maternal communication [26,27,28]. It has been stated, that aberrant gene expression either in the uterine endometrium [29] or in the embryo [29-32] is the major cause of pregnancy failure in cattle. Early embryogenesis depends on a tightly choreographed succession of gene expression patterns involved in different biological processes, which define normal development [33, 34]. Even a defect in a single gene is sufficient to cause implantation failure [35]. In this regard, all HSP40 family genes were found to be up-regulated in degenerate embryos versus blastocysts [36]. In addition, heat shock protein gene Hsp70.1 was up-regulated in blastocysts produced in vitro compared to in vivo embryos [37]. Identification of preimplantation gene regulation and functional analysis of key expressed molecular markers is crucial to understand and control important events ecompassed this period to improve farm animals' fertility. Therefore, this chapter aims to highlights research has been done in the molecular regulation of preimplantation development.

1.1. Approaches of large-scale expression analysis in bovine

The advent of high-throughput analyses of gene sequence and transcriptional regulation

has advanced our understanding of cellular and molecular activity of certain biological process. In particular, array technology is nowadays a powerful gene expression profile tool. Researchers have used gene-by-gene approach to identify gene expression before the availability of genome wide approaches such as microarray and next generation sequencing (NGS). Traditional polymerase chain reaction (PCR) has been performed to profile the expression of housekeeping genes during in vitro maturation of buffalo oocytes [38, 39]. While, quantitative real/time PCR was use to compare gene expression of key regulatory genes in bovine embryos produced either in vitro and in vivo [37]. Global approaches have been introduced to get deep insights into the molecular regulation of specific event during preimplantation development. For example, differential display and suppressive subtractive hybridization were used to define transcript abundance of genes associated with developmental competence of bovine oocytes [40]. cDNA array approach was done to identify genes differentially regulated during bovine oocyte maturation using human specific array [41]. Nevertheless, significant research efforts have been devoted to the development of cDNA resources in all major livestock species in the last few years.

Gene expression analysis using microarrays is a promising approach enabling global gene profiling to define the big picture of early embryo development. However, mRNA analysis in oocytes/embryos has to overcome many technical hurdles caused by the limited quantity of materials available and the biology of tissue studied [42]. Many universities and research institutes have tried to generate their own specific array as platform for global gene expression analysis. A large bovine microarray containing over 18,000 EST clones was developed [43]. Although this array covers a significant portion of the bovine genome, transcripts of oocyte origin may be under-represented, since the expressed sequence tags (ESTs) used for construction of this large array were derived from libraries of mixed tissue origin. A collaborative program named GINGER (Gene Index for Gene Expression profiling in Ruminants) has constructed a ruminant cDNA array with 1896 clones collected from non-normalised cDNA libraries of three tissues (muscle, embryo and mammary gland). This array was developed to be resource for gene expression profiling in ruminant tissues involved in reproduction and production (milk and beef) traits. Bovine cDNA array namely BlueChip containing ~2000 randomly selected clones was constructed from four different subtraction suppressive hybridizations (SSH) between bovine embryos and somatic tissues [42] is one of the bovine preimplantation specific array. A cDNA microarray with over 2000 randomly selected cDNA clones was generated from bovine oocyte library and was used to identify genes highly expressed in fetal ovary (an enriched source of oocytes) relative to adult spleen and liver tissues [44]. Investigation in gene expression at the level of the mRNA in mammalian reproductive tract during early embryonic development may help to identify genes, which are involved in embryo-maternal communications [45]. In the last few years both cDNA and oligonucleotide microarray technology have been successfully applied to study endometrial gene expression (reviewed in Giudice 2003). In order to, identify

embryo induced transcriptome changes in bovine endometrium a combination of SSH and cDNA microarray have been applied to compare the gene expression between uterine samples from pregnant and no pregnant heifers [46].

Functional genomics studies of oocyte competence was conducted using bovine cDNA array containing expressed sequence tags (ESTs) representing approximately 15 200 unique genes [47]. Affymetrix bovine-specific DNA microarray is the biggest available array (with >23,000 transcripts) was used for global transcription analysis in matured bovine oocytes and 8-cell embryos [48]. Global gene expression profiles of mouse and human preimplantation embryos from the GV oocyte to blastocyst stages have been established via microarray analyses using in vitro-transcribed antisense RNA as amplified target material [49]. In addition, cDNA microarrays contained 932 bovine EST clone inserts has identified a range of mRNA transcripts that are differentially expressed between bovine blastocysts derived from in vitro versus in vivo culture [50]. The transcriptome dynamics throughout preimplantation development o bovine was done using NGS to find out distinct cluster of gene regulators [51]. Furthermore, a multi-species cDNA microarray containing 3,456 transcripts from three distinct oocyte-libraries from bovine, mouse and Xenopus laevis were constructed to identify genes expressed in oocytes and conserved in these distant species [52]. Recently, the integrated interaction of ovarian miRNA and mRNA was performed in sheep to detect genes regulating prolificacy trait using NGS [53, 54].

2. Sperm RNA Population

Sperm is a differentiated cell, has a specific function which deliver the haplotype to the oocyte, it seems a simple mission, among species sperm phenotype shows a high degree of variation such as sperm size [55], studies documented that sperm not only delivers the DNA to egg but also complex RNA which it is difficult to explain [56,57]. During the replacement protamines with histones to compact DNA, a lot of changes occur in chromatin so RNA originates not from DNA transcription [56,58] and not dismiss from sperm formation process for two reasons, firstly RNA stored in sperm cell used as a substrate to activate RNA translation process [56], secondly RNA share during fertilization and embryo development [56,57,59].

The sperm has a large RNA population which is identified in many species including insects [56] and plant [60] and mainly localized in sperm head (Johnson et al. 2015) including messenger RNA (mRNA), micro- RNA (miRNA), interference RNA (iRNA), and antisense RNA [61]. and also can be characterized as coding RNAs, long non-coding RNAs (lncRNAs) and small non-coding RNAs (sncRNAs) [62] (Das et al. 2013; Jodar et al. 2013; 2015, Sendler et al. 2013; Pantano et al. 2015; Selvaraju et al. 2017; Zhang et al. 2017). Sperm RNA transcripts heat shock proteins, cytochrome P450 aromatase and wide range of receptors [61]. Large number of non-coding RNAs has potential biological functions (Jodar et al. 2013), whereas

a large number of sperm-specific non-coding RNAs have been identified, including intron retained regions and short expression regions (Jodar et al. 2013, Sendler et al. 2013, Selvaraju et al. 2017). Around 880 sperm lncRNAs seem conserves between human and mouse, however their functions are unknown (Zhang et al. 2017).

The RNA-sequencing technology (RNA-seq) is a useful tool in studying of spermatozoa ribosomal RNAs (rRNA) and has revealed that ribosomal RNAs (rRNAs) represent in from human, pig, stallion and bull sperms (around 80% of total RNA), but in mice the rRNAs represent only 30% of total RNA (Das et al. 2013; Jodar et al. 2013; Johnson et al. 2015; Selvaraju et al. 2017; Gòdia et al. 2018a). The detection of mature sperm RNA explains the role of coding RNA fermentation in transcriptional shutdown during this stage. The spermatozoon's intact transcripts selectively protected from degradation and it may have a vital role during spermatid maturation, fertilization and early embryogenesis (Sendler et al. 2013; Selvaraju et al. 2017).

2.1. Transcription and RNA storage during spermatogenesis

During spermatids maturation the absence of protein synthesis synchronize with a progressive decline in stored RNA. DNA transcription to RNA is also canceled in spermatids before and during the DNA condensation onto protamines [56], [58] because the DNA-protamine is condensed at least six times efficient than DNA-histone (minimization the volume of the nucleus) [63] and DNA toroid structures formation occur when protamine DNA becomes super condensed in later stage of spermatids formation. This toroid structure can be microscopically visualized approximately 50,000 base pairs of DNA [64] instead of the 146 base pairs of DNA for coiled twice [65] and linked to other toroids to form (DNase sensitive toroid) linked with region in which the DNA remains folding with histones [66]. The DNA toroids have not enough space to allow for RNA storage in opposite during spermatid chromatin condensation. The toroids links with the periphery of the nucleus and called (the peri-nuclear theca) [67]. These toroid structures protect the DNA from mutation, toxies and free radical [68]. The DNA amount is wrapped to protamines showed a different percentage for most mammalian species >98% of total DNA [69, 70], but for human sperm approximately 90% [68]. The super condensation minimize the volume leading to cellular process silencing and this is required for maintaining the sperm ability as a specialized cell deliver the haploid to the oocyte.

2.2. Biological roles of sperm molecules delivers to the oocyte

The microgamete sperm cell with delivers only the haploid genome to the oocyte which is called a macrogamete to contribute the cellular organelle required for embryogenesis as cytosol [71] and mitochondria because sperm structures are destroyed by the fertilized oocyte [72]. But it was observed that the meiosis II division activation in the fertilized oocyte [71] related to the sperm's centrosome (non-genomic) which is critical factor for embryo development in mammals not in rodents [73], [74] and prove that the sperm can deliver more than genomic

material [75].

Also sperm cell transports specific phosphor-lipase C-z to the oocyte, which is present in pre-nuclear theca of head and necessary for embryonic development activation [76], [77].

The increase of Ca2+ during fertilization induces the oocyte to complete meiosis and subsequently to begin in embryonic development. The signals required for oocytes calcium oscillations begin after fertilization and showed as PLC-z [76,78]. In addition, peri-nuclear theca proteins coding other molecules working as a signals involved in different protein kinase pathways but other transcriptional factors and structural proteins [79,80], activate the oocyte meiosis activation process and pronuclear development [57] need to be deeply studied. Some of sperm components are believed that slowly degrade such as mitochondria and others preserve until late embryonic stages [57,81].

2.3. RNA transfer to the oocyte and its functions

At early studies on sperm RNA, there was a belief that sperm RNA is non-functional and remain from the spermatid gene expression, on the other side, it was predicted that sperm RNA has a role after fertilization in formation of male pronucleus [82,83]. Recently among other cellular factors, is supposed that RNA affect on embryo development [84]. The first time that the three different types of sperm mRNA can be identified, the fertilizing sperm can transfer mRNA into the oocyte, which can be intact for at least 3 h post-fertilization. At least five sperm specific mRNA were recovered in oocytes post-fertilization, although they were absent in unfertilized oocyte [85].

2.4. mRNA without function

Some mRNA is specific and only expressed during spermatid differentiation such as mRNA encoding protamine-2 which expressed before, and during the DNA condensation phase when histones are replaced to protamine-2. Also protamine-2 role in chromatin coiling synchronizes with spermatid differentiation by encoding mRNA could be involved in differentiation process. But the protamine mRNA degradation is very rapid in fertilized ova explaining its deleterious expression after fertilization [86]. Other sperm cell mRNA may be residual from the last spermatid expression phase. Recently, there is a thought that the analysis of sperm mRNA composition may be an indicator for male fertility [87, 88]. A group of genes known as GA17, COX5B and TFAM mRNAs exist in large quantities in all individual human ejaculates [89] but they are non-functional and cannot use in translation or trans-membrane in mature sperm [90]. GA17 coding for a putative fusogenic protein that may be important for sperm–oocyte interaction [91,92] COX5B is a subunit of the terminal mitochondrial respiratory transport enzyme and the mitochondrial transcription factor A (TFAM) genes are coded in nuclear but located in mitochondria. COX5B and TFAM mRNA imported to the mitochondria

matrix can be translated by the ribosomes then their products will be exported to the cytosol but this suggestion is not correct because the last described phenomena have not been occurred in the mitochondria of any cell type [93]. A more suitable explanation would be the presences of some remnant cytosolic ribosomes responsible for detecting the mRNA translation. RNA is absent in the sperm mitochondria and in the mid-piece [82]. This study agree with the suggestion that sperm mitochondria proteins do not involved in transcription and translation [94].

2.5. Sperm-egg binding

The oocyte plasma membrane consists of two regions, a microvilli-free region and a microvilli-rich region. The sperm fuses the oocyte in the microvilli-rich region [95,96]. The interaction between the sperm and oocyte involves sperm cell-oocyte cell adhesion, followed by the fusion of two gametes membranes [97]. The inner acrosomal membrane of the sperm comes into the oocyte membrane [98] through the equatorial region [99,100].

Many molecules present in sperm and oocytes and are crucial for successful gamete binding as Fertilin α or ADAM1, fertilin β or ADAM2 and cyritestin or ADAM3. The role of ADAM1, ADAM2 and ADAM3 appear clearly in sperm oocyte binding [97]. Fertilin β is not essential for plasma membrane binding and fusion but poor adhesion to zona pellucida was observed in fertilin β and cyritestin knockout mice [101,102].

Oocytes integrins which found on the membrane surface are thought to be ADAMs sperm receptors. Some studies discovered that α6β1 integrin is an oocyte receptor for fertilin β [103,104] but other studies revealed that α9β1 integrin is a receptor for fertilin β [105,106]. CD46 express in rodents on the sperm acrosomal membrane [107] and maintain the membrane stability [108]. In human cells, CD 46 directly interacts with β1 integrin and indirectly with tetraspanins [109].

CD9 exists in oocytes membrane surface, one of tetraspanin protein family and is important for sperm-oocyte interactions [110]. The role of CD9 in sperm oocyte fusion has been detected in a numerous studies with CD9-null oocytes which the ability for strong sperm adhesion was reduced [111] the after fertilization reorganize microvilli distribution to enhance membrane block (Żyłkiewicz et al., 2010). CD9 deficiency in mice caused a reduction in fertility [112,113] also CD81 is another member, expressed on the surface of oocyte, its specific role is not fully studied until now but it interacts with CD9 [114]. CD81 gene silencing caused a reduction in fertility [115,116].

CRISP1 is a sperm protein expressed by the cumulus cells surrounding the oocyte, induces sperm direction through the modification of sperm hyper-activation and it may regulate Cat Sper function [117] and sperm chemo-attraction in female reproductive tract to help in

successful in-vivo insemination (Blasco, 2014).

IZUMO is a specific protein, expressed in sperm and essential for sperm-oocyte plasma membrane binding and fusion [118]. IZUMO interacts directly with some oolema molecules. Helical dimer of fragments of IZUMO N-terminus domain involved in sperm-oocyte fusion [119]. Dimers are formed by the connection between IZUMO and other proteins via its N-terminal domain [118]. Moreover, IZUMO considered a key role for organizing and stabilizing of protein-like complex which is crucial for membrane fusion. Also protein, angiotensin protein which has the ability to convert enzyme 3 (ACE3) on the sperm acrosomal cap, capable of interacting with IZUMO [120]. On the oocyte membrane, Juno belongs to the folate receptor family and recognizes the sperm IZUMO to facilitate fertilization. It has been demonstrated that mice lacking Juno on the surface of their egg cells are infertile female mice with lacking Juno failed in normal sperm fusion. The rapid absence of Juno from the oocyte membrane immediately after fertilization implies the essential role of shedding Juno in the fertilization process to prevent poly-spermy occurrence in mammals [121].

Trypsin-like acrosin and spermosin proteases are two different molecules involved in the first physical contact of the oocyte and sperm, it was suggested that aproteasome system participate in helping the sperm to penetrate the oocyte or in the process of sperm binding proteins [116]. Although sperm hyaluronidases are believed to be a limiting factor for fertilization in mammals, and sperm-specific SPAM1 and HYAL5 hyaluronidase have been suggested to paticipate in sperm-ZP binding in mice, the recent researches proved that hyaluronidases are not essential requirement for fertilization [122,123].

The oviduct tube which is the fertilization environment and secretions also play an essential role in the transport and interaction between male and female gametes. The lactoferrin expression in a human oviduct regulates polyspermy prevention process but in vitro inhibits gametes interaction (Yoon, 2014), also causes a modification in sperm function by decreasing sperm α-D-mannose binding sites and increasing the tyrosine phosphorylation of sperm proteins (Zumoffen, 2013).

3. Oocyte Transcriptomics

In the natural reproductive cycle, around 80% of the ovulated oocytes will be fertiliyed and developed to blastocyst [124]. A sharp drop in development of bovine embryo occurred when in vivo recovered oocytes are continue matured under in vitro condition compared with their counterparts that are matured in vivo [125,126]. It is supposed that COCs that are matured in vivo have accumulated all molecules such as RNA, proteins that are required for orchestrating early-cleaved embryos (Hyttel et al., 1997). During the initial cleavage divisions, embryonic development is supported by maternal mRNAs and proteins synthesized and stored during oogenesis [44]. Oocyte-expressed genes are not only important for follicular growth

and development but also are crucial for early embryogenesis however, our understanding of composition of the oocyte transcriptome and the identity of key oocyte-expressed genes with important regulatory roles in folliculogenesis and early embryonic development is far from complete [44]. In addition, investigation on the molecular characteristics of oocytes of poor developmental competence is critical to form a foundation for the development of future classification criteria for the selection of oocytes with superior developmental capacity [47]. Using oocyte-specific cDNA microarray, six genes were overexpressed in fetal ovary relative to [ribosomal protein L7a, dynein light chain, Doc2$_\alpha$, calmodulin, leucine-rich protein, and the novel gene clone (Begg20_H6)] [44]. Following cross-species hybridizations (bovine, mouse and Xenopus laevis), 268 transcripts were reported to be preferentially expressed in the oocyte of these three species [52]. In this study, transcripts of SMFN (Small fragment nuclease), Spin (Spindlin), and PRMT1 (Protein arginine methyltransferase 1) were identified in oocytes and conserved in three evolutionarily distant species. Recent report has evidenced that reduced transcript abundance for follistatin is associated with poor developmental competence of bovine oocyte [47].

Analysis of the relative abundance of transcripts during oocyte maturation will help to identify potential marker genes for bovine oocyte competence. Using heterologous human cDNA array, approximately 300 genes were expressed in the bovine oocyte, of which 70 were differentially expressed during meiotic maturation, the expressed genes were associated with cell cycle regulation (CCNB1 and CDC2), DNA transcription (TIF1 and GTF2H) and apoptosis regulation (DAD1, CASP4, FASTK and BCL2L1) [41]. In array study conducted by [48], has showed that genes controlling DNA methylation (DNMT1 and DNMT2), transport (IGF2R, VDP and ATP2B1) and metabolism (HSD11B2, MUT, SLC3A2 and PLCG1) were up-regulated in matured oocytes compared to 8-cell stage embryos. Many genes (polyA, CPSF) and CPEB) related to cytoplasmic polyadenylation element (CPE)-dependent polyadenylation complex machinery were found to be expressed in bovine oocytes pre- and post-resumption of meiotic maturation. Furthermore, the differential expression of the majority of these genes further underlines the tight temporal control of protein synthesis required for oocyte maturation and in preparation of subsequent fertilization and early embryo development [127].

Previous studies have shown that development of early embryos to the blastocyst stage was greater when oocytes were obtained during follicular growth/stagnation phase (G/S) than in the dominance/regression phase (D/R) [58,128,125, 2,129,130]. The dominant follicle exerts a direct inhibitory effect on the development of subordinate follicles in cattle [131]. causing them to undergo atresia [132], which may lead to lower in vitro developmental competence compared to their counterparts at growth phase (as measured by blastocyst rate) [128]. Moreover, blastocysts derived from oocytes collected from both medium and small follicles at growth/stagnation G/S stage or dominance/regression D/R stage were reported to be different

in relative abundance of developmentally related transcripts (Cx43) [133]. However, the molecular properties of these oocytes in bovine have not yet been investigated. Therefore, in one of our studies we have compared the transcript abundance of bovine oocytes retrieved from small follicles at growth and dominance phases of the first follicular wave using custom cDNA microarray. Comparative gene expression analysis of oocytes from growth and dominance phases and subsequent data analysis using Significant Analysis of Microarray (SAM) revealed a total of 51 genes to be differentially regulated. Hierarchical clustering and heatmap was performed to show the general and magnitude expression of differentially regulated genes **(Figure 1)**. Furthermore, gene ontology (GO) has classified expressed transcripts functionally into different clusters based on their molecular functions **(Figure 2)**. Accordingly, differentially regulated genes were found to represent transcripts with known function [70% (36/51)], with unknown function [12% (6/51)] and novel transcripts [18% (9/51)] **(Figure 2)**. Transcripts with known function showed to be involved in protein biosynthesis (18%), transcription (10%), cytoskeleton (8%), cell cycle (8%), NADH dehydrogenase activity (4%), calcium ion binding (4%), nucleotide binding (4%) and other molecular functions (10%) **(Figure 2)**. Quantitative real-time PCR has confirmed the expression profile of 80% (8/10) in independent oocyte populations from both growth and dominance phases to be in the same trend of microarray data **(Figure 3).** The reported differences in developmental capacity of bovine oocytes derived from small follicles at growth and dominance phases of follicular development are also accompanied by differences in the relative abundance of transcripts related to the various molecular events and processes governing oocyte growth and follicular development.
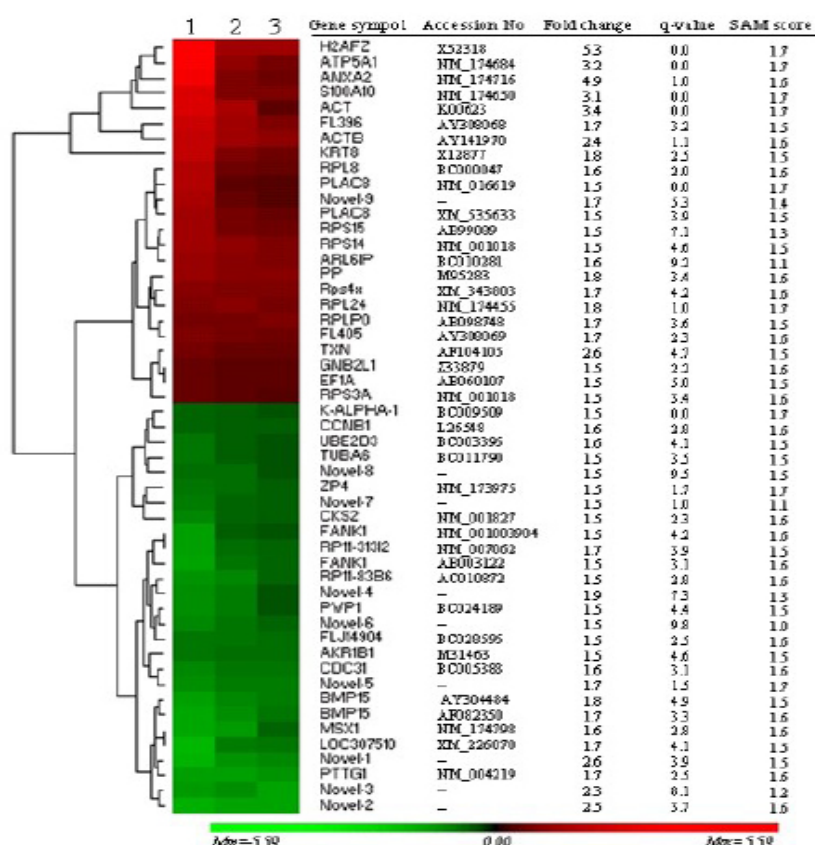

Figure 1: Hierarchical clustering and heatmap of 51 differentially expressed genes. The red blocks represent up-regulated genes while the green blocks represent down-regulated genes in oocytes recovered at growth phase.
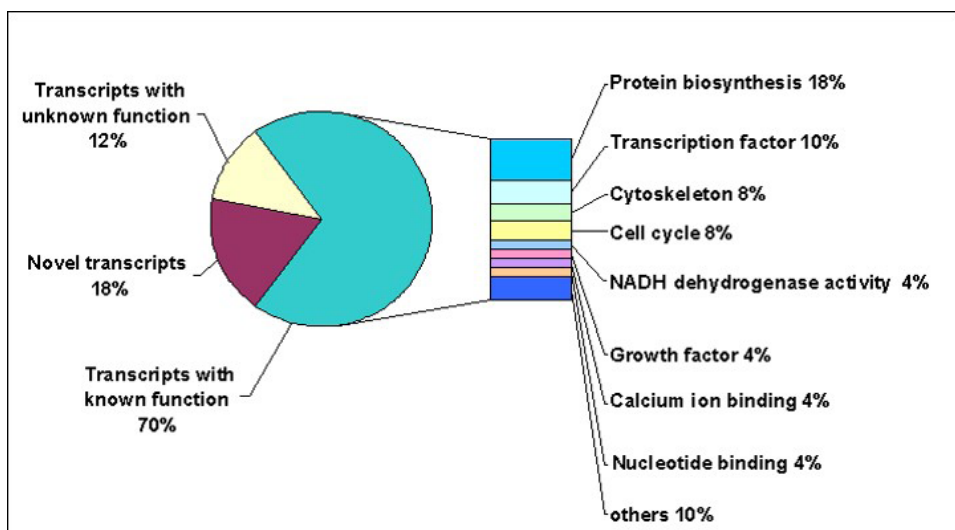
Figure 2: Differentially expressed genes as classified based on the Gene Ontology Consortium classifications (http://www.geneontology.org).
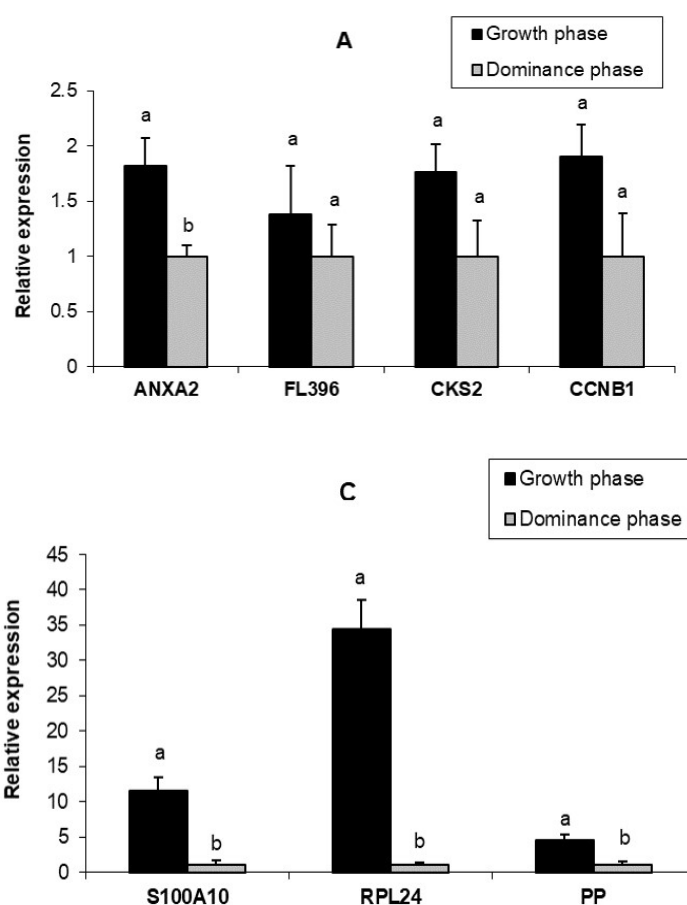

Figure 3: Quantitative real-time PCR validation of 10 differentially expressed genes in bovine oocytes recovered at growth phase (Day 3) vs. dominance phase (Day 7) as identified by microarray analysis (A, B, C). The relative abundance of mRNA levels represents the amount of mRNA compared to the calibrator (with the lowest normalized value). Bars with different superscripts (a, b) are significantly different at $P < 0.05$.

3.1. Transcriptome profile of cumulus cells

It is well established that integrated bilateral communication between the cumulus cells and its enclosed oocyte is key biological factor in acquisition of developmental competence to support preimplantation embryogenesis. Therefore, the molecular messages stored in cumulus cells are possible indicators of the further developmental fate of the oocytes until term.

Several studies have been conducted using farm animals and human granulosa cells to identify genomic signature(s) as molecular markers of developmental potential of oocyte to support embryogenesis and to establish pregnancy [134-136]. Suppressive subtractive hybridization combined with microarray were used to identify several potential cumulus cell markers of bovine COCs quality that includes several growth differentiation factor GDF9 downstream target genes like GREM1, HAS2, PTGS2, and TNFAIP6 [134]. In addition, epidermal growth factor receptor (EGFR), inhibin beta a (INHBA), betacellulin (BTC) and CD44 molecule was among candidate molecular markers that induce good potential of COCs. In another study, the transcript abundance of genes controlling of cumulus expansion process such as TNFAIP6 and nuclear maturation of oocyte like INHBA and FST were up-regulated in bovine in these cells as potential predictors of COCs quality when matured under *in vivo* [136]. A study using prepubertal bovine calf oocytes as a model of poor oocyte competence; microarray analysis detected genes encoding the cathepsin family of cysteine proteinases (CTSB, CTSS and CTSZ) are linked with reduced competence of bovine oocytes [135]. In search of potential markers of human granulosa cells, a study done by Feuerstein et al., (2007) has identified steroidogenic acute protein (STAR), prostaglandin-endoperoxide synthase 2 (PTGS2), stearoyl-co-enzyme A desaturase 1 and 5 (SCD1 and SCD5) and amphiregulin (AREG) are crucial regulators of nuclear maturation and their profile are increased after meiosis resumption. Noteworthy, reduced expression of connexin 43 (CX43) in cumulus is a good marker for nuclear maturation and further embryonic development upto blastocysts (Feuerstein et al. 2007).

3.2. Changes in gene expression during cleavage stages

In in vitro derived bovine embryos, estimates of total RNA content indicate that it declines from the mature oocyte to the morula stage, only to increase again at the blastocyst stage [137]. These estimates are based on Northern blot hybridization using probes for 28S and 18S rRNA, with the abundance of 5S rRNA following a similar pattern [137]. This pattern of RNA loss and reaccumulation mimics the patterns observed in the mouse although in the mouse the increase occurs by the 8- to 16-cell stage likely owing to the earlier onset of zygotic gene activation in this species (Piko and Clegg, 1982). In both species, the timing and the increase in abundance of specific mRNA transcripts occurs in a transcript specific manner. Examples of changes in steady state levels of various

During early development, the embryonic genome is inactive and the embryo relies on maternal messenger ribonucleic acid (mRNA) for protein synthesis (Thelie et al. 2009). The recruitment mechanisms by which dormant RNA is either targeted for translation or decay are still largely uncharacterized. The current model involves lengthening of the poly(A) tail, which triggers binding of the poly(A) binding protein and binding of translation initiation factors (Memili and First 2000; Groisman et al. 2002). RNA concentration is highest in the germinal vesicle stage oocyte and from then until the 8-cell stage, RNA is gradually depleted (Gilbert

et al. 2009; Vallée et al. 2009). Evidence in the mouse suggests that this decline is important for activation of the embryonic genome (Li et al. 2010). Depletion of maternal argonaute 2 (Ago2), which encodes a catalytic RNA hydrolase (RNase), disrupts gene expression and the 2 cell embryo fails to become a blastocyst (Li et al. 2010). In the bovine, embryonic genome activation (EGA) occurs at the 8 to 16-cell stage (Memili and First 2000) through an unknown mechanism.

3.3. Embryo transcriptomics

In mammals, maternally inherited transcripts stored within the oocyte regulate the earliest stages of embryogenesis. After fertilization, the embryonic genome becomes transcriptionally active and the expression some of embryonic genes begins in a stage-specific manner, which contribute to the early development process [137]. In cattle, global embryonic genome activation (EGA) begins during the 8-cell to 16-cell stage and it is the most critical event in early embryonic development. However, the identities of embryonic genes expressed and the mechanism(s) of EGA are poorly defined in the bovine. In addition, understanding of EGA will contribute to our understanding of nuclear reprogramming in somatic cell nuclear transfer experiments. Transcripts expressed at the 8-cell stage (EGA) include regulators of different molecular functions like transcription (NFY and USF2), cell adhesion (DSC2 and COL12A1), signal transducers (PTGER4) and transporter (CRABP1), metabolism (NEU3) and immune response (CXCL6) [48].

Accurate assessment of embryo viability is crucial for successful establishment and maintenance of pregnancy following embryo transfer. Evaluation of embryo quality is in particular of high impact for in vitro-produced embryos as these embryos differ in many aspects from their in vivo derived counterparts. The temporal or spatial and qualitative or quantitative shifts in the well-orchestrated expression patterns of developmentally important genes have been investigated in preimplantation bovine embryos following in vitro embryo manipulation. So far, studies in bovine embryos indicate that many of the differences in quality of in vitro- and in vivo-derived blastocysts can be related to culture environment-induced changes in mRNA abundance. The post-fertilization embryo culture environment has a dramatic effect on the pattern of gene expression in embryos, which in turn has serious implications for the normality of blastocyst development [138, 139]. This is the case, not only when one compares in vitro and in vivo culture systems, but also comparing different in vitro culture systems [140]. Recently, it was reported that in vitro-cultured embryos showed down-regulation of genes that are involved in transcription and translation (CCR4-NOT, EEF1G, PABPN1, FOXO3A, HMG2, GNB2L1 and DOT1L) events compared with in vivo counterparts, suggesting that in vitro-derived embryos are of inferior quality compared with in vivo-derived embryos due to a deficiency of the machinery associated with transcription and translation [50].

Imprinted genes appear to be more susceptible to alterations in epigenetic modifications [141]. especially after IVP of ovine [142] or bovine embryos [143]. Significant differences in the expression of non-imprinted genes have also been reported in bovine IVP and somatic nuclear transferred (sNT) derived embryos compared to their in vivo counterparts [144]. Differences in gene expression patterns between IVP and sNT-derived embryos and their in vivo counterparts may originate from all steps of the manipulation procedures, including in vitro maturation, in vitro fertilization, and in vitro culture and, for sNT, from different somatic nuclear transfer protocols [145]. In a recent study, it was found that there is a reduced levels of many genes required for the viability of every cell in the nuclear transferred (NT) embryo's cellular machinery [146]. In this study, transcripts of mitochondria (12S and 16S rRNA and cytochrome C oxidase I), cytoskeletal (TUBB, TPX2, KRT18, TMSB4X and ACTB), protein biosynthesis (EEF1A1, EFG2, BWZ1 and EIF5A) and ribosomal proteins (RPL4, RPL5, RPL21 and RPS20), protein binding/folding (GORASP2, HSPA9B, HSPA5 and LGALS3) and etabolism/biosynthesis (ADH5, PTGS2, SCP2, ACSL3, NDUFA1) were decreased in NT compared to in vitro produced blastocysts.

There is a clear relationship between altered transcript abundance patterns and some aspects of embryo quality (i.e. cryotolerance), which render the embryo capable o f establishing a pregnancy, if transferred fresh, but incapable of withstanding cryopreservation [147], [25]. Various studies in both mice and bovine have shown that the in vitro production of embryos under specific culture environments resulted in not only altered gene expression of transcripts related to metabolic and growth but also altered conceptus and fetal development following transfer [148,149]. Despite the fact that data on transcriptional analysis of transferable blastocysts of various origins have been accumulated, so far no direct connection of gene expression and developmental competence has been established. However, a well-established biopsy technique is needed to obtain cells from embryos before transfer without any lethal effect on the embryo during further development. For this, one study conducted in our laboratory to establish connection between transcriptional profile of embryos and the pregnancy success based on gene expression analysis of blastocyst biopsies taken prior to transfer to recipients [150]. Microarray data analysis revealed a total of 52 and 58 genes **(Figure 4 and 5)** were differentially regulated during comparison between embryo biopsies resulting in no pregnancy (G1) vs. calf delivery (G3) and those resulting in resorbed embryos (G2) vs. calf delivery (G3). Ontological classification has showed different functional clusters of genes **(Figure 6 and 7)**. In addition, differentially regulated genes represent genes with known functions (77%), ESTs (11.5%), and novel transcripts (11.5%) (**Figure 4 and 5**). Biopsies resulted in calf delivery were enriched with genes necessary for implantation (COX2 and CDX2), carbohydrate metabolism (ALOX15), growth factor (BMP15), signal transduction (PLAU), and placenta-specific 8 (PLAC8). Biopsies from embryos resulting in resorption are enriched with transcripts involved protein phosphorylation (KRT8), plasma membrane (OCLN), and glucose metabolism (PGK1

and AKR1B1). Biopsies from embryos resulting in no pregnancy are enriched with transcripts involved inflammatory cytokines (TNF), protein amino acid binding (EEF1A1), transcription factors (MSX1, PTTG1), glucose metabolism (PGK1, AKR1B1), and CD9, which is an inhibitor of implantation. The expression of those unknown and novel ESTs showed profiles similar to those of the annotated genes, as determined by tree hierarchical clustering analyses **(Figure 4 and 5)**. Quantitative real-time PCR has validated the expression of 87% (13/15) of the genes generated from the array hybridization. Thus, several genes identified in this experiment may be associated with embryo loss or survival in blastocysts during preimplantation period.
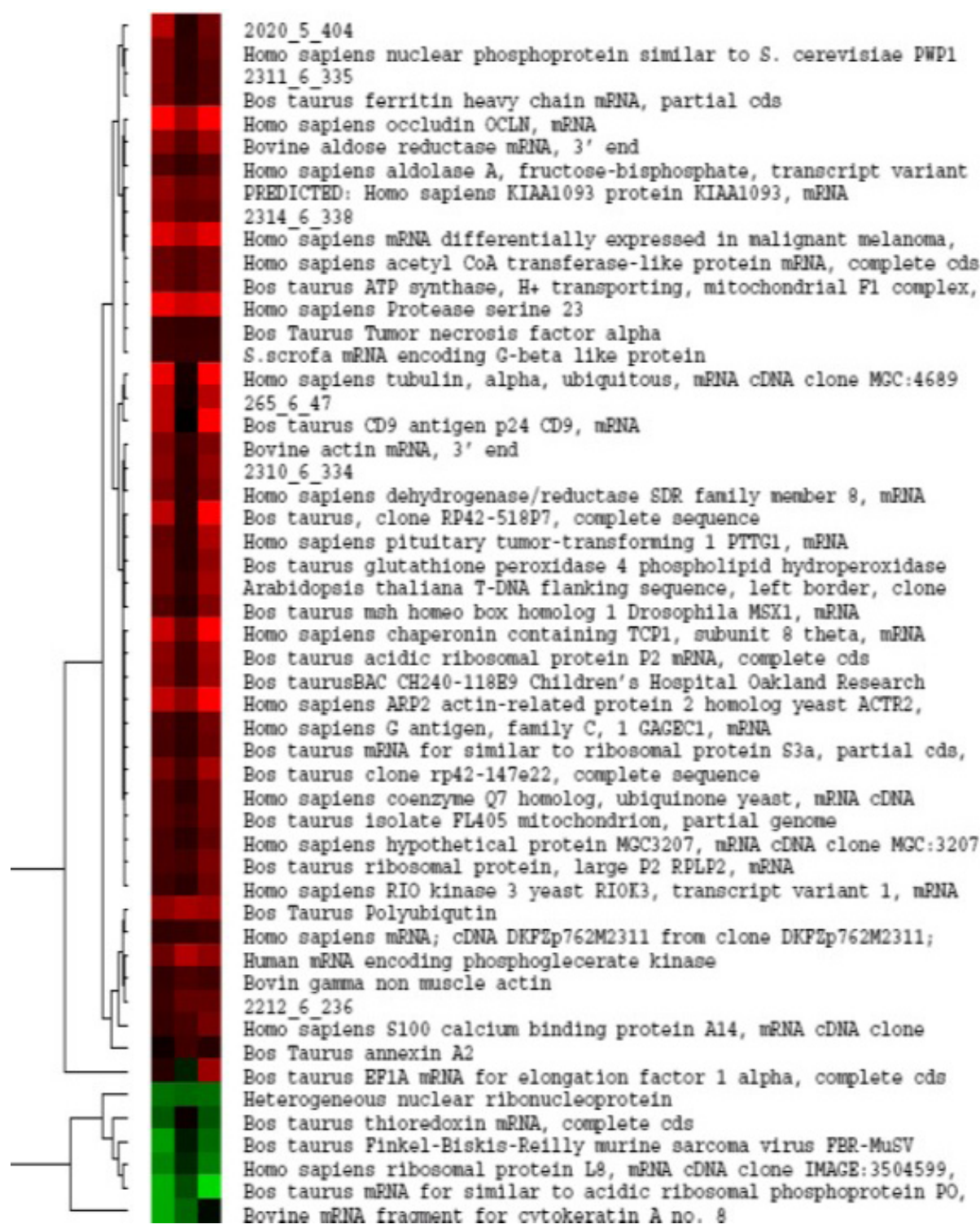

Figure 4: Hierarchical clustering for the differentially expressed genes between biopsies derived from blastocysts resulted in no pregnancy (G1) and calf delivery (G3). The columns represent the replicates. The rows represent 52 genes found to be differentially regulated between G1 and G3.
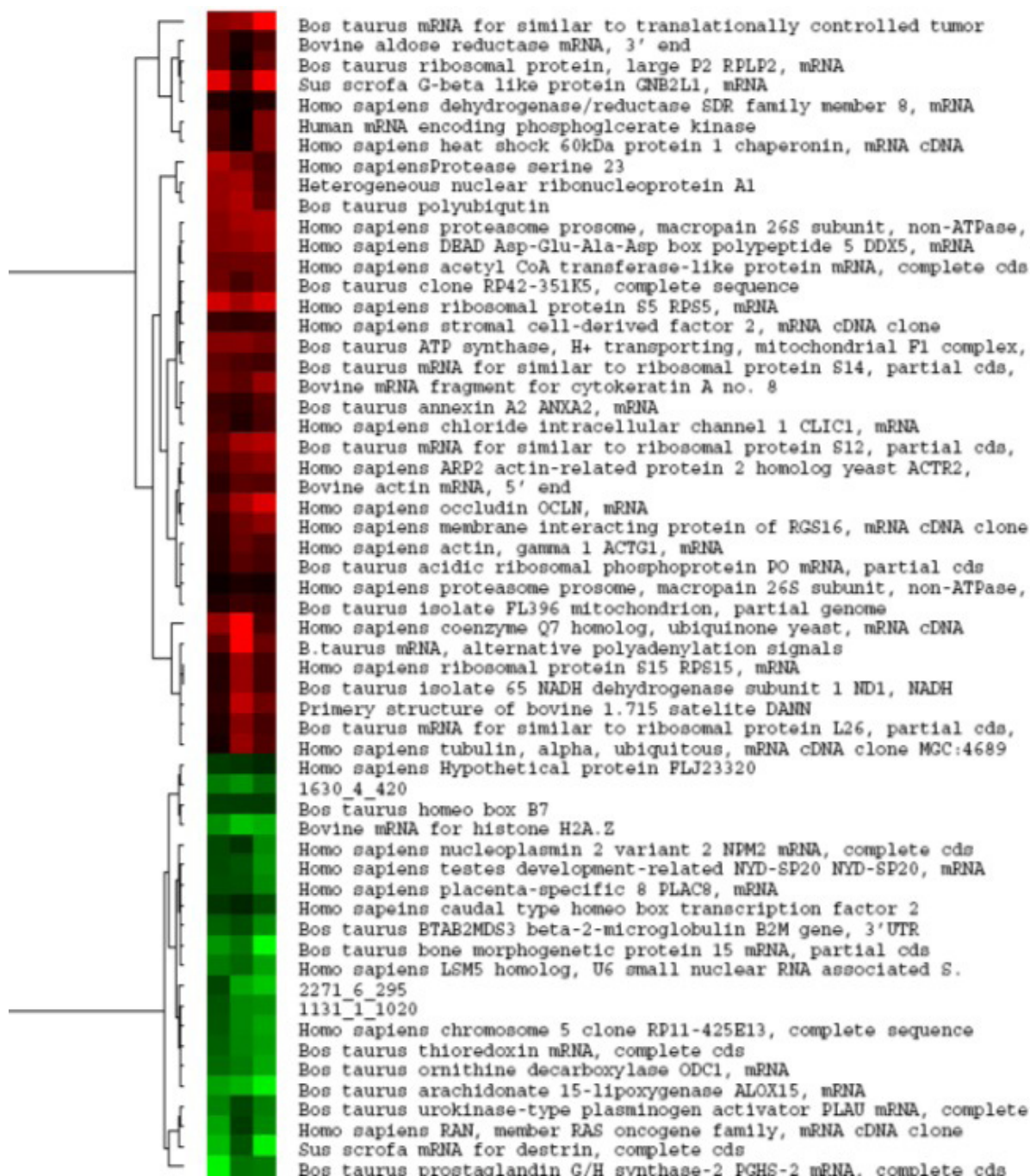
Bos taurus mRNA for similar to translationally controlled tumor
Bovine aldose reductase mRNA, 3' end
Bos taurus ribosomal protein, large P2 RPLP2, mRNA
Sus scrofa G-beta like protein GNB2L1, mRNA
Homo sapiens dehydrogenase/reductase SDR family member 8, mRNA
Human mRNA encoding phosphoglcerate kinase
Homo sapiens heat shock 60kDa protein 1 chaperonin, mRNA cDNA
Homo sapiensProtease serine 23
Heterogeneous nuclear ribonucleoprotein A1
Bos taurus polyubiqutin
Homo sapiens proteasome prosome, macropain 26S subunit, non-ATPase,
Homo sapiens DEAD Asp-Glu-Ala-Asp box polypeptide 5 DDX5, mRNA
Homo sapiens acetyl CoA transferase-like protein mRNA, complete cds
Bos taurus clone RP42-351K5, complete sequence
Homo sapiens ribosomal protein S5 RPS5, mRNA
Homo sapiens stromal cell-derived factor 2, mRNA cDNA clone
Bos taurus ATP synthase, H+ transporting, mitochondrial F1 complex,
Bos taurus mRNA for similar to ribosomal protein S14, partial cds,
Bovine mRNA fragment for cytokeratin A no. 8
Bos taurus annexin A2 ANXA2, mRNA
Homo sapiens chloride intracellular channel 1 CLIC1, mRNA
Bos taurus mRNA for similar to ribosomal protein S12, partial cds,
Homo sapiens ARP2 actin-related protein 2 homolog yeast ACTR2,
Bovine actin mRNA, 5' end
Homo sapiens occludin OCLN, mRNA
Homo sapiens membrane interacting protein of RGS16, mRNA cDNA clone
Homo sapiens actin, gamma 1 ACTG1, mRNA
Bos taurus acidic ribosomal phosphoprotein PO mRNA, partial cds
Homo sapiens proteasome prosome, macropain 26S subunit, non-ATPase,
Bos taurus isolate FL396 mitochondrion, partial genome
Homo sapiens coenzyme Q7 homolog, ubiquinone yeast, mRNA cDNA
B.taurus mRNA, alternative polyadenylation signals
Homo sapiens ribosomal protein S15 RPS15, mRNA
Bos taurus isolate 65 NADH dehydrogenase subunit 1 ND1, NADH
Primery structure of bovine 1.715 satelite DANN
Bos taurus mRNA for similar to ribosomal protein L26, partial cds,
Homo sapiens tubulin, alpha, ubiquitous, mRNA cDNA clone MGC:4689
Homo sapiens Hypothetical protein FLJ23320
1630_4_420
Bos taurus homeo box B7
Bovine mRNA for histone H2A.Z
Homo sapiens nucleoplasmin 2 variant 2 NPM2 mRNA, complete cds
Homo sapiens testes development-related NYD-SP20 NYD-SP20, mRNA
Homo sapiens placenta-specific 8 PLAC8, mRNA
Homo sapeins caudal type homeo box transcription factor 2
Bos taurus BTAB2MDS3 beta-2-microglobulin B2M gene, 3'UTR
Bos taurus bone morphogenetic protein 15 mRNA, partial cds
Homo sapiens LSM5 homolog, U6 small nuclear RNA associated S.
2271_6_295
1131_1_1020
Homo sapiens chromosome 5 clone RP11-425E13, complete sequence
Bos taurus thioredoxin mRNA, complete cds
Bos taurus ornithine decarboxylase ODC1, mRNA
Bos taurus arachidonate 15-lipoxygenase ALOX15, mRNA
Bos taurus urokinase-type plasminogen activator PLAU mRNA, complete
Homo sapiens RAN, member RAS oncogene family, mRNA cDNA clone
Sus scrofa mRNA for destrin, complete cds
Bos taurus prostaglandin G/H synthase-2 PGHS-2 mRNA, complete cds

Figure 5: Results of hierarchical clustering for the differentially expressed genes between biopsies derived from blastocysts resulted in resorption (G2) and calf delivery (G3) identified by microarray analysis. The columns represent the replicates.The rows represent 58 genes found to be differentially regulated between the two groups of biopsies.
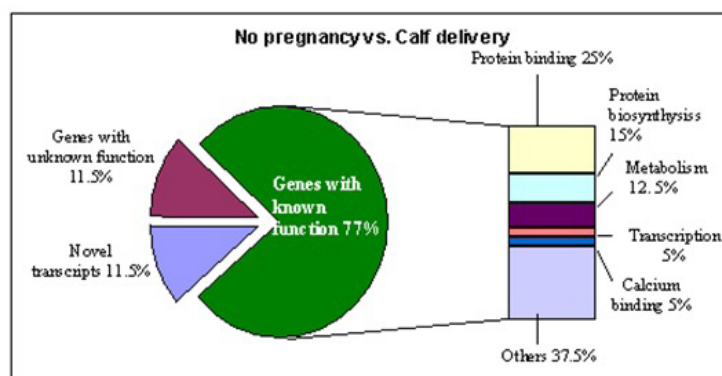

Figure 6: Ontology classification for differentially expressed transcripts between biopsies derived from blastocysts resulted n no pregnancy and calf delivery. The known genes were classified functionally based on the Gene Ontology Consortium classification (http://www.geneontology.org)
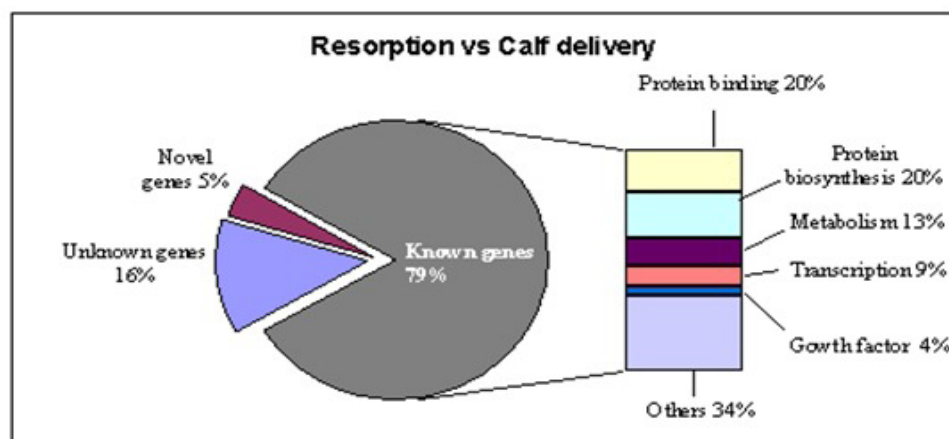
Figure 7: Ontology classification for differentially expressed transcripts between biopsies derived from blastocysts resulted in resorption and calf delivery. The known genes were classified functionally based on the Gene Ontology Consortium classification (http://www.geneontology.org).
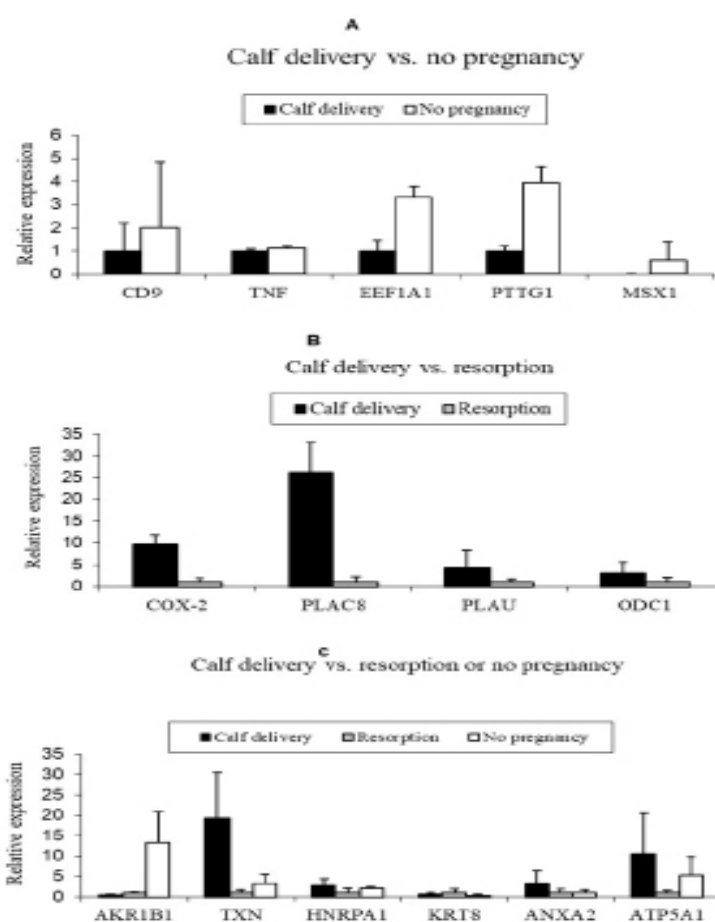

Figure 8: Quantitative real time PCR confirmation of selected transcripts between biopsies from blastocysts resulted in calf delivery versus no pregnancy (A) and calf delivery versus resorption group (B) and those resulted in calf delivery versus resorption or no pregnancy (C).

4. Characterization and Functional Analysis of Candidate Genes

To correlate transcript level with corresponding protein level and to elucidate embryonic cellular function, detailed characterisation is necessary at the protein level. Oogenesin gene is expressed during oogenesis and early embryogenesis in mouse and its protein is synthesised from the oocyte to four-cell embryo stages, suggesting a possible role during oocyte maturation and/or embryonic genome activation [151].

In one of our studies, MSX1 was selected as candidate gene for protein localization in early embryonic development and throughout follicular turnover. MSX1 protein was found to be localized at higher levels in the oocytes cytoplasm than in the surrounding cumulus cells **(Figure 9d, h, p)** or other cellular layers of the growing follicle **(Figure 9b, f, n)** at all stages of follicular development except at growth phase **(Figure 7j, l).**

The MSX1 protein was found to be dispersed in the cytoplasm of immature and matured oocytes and early zygote stages **(Figure 10a, b, c)** but tends to be localized around the nucleus at advanced zygote, 2-cell, 4-cell and 8-cell cleavage stage embryos **(Figure 10d, e, f, g)**. Comparative analysis of protein signals between oocytes showed that fluorescence signals were reduced after maturation **(Figure 10b).** Moreover, the in situ hybridization experiment results showed that MSX1 mRNA was localized in the oocytes, cumulus cells and follicular wall during the periods of follicular turnover under investigation **(Figure 11).**
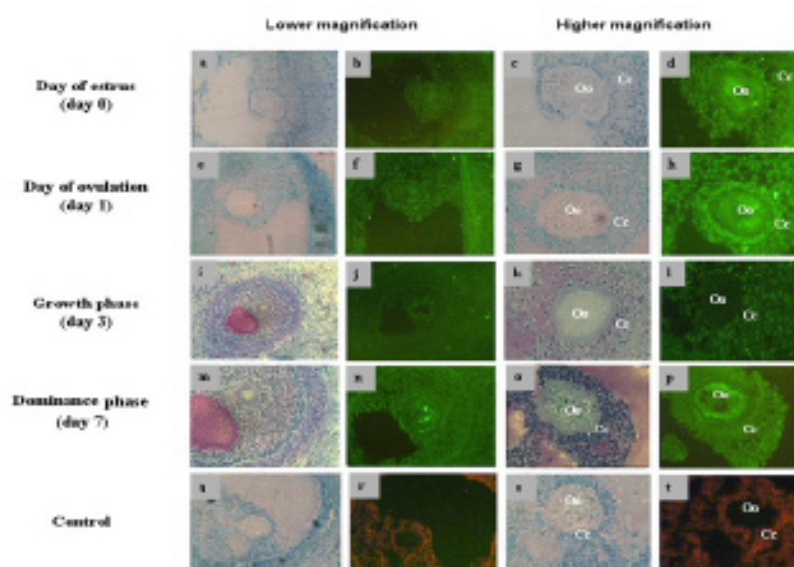
Figure 9: Immunohistochemical localisation of MSX1 protein in bovine ovarian sections at day of estrus (b, d), day of ovulation (f, h), growth phase (j, l), dominance phase (m, q). Cumulus cells are marked with Cc and oocytes are marked with Oo. Negative controls were processed without addition of primary anti-MSX1 antibody (r, t). Sections were counterstained with toluidine blue (a, c, e, g, i, k, m, o, q and s). Images from the same ovarian sections were captured with lower and higher magnification.
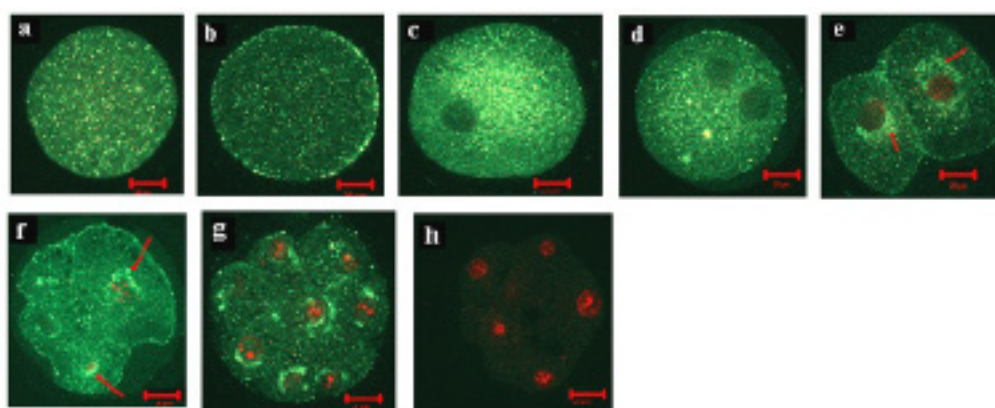

Figure 10: Subcellular localization of bovine MSX1 protein in bovine oocytes and early cleavage embryonic stages [immature oocyte (a), matured oocyte (b), zygote (c), advanced zygote (d), 2-cell (e), 4-cell (f) and 8-cell (g)]. Negative control (h) was processed without addition of primary anti-MSX1 antibody. Nuclei are stained with propidium iodide (red). Scale bars represent 20 μm.
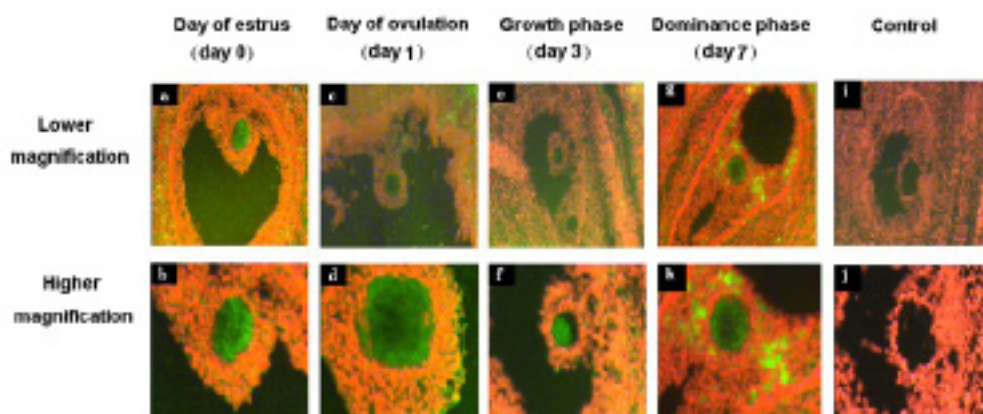
Figure 11: Fluorescent in situ hybridization of MSX1 mRNA conducted with DIG labelled RNA antisense probe in bovine ovarian sections at day of estrus (A, B), day of ovulation (B, C), growth phase (D, E), dominance phase (F, G). Cytoplasms of the oocytes (Oo) are darkly stained with green fluorescent compared to cumulus cells (Cc). Negative controls were hybridized with DIG labelled RNA sense probe (H, I). Images from the same ovarian sections were captured with lower and higher magnification.

5. References

1. Le Naour F, Rubinstein E, Jasmin C, Prenant M and Boucheix C: Severely reduced female fertility in CD9-deficient mice. Science 287: 319-321, 2000.

2. Leibfried-Rutledge ML (1999): Factors determining competence of in vitro produced cattle embryos. Theriogenology 51, 473-485.

3. Flesch FM, Gadella BM. Dynamics of the mammalian sperm plasma membrane in the process of fertilization. Biochim Biophys Acta 2000; 1469: 197–235.

4. Kadivar A, Heidari Khoei H, Hassanpour H, Ghanaei H, Golestanfar A, Mehraban H et al. Peroxisome proliferator-activated receptors (PPARα, PPARγ and PPARβ/δ) gene expression profile on ram spermatozoa and their relation to the sperm motility. Vet Res Forum 2016; 7: 27-34.

5. Kim KU, Pang WK, Kang S, Ryu DY, Song WH, Rahman MS et al. Sperm solute carrier family 9 regulator 1 is correlated with boar fertility. Theriogenology 2019; 126:254-60.

6. Parthipan S, Selvaraju S, Somashekar L, Arangasamy A, Sivaram M, Ravindra JP. Spermatozoal transcripts expression levels are predictive of semen quality and conception rate in bulls (Bos taurus). Theriogenology, 2017; 98:41-49.

7. Bissonnette N, Lévesque-Sergerie JP, Thibault C, Boissonneault G. Spermatozoal transcriptome profiling for bull sperm motility: a potential tool to evaluate semen quality. Reproduction 2009;138: 65–80.

8. Boerke A, Dieleman SJ, Gadella BM. A possible role for spermatozoa RNA in early embryo development. Theriogenology 2007; 68:147–55.

9. Macmillan KL, Lean IJ, Westwood CT (1996): The effects of lactation on the fertility of

10. Lucy, MC (2001): Reproductive loss in high-producing dairy cattle: Where will it end?.J Dairy Sci. 2001 Jun;84(6):1277-93.

11. Marai, I.F.M and Haeeb A.A.M. (2010). Buffalo's biological functions as affected by heat stress - a review. Livest. Sci.,(127):89 - 109.

12. Al-Katanani YM, Paula-Lopes FF, Hansen PJ. Effect of Season and Exposure to Heat Stress on Oocyte Competence in Holstein Cows J Dairy Sci. 2002; 85(2):390-6.

13. Gendelman M, Roth Z. Seasonal effect on germinal vesicle-stage bovine oocytes is further expressed by alterations

in transcript levels in the developing embryos associated with reduced developmental competence. Biol Reprod. 2012 Jan 16;86(1):1-9.

14. Sadeesh EM, Sikka P, Balhara AK, Balhara S. Developmental Competence and Expression Profile of Genes in Buffalo (Bubalus Bubalis) Oocytes and Embryos Collected Under Different Environmental Stress. Cytotechnology. 2016; 68(6):2271-2285.

15. Abdoon AS, Gabler C, Holder C, Kandil OM, Einspanier R.Seasonal variations in developmental competence and relative abundance of gene transcripts in buffalo (Bubalus bubalis) oocytes. Theriogenology. 2014 Nov;82(8):1055-67.

16. Maya-Soriano MJ, López-Gatius F, Andreu-Vázquez C, López-Béjar M. Bovine Oocytes Show a Higher Tolerance to Heat Shock in the Warm Compared With the Cold Season of the Year. Theriogenology. 2013; 79(2):299-305.

17. Edwards JL, Hansen PJ. Differential responses of bovine oocytes and preimplantation embryos to heat shock. Mol Reprod Dev. 1997; 46(2):138-45.

18. Nabenishi H, Ohta H, Nishimoto T, Morita T, Ashizawa K, Tsuzuki Y. The effects of cysteine addition during in vitro maturation on the developmental competence, ROS, GSH and apoptosis level of bovine oocytes exposed to heat stress. Zygote. 2012; 20(3):249-59.

19. Armon L, Ben-Ami I, Ron-El R and Eisenbach M: Human oocyte-derived sperm chemoattractant is a hydrophobic molecule associated with a carrier protein. Fertil Steril 102: 885-890, 2014.

20. Yadav A, Singh KP, Singh MK, Saini N, Palta P, Manik RS, Singla SK, Upadhyay RC, Chauhan MS. Effect of physiologically relevant heat shock on development, apoptosis and expression of some genes in buffalo (Bubalus bubalis) embryos produced in vitro. Reprod Domest Anim. 2013 Oct;48(5):858-65.

21. Snijders SEM, Dillon P, O'Callaghan D, Boland MP (2000): Effect of genetic merit,

22. Donnison M, Pfeffer PL (2004): Isolation of genes associated with developmentally competent bovine oocytes and quantitation of their levels during development. Biol Reprod 71, 1813-1821.

23. Ghanem N, Hölker M, Rings F, Jennen D, Tholen E, Sirard MA, Torner H, Kanitz W, Schellander K, Tesfaye D, 2007: Alterations in transcript abundance of bovine oocytes recovered at growth and dominance phases of the first follicular wave. BMC Dev Biol 7, 90.

24. Rizos D, Ward F, Duffy P, Boland MP, Lonergan P (2002): Consequences of bovine

25. Rizos D, Gutiérrez-Adán A, Pérez-Garnelo S, de la Fuente J, Boland MP, Lonergan P (2003): Bovine embryo culture in the presence or absence of serum: implications for blastocyst development, cryotolerance, and messenger RNA expression. Biol Reprod 68, 236-243.

26. Rodriguez-Zas S, Schellander K, Lewin H, 2008: Biological interpretations of transcriptomic profiles in mammalian oocytes and embryos. Reproduction 135, 129-39.

27. Morris RL, Brown HM, Wright BD, Sharp DJ, Sullivan W, Scholey JM, 2001: Microinjection methods for analyzing the functions of kinesins in early embryos. Methods Mol Biol 164,163-172.

28. Geisert RD, Morgan GL, Short EC Jr, Zavy MT, 1992: Endocrine events associated with endometrial function and conceptus development in cattle. Reprod Fertil Dev 4, 301-305.

29. Salilew-Wondim D, Hölker M, Rings F, Ghanem N, Ulas-Cinar M, Peippo J, Tholen E, Looft C, Schellander K, Tesfaye D, 2010: Bovine pretransfer endometrium and embryo transcriptome fingerprints as predictors of pregnancy success after embryo transfer. Physiol Genomics 42, 201-218.

30. El-Sayed A, Hoelker M, Rings F, Salilew D, Jennen D, Tholen E, Sirard M-A, Schellander K, Tesfaye D, 2006: Large-scale transcriptional analysis of bovine embryo biopsies in relation to pregnance success after transfer to recipi-

ents. Physiol. Genomics 28, 84-96.

31. Gad A, Besenfelder U, Rings F, Ghanem N, Salilew-Wondim D, Hossain MM, Tesfaye D, Lonergan P, Becker A, Cinar U, Schellander K, Havlicek V, Hölker M, 2011: Effect of reproductive tract environment following controlled ovarian hyperstimulation treatment on embryo development and global transcriptome profile of blastocysts: implications for animal breeding and human assisted reproduction. Hum Reprod 26,1693-1707.

32. Ghanem N, Salilew-Wondim D, Gad A, Tesfaye D, Phatsara C, Tholen E, Looft C, Schellander K, Hoelker M, 2011: Bovine blastocysts with developmental competence to term share similar expression of developmentally important genes although derived from different culture environments. Reproduction 142, 551-564.

33. Niemann H, Carnwath J, Kues W, 2007: Application of DNA array technology to mammalian embryos. Theriogenology 68, S165-177.

34. Ruddock-D'Cruz NT, Hall VJ, Tecirlioglu RT, French AJ, 2007: Gene expression analysis of single preimplantation bovine embryos and the consequence for developmental potential. Soc Reprod Fertil Suppl 64, 341-363.

35. Copp AJ (1995): Death before birth: clues from gene knockouts and mutations. Trends Genet 11, 87-93.

36. Zhang B, Peñagaricano F, Driver A, Chen H, Khatib H, 2011: Differential expression of heat shock protein genes and their splice variants in bovine preimplantation embryos. J Dairy Sci 94, 4174-4182.

37. Niemann H, and Wrenzycki C, 2000: Alterations of expression of developmentally important genes in preimplantation bovine embryos by in vitro culture conditions: implications for subsequent development. Theriogenology 53, 21- 34.

38. Aswal APS, Raghav S, De S, Thakur M, Goswami SL, Datta TK, 2007a: Expression stability of two housekeeping genes (18S rRNA and G3PDH) during in vitro maturation of follicular oocytes in buffalo (Bubalus bubalis). Anim Reprod Sci 103, 164–171.

39. Aswal APS, Datta TK, Raghav S, De S, Yadav P, Goswami SL, 2007b: Development of a competitive quantitative PCR strategy for evaluating the expression stability of 18s rRNA during in vitro maturation of buffalo (Bubalus bubalis) follicular oocytes. Reprod Domest Anim 42, 195–201.

40. Robert C, Gagne D, Bousquet D, Barnes FL Sirard, MA (2001): Differential display and suppressive subtractive hybridization used to identify granulosa cell messenger RNA associated with bovine oocyte developmental competence. Biol Reprod 64, 1812-1820.

41. Dalbiès-Tran R, Mermillod P (2003) Use of heterologous complementary DNA array screening to analyze bovine oocyte transcriptome and its evolution during in vitro maturation. Biol Reprod 68, 252-261.

42. Sirard MA, Dufort I, Vallee M, Massicotte L, Gravel C, Reghenas H, Watson AJ, King WA, Robert C (2005): Potential and limitations of bovine-specific arrays for the analysis of mRNA levels in early development: preliminary analysis using a bovine embryonic array. Reprod Fertil Dev 17, 47-57.

43. Suchyta SP, Sipkovsky S, Kruska R, Jeffers A, McNulty A, Coussens MJ, Tempelman RJ, Halgren RG, Saama PM, Bauman DE, Boisclair YR, Burton JL, Collier RJ, DePeters EJ, Ferris TA, Lucy MC, McGuire MA, Medrano JF, Overton TR, Smith TP, Smith GW, Sonstegard TS, Spain JN, Spiers DE, Yao J, Coussens PM. (2003): Development and testing of a high-density cDNA microarray resource for cattle. Physiol Genomics 15, 158-164.

44. Yao J, Ren X, Ireland JJ, Coussens PM, Smith TP, Smith GW (2004): Generation of a bovine oocyte cDNA library and microarray: resources for identification of genes important for follicular development and early embryogenesis. Physiol Genomics 19, 84-92.

45. Wolf E, Arnold GJ, Bauersachs S, Beier HM, Blum H, Einspanier R, Fröhlich T, Herrler A, Hiendleder S, Kölle S, Prelle K, Reichenbach HD, Stojkovic M, Wenigerkind H, Sinowatz F 2003 Embryo-Maternal communication in bovine-Strategies for deciphering a complex cross-talk. Reprod Dom Anim 38, 276-289.

46. Bauersachs S, Ulbrich SE, Gross K, Schmidt SEM, Meyer HHD, Wenigerkind H, Vermehren M, Sinowatz F, Blum H, Wolf E 2006 Embryo-induced transcriptome changes in bovine endometrium reveal species-specific and common molecular markers of uterine receptivity. Reproduction 132, 319-331.

47. Patel OV, Bettegowda A, Ireland JJ, Coussens PM, Lonergan P, Smith GW (2007): Functional genomics studies of oocyte competence: evidence that reduced transcript abundance for follistatin is associated with poor developmental competence of bovine oocytes. Reproduction 133, 95-106.

48. Misirlioglu M, Page GP, Sagirkaya H, Kaya A, Parrish JJ, First NL, Memili E (2006): Dynamics of global transcriptome in bovine matured oocytes and preimplantation embryos. Proc Natl Acad Sci 103, 18905-18910.

49. Kocabas AM, Crosby J, Ross PJ, Out HH, Beyhan Z, Can H, et al. 2006. The transcriptome of human oocytes. Proc Natl Acd Sci USA. 103:14027-32.

50. Corcoran D, Fair T, Park S, Rizos D, Patel OV, Smith GW, Coussens PM, Ireland JJ, Boland MP, Evans ACO, Lonergan P (2006): Suppressed expression of genes involved in transcription and translation in in vitro compared to in vivo cultured bovine embryos. Reproduction 131, 651-660.

51. Kues WA, Sudheer S, Herrmann D, Carnwath JW, Havlicek V, Besenfelder U, Lehrach H, Adjaye J, Niemann H. Genome-wide expression profiling reveals distinct clusters of transcriptional regulation during bovine preimplantation development in vivo. Proc Natl Acad Sci U S A. 2008 Dec 16;105(50):19768-73.

52. Vallée M, Robert C, Méthot S, Palin M-F, Sirard M-A.(2006): Cross-species hybridizations on a multi-species cDNA microarray to identify evolutionarily conserved genes expressed in oocytes. BMC Genomics 7,113.

53. Hu X, Pokharel K, Peippo J, Ghanem N, Zhaboyev I, Kantanen J, Li MH (2016): Identification and characterization of miRNAs in the ovaries of a highly prolific sheep breed. Animal Genetics 47(2):234-239.

54. Pokharel K, Peippo J, Honkatukia M, Seppälä A, Rautiainen J, Ghanem N, Hamama TM, Crowe MA, Andersson M, Li MH, Kantanen J (2018) : Integrated ovarian mRNA and miRNA transcriptome profiling characterizes the genetic basis of prolificacy traits in sheep (Ovis aries).BMC Genomics, 29;19(1):104.

55. Pitnick, S. et al. (2009) Sperm morphological diversity. In Sperm Biology: An Evolutionary Perspective (Birkhead, T.R. et al., eds), pp. 69–149, Academic Press

56. Fischer, B.E. et al. (2012) Conserved properties of Drosophila and human spermatozoal mRNA repertoires. Proc. R. Soc. B 279, 2636–2644 8 Hecht, N.B. (1998) Molecular mechanisms of male germ cell differentiation. Bioessays 20, 555–561 9.

57. Miller, D. et al. (2005) The controversy, potential and roles of spermatozoal RNA. Trends Mol. Med. 11, 156–163

58. Hagemann LJ, Weilert LL, Beaumont S, Tervit HR (1998): Development of bovine embryos in single in vitro production (sIVP) systems. Mol Reprod Dev 51, 143-147.

59. Boerke, A. et al. (2007) A possible role for sperm RNA in early embryo development. Theriogenology 68S, S147–S155

60. Bourc'his, D. and Voinnet, O. (2010) A small-RNA perspective on gametogenesis, fertilization, and early zygote development. Science 330, 617–622

61. Dadoune, J-P. (2009) Spermatozoal RNAs: what about their functions? Microsc. Res. Tech. 72, 536–551. dairy cows. Aust vet J. 73, 141-147.

62. Krawetz SA. Paternal contribution: new insights and future challenges. Nat Rev Genet 2005; 6:633–42.

63. Gardener, A. and West, S.A. (2009) Green beards. Evolution 64, 25–38.

64. Curry, E. et al. (2011) Differential expression of porcine sperm microRNAs and their association with sperm mor-

phology and motility. Theriogenology 76, 1532–1539

65. Yan, W. et al. (2008) Birth of mice after intra cytoplasmic injection of single purified sperm nuclei and detection of messenger RNAs and MicroRNAs in the sperm nucleus. Biol. Reprod. 78, 896–902

66. Liu, W-M. et al. (2012) Sperm-borne microRNA-34c is required for the first cleavage division in mouse. Proc. Natl. Acad. Sci. U.S.A. 109, 490-494.

67. Gapp, K. et al. (2014) Implication of sperm RNAs in transgenerational inheritance of the effects of early trauma in mice. Nat. Neurosci. http:// dx.doi.org/10.1038/nn.3695

68. Hamilton, W.D. (1964) The genetical evolution of social behavior I & II. J. Theor. Biol. 7, 1–52.

69. Pomiankowski, A. (1999) Intragenomic conflict. In Levels of Selection (Keller, L., ed.), pp. 121–152, Princeton University Press

70. Leigh, E.G. (1999) Levels of selection, potential conflicts, and their resolution: the role of the 'common good'. In Levels of Selection (Keller, L., ed.), pp. 15–30, Princeton University Press

71. Fisher, H.S. and Hoekstra, H.E. (2010) Competition drives cooperation among closely related sperm of deer mice. Nature 463, 801–803.

72. Holman, L. and Snook, R.R. (2008) A sterile sperm caste protects brother fertile sperm from female-mediated death in Drosophila pseudoobscura. Curr. Biol. 18, 292–296.

73. Higginson, D.M. and Pitnick, S. (2011) Evolution of intra-ejaculate sperm interactions: do sperm cooperate? Biol. Rev. 86, 249–270.

74. Immler, S. et al. (2007) By hook or by crook? Morphometry, competition and cooperation in rodent sperm. PLoS ONE 2, e170.

75. Moore, H.D. et al. (2002) Exceptional sperm cooperation in the wood mouse. Nature 418, 174–177.

76. Arnqvist, G. and Nilsson, T. (2000) The evolution of polyandry: multiple mating and female fitness in insects. Anim. Behav. 60, 164-145.

77. Jennions, M.D. and Petrie, M. (2000) Why do females mate multiply? A review of the genetic benefits. Biol. Rev. 75, 21–64.

78. Hosken, D.J. and Stockley, P. (2003) Benefits of polyandry: a life history perspective. Evol. Biol. 33, 173–194.

79. Parker, G.A. (1970) Sperm competition and its evolutionary consequences in insects. Biol Rev. 45, 525–567.

80. Birkhead, T.R. and Moller, A.P. (1998) Sperm Competition and Sexual Selection, Academic Press.

81. Simmons, L.W. (2001) Sperm Competition and its Evolutionary Consequences in the Insects, Princeton University Press.

82. Pessot CA, Brito M, Figueroa J, Concha II, Yanez A, Burzio LO. 1989 Presence of RNA in the sperm nucleus. Biochem Biophys Res Commun 1989; 158: 272–8.

83. Swain JL, Stewart TA, Leder P. Parental legacy determines methylation and expression of an autosomal transgene: a molecular mechanism for parental imprinting. Cell 1987;50: 719–27.

84. Cummins JM. Cytoplasmic inheritance and its implications for animal biotechnology. Theriogenology 2001; 55: 1381–99.

85. Ostermeier GC, Miller D, Huntriss JD, Diamond MP, Krawetz SA. Reproductive biology: delivering spermatozoan

RNA to the oocyte. Nature 2004; 429: 154.

86. Ziyyat A, Lefevre A. Differential gene expression in pre-implantation embryos from mouse oocytes injected with round spermatids or spermatozoa. Hum Reprod 2001; 16: 1449–56.

87. Ostermeier GC, Goodrich RJ, DiamondMP, Dix DJ, Krawetz SA. Toward using stable spermatozoal RNAs for prognostic assessment of male factor fertility. Fertil Steril 2005; 83: 1687–94.

88. Platts AE, Dix DJ, Chemes HE, Thompson KE, Goodrich R, Rockett JC, et al. Success and failure in human spermatogenesis as revealed by teratospermic RNAs. Hum Med Gen 2007; 16: 763–73.

89. Zhao Y, Li Q, Yao C, Wang Z, Zhou Y, Wang Y, et al. Characterization and quantification of mRNA transcripts in ejaculated spermatozoa of fertile men by serial analysis of gene expression. Hum Reprod 2006; 21: 1583–90.

90. Flesch FM, Gadella BM. Dynamics of the mammalian sperm plasma membrane in the process of fertilization. Biochim Biophys Acta 2000; 1469: 197–235.

91. Miller D, Ostermeier GC. Towards a better understanding of RNA carriage by ejaculate spermatozoa. Hum Reprod Update 2006; 12: 757–67.

92. Miller* D, Ostermeier GC. Spermatozoal RNA: why is it there and what does it do? Gynecol Obstet Fertil 2006; 34: 840–6.

93. Gui LM, Joyce IM (2005): RNA interference evidence that growth differentiation factor-9 mediates oocyte regulation of cumulus expansion in mice. Biol Reprod 72, 195-199.Gur Y, Breitbart H. Mammalian sperm translate nuclear-encoded proteins by mitochondrial-type ribosomes. Genes Dev 2006; 20: 411–6.

94. Sutovsky P, Moreno RD, Ramalho-Santos J, Dominko T, Simerly C, Schatten G. Ubiquitinated sperm mitochondria, selective proteolysis, and the regulation of mitochondrial inheritance in mammalian embryos. Biol Reprod 2000; 63: 582–90.

95. Ebensperger C and Barros C: Changes at the hamster oocyte surface from the germinal vesicle stage to ovulation. Gamete Res 9: 387-397, 1984.

96. Johnson MH, Eager D, Muggleton-Harris A and Grave HM: Mosaicism in organisation concanavalin A receptors on surface membrane of mouse egg. Nature 257: 321-322, 1975.

97. Evans JP and Florman HM: The state of the union: the cell biology of fertilization. Nat Cell Biol 4: s57-s63, 2002.

98. Huang TTF Jr and Yanagimachi R: Inner acrosomal membrane of mammalian spermatozoa: Its properties and possible functions in fertilization. Am J Anat 174: 249-268, 1985.

99. Yanagimachi R and Noda YD: Physiological changes in the postnuclear cap region of mammalian spermatozoa: A necessary preliminary to the membrane fusion between sperm and egg cells. J Ultrastruct Res 31: 486-493, 1970.

100. Bedford JM, Moore HDM and Franklin LE: Significance of the equatorial segment of the acrosome of the spermatozoon in eutherian mammals. Exp Cell Res 119: 119-126, 1979.

101. Cho C, Bunch DO, Faure JE, Goulding EH, Eddy EM, Primakoff P and Myles DG: Fertilization defects in sperm from mice lacking fertilin β. Science 281: 1857-1859, 1998.

102. Nishimura H, Cho C, Branciforte DR, Myles DG and Primakoff P: Analysis of loss of adhesive function in sperm lacking cyritestin or fertilin beta. Dev Biol 233: 204-213, 2001.

103. Almeida EA, Huovila AP, Sutherland AE, Stephens LE, Calarco PG, Shaw LM, Mercurio AM, Sonnenberg A, Primakoff P, Myles DG and White JM: Mouse egg integrin α 6 β 1 functions as a sperm receptor. Cell 81: 1095-1104, 1995.

104. Chen H and Sampson NS: Mediation of sperm-egg fusion: Evidence that mouse egg α6β1 integrin is the receptor for sperm fertilin beta. Chem Biol 6: 1-10, 1999.

105. Eto K, Huet C, Tarui T, Kupriyanov S, Liu HZ, Puzon-McLaughlin W, Zhang XP, Sheppard D, Engvall E and Takada Y: Functional classification of ADAMs based on a conserved motif for binding to integrin α 9β 1: Implications for sperm-egg binding and other cell interactions. J Biol Chem 277: 17804-17810, 2002.

106. Zhu X and Evans JP: Analysis of the roles of RGD-binding integrins, α(4)/α(9) integrins, α(6) integrins, and CD9 in the interaction of the fertilin β (ADAM2) disintegrin domain with the mouse egg membrane. Biol Reprod 66: 1193-1202, 2002.

107. Mizuno M, Harris CL, Johnson PM and Morgan BP: Rat membrane cofactor protein (MCP; CD46) is expressed only in the acrosome of developing and mature spermatozoa and mediates binding to immobilized activated C3. Biol Reprod 71: 1374-1383, 2004.

108. Johnson PM, Clift LE, Andrlíková P, Jursová M, Flanagan BF, Cummerson JA, Stopka P and Dvorakova-Hortova K: Rapid sperm acrosome reaction in the absence of acrosomal CD46 expression in promiscuous field mice (Apodemus). Reproduction 134: 739-747, 2007.

109. Lozahic S, Christiansen D, Manié S, Gerlier D, Billard M, Boucheix C and Rubinstein E: CD46 (membrane cofactor protein) associates with multiple beta1 integrins and tetraspans. Eur J Immunol 30: 900-907, 2000.

110. Stein KK, Primakoff P and Myles D: Sperm-egg fusion: Events at the plasma membrane. J Cell Sci 117: 6269-6274, 2004.

111. Jégou A, Ziyyat A, Barraud-Lange V, Perez E, Wolf JP, Pincet F and Gourier C: CD9 tetraspanin generates fusion competent sites on the egg membrane for mammalian fertilization. Proc Natl Acad Sci USA 108: 10946-10951, 2011.

112. Kaji K, Oda S, Shikano T, Ohnuki T, Uematsu Y, Sakagami J, Tada N, Miyazaki S and Kudo A: The gamete fusion process is defective in eggs of Cd9-deficient mice. Nat Genet 24: 279-282, 2000.

113. Miyado K, Yamada G, Yamada S, Hasuwa H, Nakamura Y, Ryu F, Suzuki K, Kosai K, Inoue K, Ogura A, et al: Requirement of CD9 on the egg plasma membrane for fertilization. Science 287: 321-324, 2000.

114. Horváth G, Serru V, Clay D, Billard M, Boucheix C and Rubinstein E: CD19 is linked to the integrin-associated tetraspans CD9, CD81, and CD82. J Biol Chem 273: 30537-30543, 1998.

115. Takahashi Y, Bigler D, Ito Y and White JM: Sequence-specific interaction between the disintegrin domain of mouse ADAM 3 and murine eggs: Role of beta1 integrin-associated proteins CD9, CD81, and CD98. Mol Biol Cell 12: 809-820, 2001.

116. Rubinstein E, Ziyyat A, Prenant M, Wrobel E, Wolf JP, Levy S, Le Naour F and Boucheix C: Reduced fertility of female mice lacking CD81. Dev Biol 290: 351-358, 2006.

117. Ernesto JI, Weigel Muñoz M, Battistone MA, Vasen G, Martínez-López P, Orta G, Figueiras-Fierro D, De la Vega-Beltran JL, Moreno IA, Guidobaldi HA, et al: CRISP1 as a novel CatSper regulator that modulates sperm motility and orientation during fertilization. J Cell Biol 210: 1213-1224, 2015.

118. Inoue N, Ikawa M, Isotani A and Okabe M: The immunoglobulin superfamily protein Izumo is required for sperm to fuse with eggs. Nature 434: 234-238, 2005.

119. Inoue N, Hamada D, Kamikubo H, Hirata K, Kataoka M, Yamamoto M, Ikawa M, Okabe M and Hagihara Y: Molecular dissection of IZUMO1, a sperm protein essential for sperm-egg fusion. Development 140: 3221-3229, 2013.

120. Inoue N, Kasahara T, Ikawa M and Okabe M: Identification and disruption of sperm-specific angiotensin converting enzyme-3 (ACE3) in mouse. PLoS One 5: e10301, 2010. J Dairy Sci. 84, 1277-1293.

121. Bianchi E and Wright GJ: Izumo meets Juno: Preventing polyspermy in fertilization. Cell Cycle 13: 2019-2020, 2014.

122. Sawada H, Mino M and Akasaka M: Sperm proteases and extracellular ubiquitin-proteasome system involved in fertilization of ascidians and sea urchins. Adv Exp Med Biol 759: 1-11, 2014.

123. Zhou C, Kang W and Baba T: Functional characterization of double-knockout mouse sperm lacking SPAM1 and ACR or SPAM1 and PRSS21 in fertilization. J Reprod Dev 58: 330-337, 2012.

124. Besenfelder U, Havlicek V, Moesslacher G, Gilles M, Tesfaye D, Griese J, Hoelker M, Hyttel PM, Laurincik J, Brem G, Schellander K (2008): Endoscopic recovery of early preimplantation bovine embryos: effect of hormonal stimulation, embryo kinetics and repeated collection. Reprod Domest Anim 43, 566-572

125. Hendriksen PJ, Steenweg WN, Harkema JC, Merton JS, Bevers MM, Vos PL, Dieleman SJ (2004): Effect of different stages of the follicular wave on in vitro developmental competence of bovine oocytes. Theriogenology 61, 909-920.

126. Rizos D, Ward F, Duffy P, Boland MP, Lonergan P (2002): Consequences of bovine

127. Fair T, Carter F, Park S, Evans ACO, Lonergan P (2007): Global gene expression analysis during bovine oocyte in vitro maturation. Theriogenology.

128. Hagemann LJ (1999) Influence of the dominant follicle on oocytes from subordinate follicles. Theriogenology 51, 449-459.

129. Machatkova M, Jokesova E, Horky F, Krepelova A (2000): Utilization of the growth phase of the first follicular wave for bovine oocyte collection improves blastocyst production. Theriogenology 54, 543-550.

130. Machatkova M, Krausova K, Jokesova E, Tomanek M (2004): Developmental competence of bovine oocytes: effects of follicle size and the phase of follicular wave on in vitro embryo production. Theriogenology 61, 329-335.

131. Wood SC, Glencross RG, Bleach EC, Lovell R, Beard AJ, Knight PJ (1993): The ability of steroid-free bovine follicular fluid to suppress FSH secretion and delay ovulation persists in heifers actively immunized against inhibin. J Endocrinol 136, 137-148.

132. Wolfsdorf KE, Diaz T, Smitt EJP, Thatcher MJ, Drost M, Thatcher WW (1997): The dominant follicle exerts an interovarian inhibition on FSH-induced follicular development. Theriogenology 48, 435-447.

133. Nemcova L, Machatkova M, Hanzalova K, Horakovab J, Kankaa J (2006): Gene expression in bovine embryos derived from oocytes with different developmental competence collected at the defined follicular developmental stage. Theriogenology 65, 1254-1264.

134. Assidi M, Dufort I, Ali A, Hamel M, Algriany O, et al. (2008) Identification of potential markers of oocyte competence expressed in bovine cumulus cells matured with follicle-stimulating hormone and/or phorbol myristate acetate in vitro. Biol Reprod 79: 209-222.

135. Bettegowda A, Patel OV, Lee KB, Park KE, Salem M, et al. (2008) Identification of novel bovine cumulus cell molecular markers predictive of oocyte competence: functional and diagnostic implications. Biol Reprod 79: 301-309.

136. Tesfaye D, Ghanem N, Carter F, Fair T, Sirard MA, et al. (2009) Gene expression profile of cumulus cells derived from cumulus-oocyte complexes matured either in vivo or in vitro. Reprod Fertil Dev 21: 451-61.

137. Bilodeau-Goeseel S, Schultz GA (1997): Changes in ribosomal ribonucleic acid content within in vitro-produced bovine embryos. Biol Reprod 56, 1323-1329.

138. Lonergan P, Rizos D, Gutiérrez-Adán A, Moreira PM, Pintado B, de la Fuente J, Boland MP (2003a): Temporal divergence in the pattern of messenger RNA expression in bovine embryos cultured from the zygote to blastocyst stage

in vitro or in vivo. Biol Reprod 69, 1424-1431.

139. Tesfaye D, Ponsuksili S, Wimmers K, Gilles M Schellander K (2004): A comparative expression analysis of gene transcripts in post-fertilization developmental stages of bovine embryos produced in vitro or in vivo. Reprod Dom Anim 39, 396-404.

140. Wrenzycki C, Herrmann D, Lucas-Hahn A, Korsawe K, Lemme E, Niemann H (2005): Messenger RNA expression patterns in bovine embryos derived from in vitro procedures and their implications for development. Reprod Fertil Dev 17, 23–35.

141. Moore T (2001) Genetic conflict, genomic imprinting and establishment of the epigenotype in relation to growth. Reproduction 122, 185-193.

142. Young LE, Fernandes K, McEvoy TG, Butterwith SC, Gutierrez CG, Carolan C, Broadbent PJ, Robinson JJ, Wilmut I, Sinclair KD (2001): Epigenetic change in IGF2R is associated with fetal overgrowth after sheep embryo culture. Nat Genet 27, 153-154.

143. Blondin P, Farin PW, Crosier AE, Alexander JE, Farin CE (2000): In vitro production of embryos alters levels of insulin-like growth factor-II messenger ribonucleic acid in bovine fetuses 63 days after transfer. Biol Reprod 62, 384-389.

144. Lonergan P, Rizos D, Gutierrez-Adan A, Fair T, Boland MP (2003b): Oocyte and embryo quality: effect of origin, culture conditions and gene expression patterns. Reprod Domest Anim 38, 259-267.

145. Wrenzycki C, Herrmann D, Lucas-Hahn A, Lemme E, Korsawe K, Niemann H (2004): Gene expression patterns in in vitro-produced and somatic nuclear transfer-derived preimplantation bovine embryos: relationship to the large offspring syndrome?. Anim Reprod Sci 82-83, 593-603.

146. Somers J, Smith C, Donnison M, Wells DN, Henderson H, McLeay L, Pfeffer PL (2006): Gene expression profiling of individual bovine nuclear transfer blastocysts. Reproduction 131, 1073-1084.

147. Rizos D, Lonergan P, Boland MP, Arroyo-García R, Pintado B, de la Fuente J, Gutiérrez-Adán A (2002b): Analysis of differential messenger RNA expression between bovine blastocysts produced in different culture systems: implications for blastocyst quality. Biol Reprod 66, 589-595.

148. Khosla S, Dean W, Brown D, Reik W, Feil R (2001): Culture of preimplantation mouse embryos affect fetal development and the expression of imprinted genes. Biol Reprod 64, 918-926.

149. Lazzari G, Wrenzycki C, Herrmann D, Duchi R, Kruip T, Niemann H, Galli C (2002): Cellular and molecular deviations in bovine in vitro-produced embryos are related to the large offspring syndrome. Biol Reprod 67, 767-775.

150. El-Sayed A, Hoelker M, Rings F, Salilew S, Jennen D, Tholen E, Sirard MA, Schellander K, Tesfaye D (2006): Large-scale transcriptional analysis of bovine embryo biopsies in relation to pregnancy success after transfer to recipients. Physiol Genomics 28, 84-96.

151. Minami N, Aizawa A, Ihara R, Miyamoto M, Ohashi A, Imai H (2003): Oogenesin is a novel mouse protein expressed in oocytes and early cleavage-stage embryos. Biol Reprod 69, 1736-1742.